SLAC-165
(T/E/A)
UC-28

DESIGN REPORT:

THE PROPOSED RECIRCULATING LINEAR ACCELERATOR AT SLAC*

(RLA)

STANFORD LINEAR ACCELERATOR CENTER
STANFORD UNIVERSITY
Stanford, California 94305

PREPARED FOR THE U. S. ATOMIC ENERGY
COMMISSION UNDER CONTRACT NO. AT(04-3)-515

August 1973

Printed in the United States of America. Available from National Technical Information Service, U. S. Department of Commerce, 5285 Port Royal Road, Springfield, Virginia 22151.
Price: Printed copy $5.45

---

*This supersedes SLAC-139 and SLAC-139 (Revised).

PREFACE

Two previous reports[1,2] have described SLAC's earlier studies and design work on the proposed Recirculating Linear Accelerator (RLA). During the intervening period there has been substantial effort at SLAC to elaborate and improve upon the design of RLA, and to refine and extend the studies of the potential research applications of the machine. This continuing work has confirmed the soundness of the concept and has provided further evidence of the unique position that RLA would occupy in extending those areas of particle-physics research that depend on high-energy electron beams.

RLA's principal parameters may be summarized as follows: A beam energy approximately double that of the present SLAC accelerator would be achieved by a sequence that consists of first-pass acceleration through the two-mile accelerator, beam storage in the recirculator, and reinjection and second-pass acceleration of the beam. In an alternate mode of operation, a stored one-pass beam having an energy up to about 20 GeV could be gradually extracted from the recirculator for use in high duty cycle experiments (up to 7%, as compared with the present 0.06%). The maximum recirculation energy is 17 to 20 GeV, depending on the number of electrons stored. Beam-energy losses of approximately 130 MeV each turn due to synchrotron radiation are compensated by two sectors (200 meters) of standard SLAC accelerator sections operating at the standard accelerator frequency (2856 MHz). These sectors will be powered by a special klystron now under development yielding 500 kW peak power at a duty cycle of about 10%. The repetition rate of the power source is 43,000 pps, and the recirculating period is 23 microseconds, corresponding to the total storage path of 6963 meters. The initial beam energy attainable at SLAC by this method is estimated to be about 42 GeV, and future increases are possible. Some of these would occur naturally as part of the program at SLAC of increases in klystron power. A further substantial change might occur in the future by the installation of accelerator sections which can compensate for the synchrotron radiation loss at storage energies as high as 25 GeV. A combination of these improvements might eventually increase the RLA energy up to 60 GeV.

Both the higher energy and the improved duty cycle would greatly enhance the utility of SLAC for particle-physics research. Areas which will be opened up are, among others:

A. Detailed studies of elastic and inelastic lepton scattering at higher energy and momentum transfer, including studies of the final states produced.

B. Photoproduction studies of extended kinematic range.

C. Enhanced secondary-particle beams, including $\bar{p}$, $\bar{n}$, and K^- beams that have previously been unavailable at SLAC.

D. Extension and experimental use of the hybrid and rapid-cycling bubble chamber techniques.

E. The use of extraordinarily powerful and clean K^o beams.

F. Weak-interaction experiments and particle searches in new regimes.

G. Meson and hadron spectroscopy using the facilities now existing at SLAC, and possible future facilities.

The technical discussions of accelerator components and systems in the latter sections of this Report often assume that the reader will already have a general familiarity with the present SLAC two-mile accelerator. For those interested, Ref. 3 listed below is the most complete compendium of technical information about (and of additional references to) the present SLAC machine.

References

1. "Description and physics program of the proposed Recirculating Linear Accelerator," Report No. SLAC-139, Stanford Linear Accelerator Center, Stanford University, Stanford, California (1971).
2. Report No. SLAC-139 (Revised 1972).
3. R. B. Neal, editor, The Stanford Two-Mile Accelerator (W. A. Benjamin, Inc., New York, 1968).

ACKNOWLEDGEMENTS

The following members of the SLAC staff have contributed to the work described in this report.

M. A. Allen
R. A. Bell
J. Ballam
W. H. Beeger
M. M. Berndt
S. J. Brodsky
L. E. Brown
W. O. Brunk
J. K. Cobb
D. H. Coward
K. F. Crook
U. K. Cummings
W. Davies-White
S. D. Drell
R. A. Early
R. A. Ecken
Z. D. Farkas
R. J. Fuendeling
E. Garwin
R. S. Gould
F. F. Hall
R. H. Helm
W. B. Herrmannsfeldt
H. A. Hogg
D. Jeong
W. B. Johnson
J. Jurow
K. R. Kase
A. J. Keicher
W. T. Kirk
L. J. Kral
C. J. Kruse
J. V. Lebacqz
M. J. Lee
A. V. Lisin
G. A. Loew
K. B. Mallory
F. Martin
R. H. Miller
P. L. Morton
J. J. Murray
R. B. Neal
C. W. Olson
W. K. H. Panofsky
J. R. Rees
D. B. Robbins
R. M. Rowe
M. Sands
R. A. Scholl
E. J. Seppi
C. K. Sinclair
E. L. Stockbridge
R. L. Stringall
R. E. Taylor
E. A. Taylor
A. A. Tseng
D. R. Walz
K. M. Welch
P. B. Wilson
B. M. Woo

TABLE OF CONTENTS

Page

LIST OF TABLES

LIST OF FIGURES

I. HIGH ENERGY PHYSICS OBJECTIVES

A. Introduction and Summary

The potential impact of an increase in energy and duty cycle of the two-mile accelerator can be understood by considering SLAC's research program of the past six years. This program has confirmed that the study of particle physics via electron- and photon-scattering experiments plays an essential and unique role in the investigation of the structure of the hadrons. The importance of such experiments derives from the fact that the electromagnetic interaction is well understood, can be well treated in the formal analyses, and exhibits a local, point-like nature. The known electromagnetic field generated during the electron's scattering or absorption of a photon interacts with the local electromagnetic current of the hadron target and thus can probe the structure of the nucleon at arbitrarily small distances. This is in sharp contrast to hadron-hadron scattering, in which the basic interaction between the target and beam particles is both unknown and diffuse, so that it is difficult to isolate the structure of the target particle.

Since the electron interacts via a known electromagnetic force, its scattering pattern can be interpreted in terms of the structures within the target protons and neutrons from which it scatters. Indeed, the deep inelastic scattering measurements performed at SLAC have given dramatic evidence of a scale-invariant behavior of the nucleons' structure functions which is reminiscent of the original Rutherford atomic scattering patterns and which strongly hints at a rich substructure, perhaps point-like, within the nucleon itself. In a complementary manner the purely hadronic interactions studied at the high-energy proton accelerators reveal regularities and patterns in the distribution of the debris emerging from the collisions. In these two patterns -- electron scattering and debris analysis in hadron collisions -- lie the clues to progress in our understanding of elementary particles. The results of the last few years have emphasized the vital importance of advancing both electron (photon) and proton (meson) scattering frontiers.

With RLA the sensitivity of SLAC experiments to short distance and other physics effects will be significantly increased. The projected increase in energy will greatly extend the kinematic range covered by the SLAC measurements and more than double the energy that can be transferred to the target hadron. The improved duty cycle at 20 GeV will permit multiparticle final state coincidence techniques to be advanced by up to several orders of magnitude.

The key beam parameters of the RLA are summarized in Table 1 (for a more detailed explanation of beam parameters, the reader is referred to Section II of this report). The beam intensity will be of the order of 10^{14} electrons per second. By contrast, the estimated muon flux from the 500 GeV NAL proton beam will be approximately 5×10^6 muons per second at 100 GeV; this limit is set primarily by beam halo. The electron beam attainable from neutral pion decay at NAL is expected to be between 10^7 and 10^8 electrons per second. Thus, for purposes of electromagnetic physics, there is an intensity ratio of at least six orders of magnitude in favor of the recirculating SLAC accelerator so that, although the energy range will be much more limited than at NAL, the momentum-transfer range for electromagnetic scattering can be extended to larger values. Thus while NAL will probe for new threshold effects at higher energies, SLAC-RLA will probe closer and closer to the light cone by studying the high momentum transfer regions.

It will be very important to compare the results from RLA with those from the electron-positron storage ring SPEAR, since SPEAR can probe hadronic properties with time-like photons carrying photon-masses of q^2 up to 81 GeV^2, while RLA will allow the comparable space-like probes to reach values of $q^2 \sim 45\ GeV^2$. This will thus permit what can be anticipated to be highly important comparisons for elucidating the structure of hadrons.

The physics possibilities of RLA can be divided into four main categories:

1. Deep inelastic electron scattering
2. Photoproduction and photon scattering processes
3. Secondary beams for hadron and weak interaction physics
4. New particle physics

We summarize below some of the essential physics of these four areas. The latter part of Section I will then discuss the physics program in more detail. A summary of how the capabilities of the existing experimental facilities at SLAC can be extended for use with RLA will also be presented.

1. Deep inelastic electron and muon scattering

Electron or muon scattering experiments can be considered as (virtual) photoproduction experiments in which the photon mass can be controlled by varying the energy and angle of the scattered lepton. This possibility of

TABLE 1

The Principal Design Beam-Parameters For RLA

	High Energy Mode	High Duty Cycle Mode
Output Beam Energy (GeV)	42	17.5
Recirculating Beam Energy (GeV)	17.5	17.5
Peak Output Beam Current (mA)	24	0.2
Average Beam Current (e/sec)	$\sim 10^{14}$	$\sim 10^{14}$
Duty Cycle (%)	.06	7

"tuning" the photon's mass is a unique feature of lepton-induced reactions. In addition, the polarization of the incident photon (real or virtual) may also be controlled experimentally. The scattering experiments performed at SLAC to date are of two general types: (i) Inclusive measurements in which the scattered electron (or muon) is detected and all available hadron channels are summed over; these are in effect total-cross-section measurements in which the virtual photons have a particular mass and polarization. (ii) Semi-inclusive and exclusive experiments in which one or more of the emerging hadrons is detected along with the scattered electron. The projected increase in energy obtained with the RLA will greatly extend the kinematic range covered by these measurements and more than double the energy that can be transferred to the target hadron. In particular, one is anxious to learn if the proton continues to scatter as if individual point-like constituents are contributing incoherently. The high-intensity electron beam will allow detailed and precise measurements of the electroproduction cross sections and will be a necessary complement to the gross measurements possible at NAL at still higher energies. Figures 1, 2, and 3 compare the kinematic ranges and counting rates at SLAC, RLA, and NAL for the inclusive experiments.

The continued observation of scale-invariant behavior of the proton and neutron cross sections in the RLA energy and sensitivity range could imply that we are observing asymptotic features of the proton structure, and would strongly support the main hypothesis of the parton and light-cone models: that the carriers of the electromagnetic current within the hadrons are structureless and light. Observation of scaling breakdown, on the other hand, would imply a new scale for hadronic phenomena, as would be required, e.g., if there are thresholds for parton or quark production, or could reflect the structure of the partons themselves. The experimental support or failure of scaling could represent one of the most significant problems in particle physics.

Further clues to the fundamental substructure of the nucleon must come from the detailed study of the properties of the final state in deep inelastic electron scattering. The increased duty cycle of RLA will greatly enhance SLAC's ability to observe final-state hadrons in electroproduction. As in hadron-hadron experiments, this may be done by identifying all final-state particles (exclusive experiments) or by identifying only a few particles and summing over the rest (inclusive experiments). The detailed information

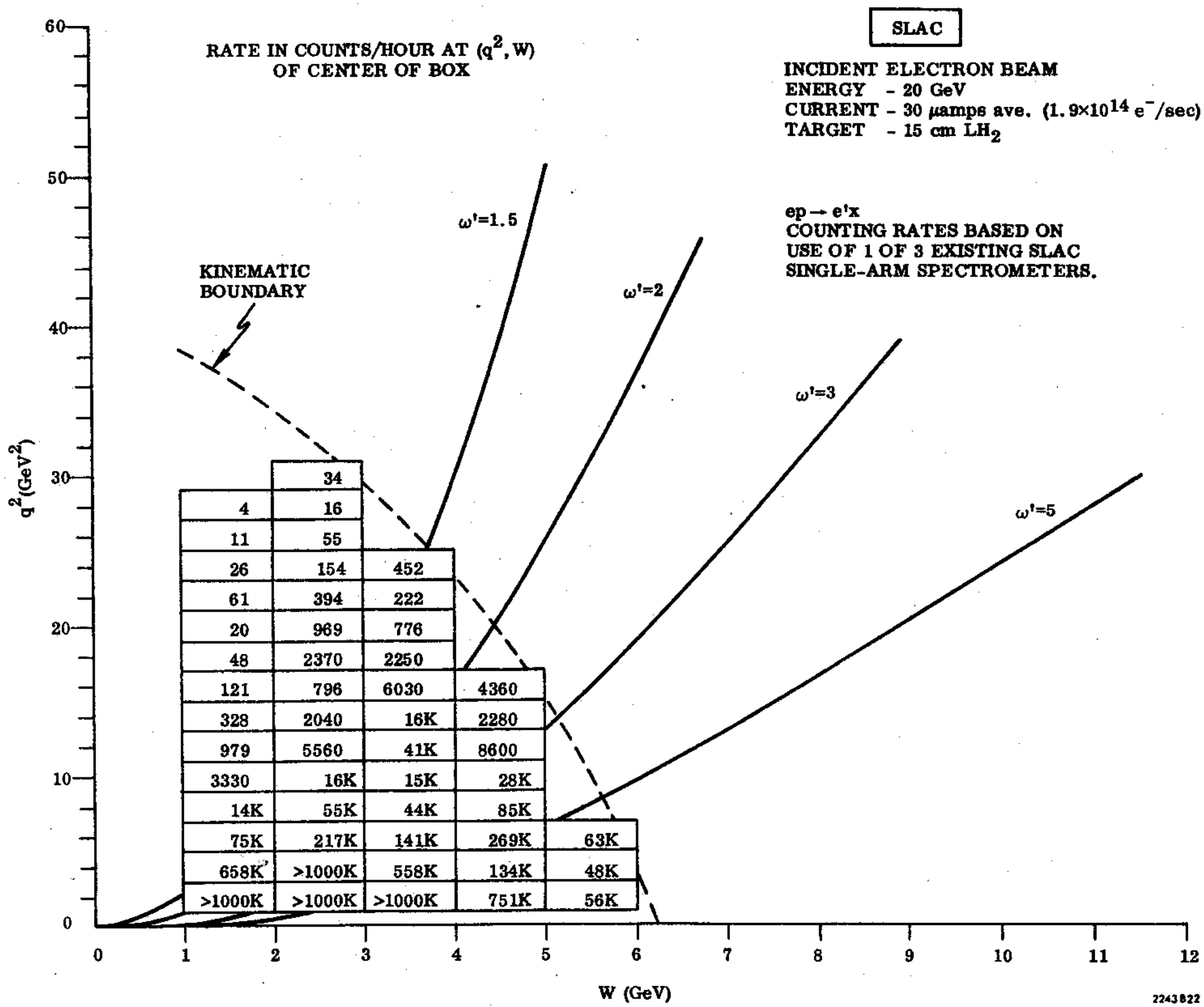

FIG. 1--The (q^2, W) region that has been explored by the present SLAC accelerator.

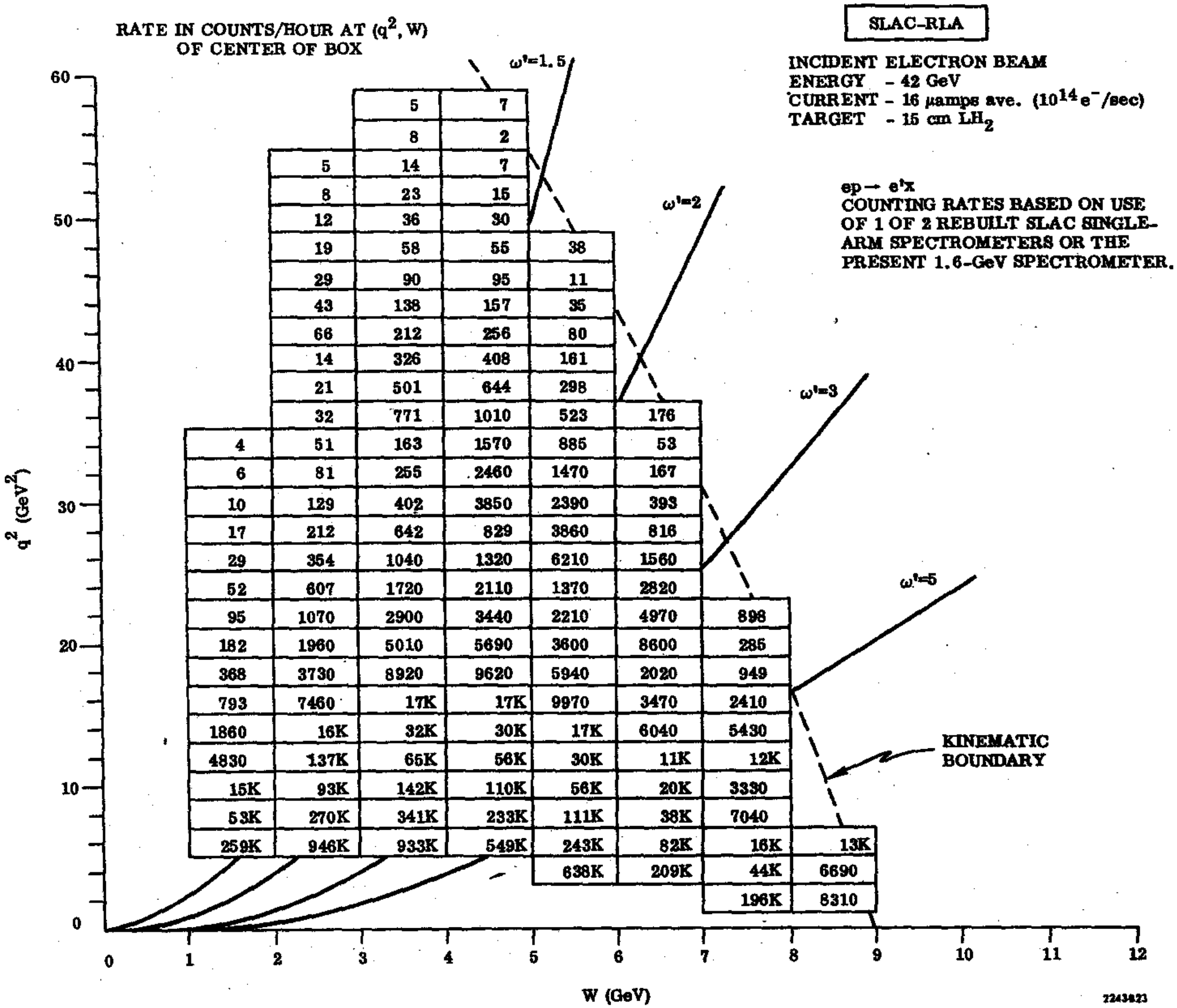

FIG. 2--The (q^2, W) region that could be explored by the SLAC Recirculating Linear Accelerator.

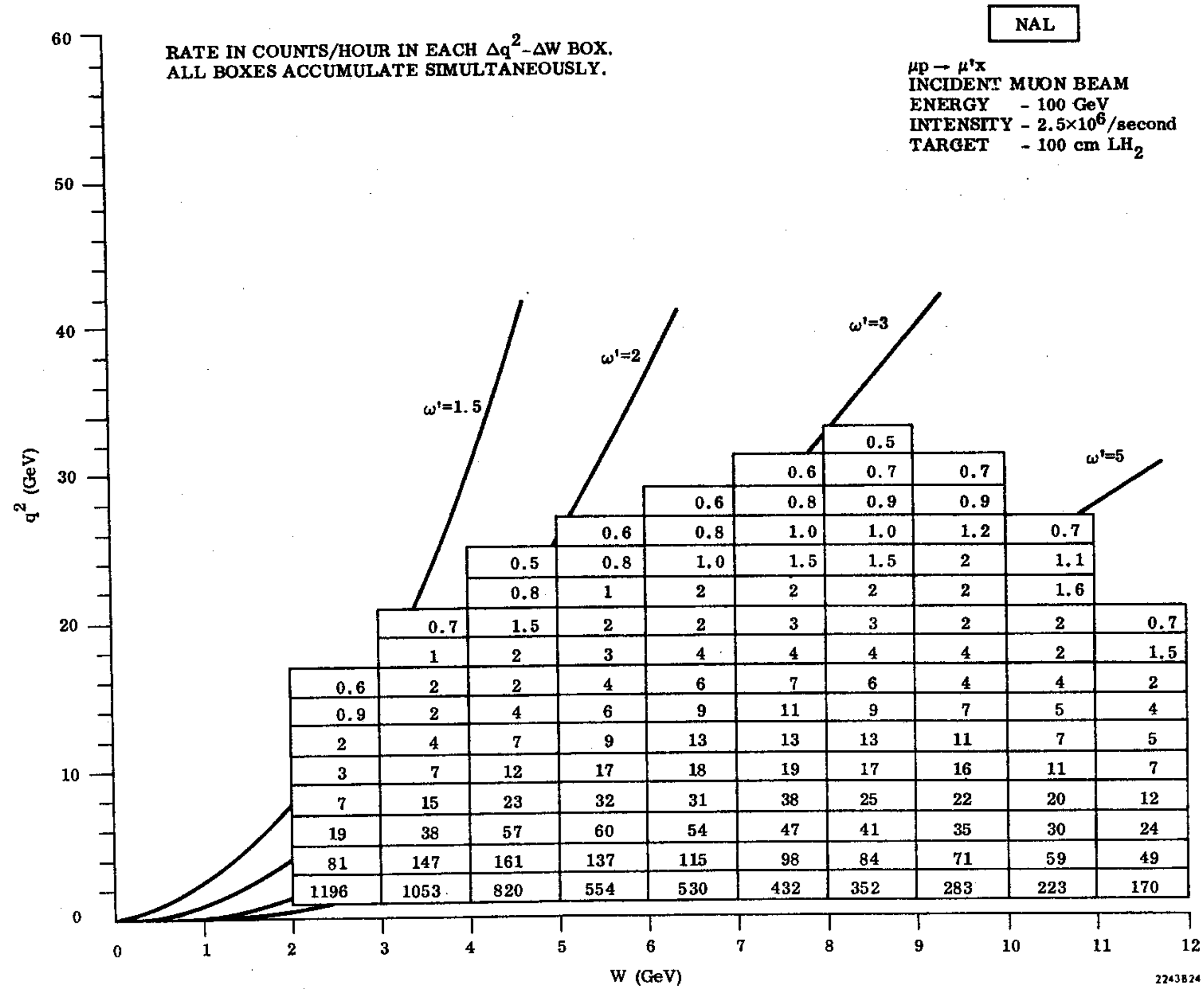

FIG. 3--The (q^2, W) region that can be explored by the NAL accelerator.

available from these experiments (i.e., multiplicities, momentum distributions, quantum numbers, correlations, etc.) will provide tests of specific predictions of the parton and other models (such as the intimate relations in the parton view between electroproduction, e^+e^- annihilation, and large-angle hadron scattering). Similarly, the photon mass and energy dependence of exclusive channels measurable at RLA will contribute much to our understanding of quasi-two-body production and will test many existing models (such as the quark model) and dynamical production mechanisms. Other general and fundamental features to be studied at large photon masses include the applicability of Regge theory analyses, the validity of sum rules based on current algebra and light-cone analyses, and the "fragmentation" of massive photons into jets of secondary hadrons.

2. Photoproduction and photon scattering processes

The study of reactions in which strongly interacting particles are produced by high-energy gamma rays (photoproduction) has been a major field of research at SLAC. These experiments have contributed directly to our understanding of the dynamics of the strong interaction, both in their own right and because they complement experiments done at other laboratories, such as Brookhaven and CERN, with incident proton and meson beams. The improvements proposed here for the SLAC machine will allow a great extension of this work. An increase in the duty cycle of the accelerator in the 15 to 20 GeV energy region by a factor of about 100 should provide an increase of the same factor of 100 in the amount of data already obtained on multiparticle momentum and angle correlations in photoproduction reactions. Most of the work to date in this multiparticle field has been devoted to the various vector-meson production reactions which have relatively large cross sections. The increase in data rate allowed by the improvement in duty cycle will allow experiments to be done on reactions with smaller cross sections, and hence broaden the spectrum of experiments which complement the work done in the same energy range at Brookhaven and CERN.

Photoproduction data bears directly on the electroproduction work at SLAC by furnishing a reference point at $q^2=0$. An understanding of the transition from photons with $q^2=0$, which exhibit mostly hadronic behavior, to high q^2 photons, where scaling appears to hold, is one of the fundamental challenges in high-energy phenomenology.

There are unique characteristics of the photon-initiated exclusive reactions that can be explored at high energies for uncovering the ways in which a photon is similar to and differs from a hadron. Subtle differences in Regge limiting behavior or the possible appearance of "fixed poles" in photon-induced reactions can be probed. Photon-initiated diffraction-dissociation events viz., γ + target $\rightarrow$ (hadronic system with the photon's quantum numbers) + target, can be probed to higher energies as well as higher massive hadronic states with RLA. To cite one very clear special feature as an example: the mechanism turning a γ into a ϕ is purely diffractive via Pomeron exchange and, with other background contributions absent, the pure diffraction character of the amplitude can be more readily observed. The studies of other "hadronic" features of a photon beam such as the shadowing effects as it traverses nuclear matter can also be explored in detail.

Scatterings with a large transverse momentum transfer correspond to small impact parameter collisions and also probe the short-distance structure of hadrons. Whether the probes are hadrons themselves, as at CERN, Brookhaven and NAL, or photons, as at SLAC, new types of scaling behavior are anticipated based on constituent models of the hadron as developed from the deep inelastic electron scattering results. Thus photoproduction and Compton scattering will be important processes to study -- and it is important to extend the measurements to as large a value of momentum transfer and to as small a value of the cross section as possible. In particular, comparison of exclusive vector-meson photoproduction and elastic Compton scattering in this region will be important for comparing the short-distance behavior of photons and mesons. In this domain all the processes, exclusive and inclusive, initiated by electromagnetic currents will require RLA's high fluxes to allow the measurements to probe to large momentum transfers.

For example, with the full photon flux of SLAC at 7.5 GeV, it has been possible to probe two-body photoproduction cross sections out to the kinematic limit of $\sim 13\ (\mathrm{GeV}/c)^2$ for the momentum transfers, corresponding to a minimum cross section value of $\sim 10^{-34}\ \mathrm{cm}^2/\mathrm{GeV}^2$. Since these observations show a cross section falling rapidly with $p_\perp$ (as $p_\perp^{-14}$) the importance of very high photon fluxes for studying such processes is clear.

Another example of high-energy limiting behavior comes from very inelastic photoproduction of massive μ-pairs, which can be studied for scaling laws similar to those found in deep inelastic scattering of electrons by protons. Comparison with the production of massive μ-pairs in proton-proton collisions will provide new information on possible differences of the photon and hadron interactions. Inclusive measurements at large momentum transfer of deep inelastic Compton scattering, $\gamma + p \rightarrow \gamma + X$, and wide-angle bremsstrahlung, $e + p \rightarrow e + \gamma + X$, are also important tests of predictions based on point-like constituents within the hadrons. Furthermore, measurements of the difference between electron and positron wide-angle bremsstrahlung, $e^{\pm} + p \rightarrow e^{\pm} + \gamma + p$, provide a direct determination of the real part of the Compton amplitude, which is a fundamental quantity in particle physics.

In photoproduction the use of a quasi-monochromatic polarized photon beam is important because it provides the only practical boson beam with spin. Consequently, it is a unique tool in the study of the spin dependence of meson processes. SLAC has been very successful in developing such a beam, and experiments with it have shown that ρ^{o}, ω and ϕ photoproduction tends to conserve the s-channel helicity of the photon; i.e., the spin of the vector meson is along its direction of motion. The polarized photon beam also allows a clean separation of the interactions due to exchange of natural and unnatural parity particles or "trajectories"; in this case only one beam is necessary, as opposed to the hadron beam case, where cross sections from different types of reactions are needed to make the separation.

The high-intensity, good-duty-cycle photon beams at RLA will make possible measurements of the η and η' lifetimes by the Primakoff effect, and may permit a more general study of even-charge-conjugation hadronic states in photon-photon collisions. The study of the interference of the electromagnetic and hadronic production amplitudes is also valuable.

3. Secondary beams for hadron and weak interaction physics

RLA will also be a copious and effective source of secondary hadron beams, as shown in Table 2. While the improved duty cycle will allow some experiments with pion beams which cannot be done now, the greatest interest will lie in the 25-45 GeV region. Also, the variety of experiments will be enhanced over the present ones by the introduction of useful K^{-}, $\bar{p}$ and $\bar{n}$ beams. Although the hadron beams at RLA are neither unique nor of exceptionally high flux,

TABLE 2

The Expected Secondary Particle Yields From RLA

Particle	Particles/sec
$\pi^{\pm}$	$\sim 10^6$
K^+	few $\times 10^4$
K^-	$\sim 10^4$
$\bar{p}(\bar{n})$	few $\times 10^3$
p(n)	$\sim 10^4$
K_L^o	few $\times 10^4$

Note: These yields are applicable to beams similar to those now in existence at SLAC.

neutral K^0 and $\bar{n}$ beams at SLAC will be clean compared to those at NAL, since they will be relatively free of neutron backgrounds. Reasonable momentum measurements of these neutrals can be made up to energies of 7 GeV by time-of-flight methods based on the intrinsically short rfbunches (10^{-11} sec) in the SLAC pulse.

Some of the interesting processes that RLA can study include:

(a) Determination of the energy dependence of specific processes and tests of duality, factorization, etc.

(b) The isolation of diffraction from exchange processes, and the illumiation of diffractive-dissociation mechanisms.

(c) The search for exotic exchanges.

(d) The search for heavy mesons.

(e) The study of relatively low-cross-section hadron processes induced by pions, such as backward-produced pion resonances, quasi-two-body final states involving high-mass nucleon resonances, etc., will be possible for the first time at SLAC since a large fraction of the full pion intensity in the energy range 10-20 GeV will be utilized.

(f) The study of parton-model scaling laws which predict energy-independent angular distributions at large center-of-mass angles.

(g) K-meson decays, regeneration, and associated weak interaction and CP-violating processes.

The high repetition rate at SLAC allows application of an important new technology in the area of fast-cycling bubble chambers operating in a triggered mode. The large aperture solenoid spectrometer (LASS) now being developed at SLAC allows a huge event capability with reasonable acceptance and high mass resolution. These facilities, and others such as the already existing streamer chamber and spectrometer systems, combined with RLA indicate that a strong program in hadron physics will continue at SLAC.

The yields given in Table 2 are for secondary beams of momenta of 10-40 GeV. Despite the fact that these yields are lower than that of NAL (by a factor of 10-100 for an NAL current of 5×10^{12} protons/sec), for reasonable cross sections in which the flux exceeds or matches the capacity of the data-handling system, SLAC will be a valuable complementary facility to NAL, as it now serves to Brookhaven and CERN.

4. New particle physics

Among the great mysteries of particle physics are the role of the muon and the possible existence of new leptons or heavy particles (W's, Z's) which carry the weak current. Since any particle with charge or magnetic moment is pair-produced, there will be great interest in experimental searches for such particles using the high-intensity higher energy electromagnetic beams of RLA. Further channel-by-channel comparisons of muon and electron interactions can be made to search for a possible difference in their interactions with hadrons. Tests of lepton conservation at high momentum transfer can also be done.

B. General Areas of Research - Detailed Discussion

1. Deep inelastic processes

The deep inelastic electron scattering results at SLAC have clearly shown that there are very large reaction rates as well as many contributing channels. To be more specific, consider the process in which an electron scatters inelastically and is detected after transferring energy ν and invariant four-momentum square q^2 to a target nucleon (hadron of mass M). For values of $\nu/M > 1$ and $q^2/M^2 > 1$, i.e., the deep inelastic region, the data indicate cross sections much larger than the partial cross sections to individual nucleon ground and resonance states. In fact, the structure functions for the inelastic cross section are observed to be functions of the dimensionless variable $\omega = 2m\nu/q^2$ and consequently do not fall as q^2 increases. The resonance bumps disappear into the large continuum tail as q^2 rises, and the scattering behaves as if it occurs from point-like constituents (anticipated by Bjorken and called "partons" by Feynman) in the proton, each contributing independently of the others, just as individual electrons add incoherently to make up the atomic cross section for highly inelastic scattering from atoms.

One of the primary questions to be answered by RLA is whether scaling continues to persist in the larger kinematic domain. With the higher energy beam in the 40-50 GeV region, it will be possible to extend greatly the range of ν (from 18 to ~40 GeV) and q^2 (from 20 to 40 GeV^2), as already illustrated in Figures 1 and 2, and to explore further into this deep inelastic scattering range. Whether scaling continues or not will help answer if we are truly probing the elementary, structureless building blocks of the hadrons or if we are uncovering a new layer of structure dominated by another mass scale (i.e., if the hadron constituents possess structure themselves). Also of great importance is the separation of $\sigma_L(\nu, q^2)$ and $\sigma_T(\nu, q^2)$ (the longitudinal and transverse total virtual photon cross sections). This requires large-angle lepton scattering and places severe requirements on the event rate. Thus, whereas NAL will probe to higher values of ν, the separation of σ_L and σ_T requires large-angle scattering and can be performed only with SLAC intensities. Indeed, one of the most interesting results from SLAC to date is the small value (~ 0.18) of σ_L/σ_T which suggests the dominance of spin-$\frac{1}{2}$ partons.

The state of theory is now such that in deep inelastic lepton scattering experiments, accuracy of measurement is becoming important. Specifically, alternate models differing in their fundamental aspects (such as the "anomalous dimensions" concept of K. Wilson) predict variances only discernible with high energy.

Further clues to the nature of the deep inelastic process, and the unravelling of the properties and interactions of the constituents, requires detailed study of the distribution and multiplicities of secondary particles emerging from the proton, as well as the dominant individual final-state channels, their mass distributions and dependence on momentum transfer. These are the analogues of the richly rewarding studies with incident baryon and pion beams that have paced the understanding of hadron dynamics and are the processes that the recirculating linear accelerator with a higher duty cycle would first open to our view.

The improvement in duty cycle by a factor of 100 or more at present energies provided by RLA means that event rates for these coincidence measurements would be increased by a comparable factor, allowing the determination of detailed effects and the measurements of small cross sections for specific channels.* With good duty cycle in the 15-25 GeV range at SLAC, one can explore this essential physics without expensive and major new detectors in the experimental area. Not only can the photon mass and energy dependence of these channels be mapped out, but also (by correlation with the scattering angle of the electron) the polarization of the incident virtual photon can in principle be controlled. In contrast, the hadron processes only allow variation of the incident energy but not the mass of the incident target.

*Some examples of experiments with RLA using existing SLAC experimental apparatus are discussed in part C of this section.

One such detector that has been successfully used at SLAC energies is an electroproduction apparatus consisting of a hydrogen target followed by a superconducting tube to reduce drastically the background due to Bethe-Heitler processes. The rest of the apparatus is a large magnet followed by wire chambers to detect forward-going hadrons while shower counters detect the scattered electrons. The superconducting tube has allowed electron intensities as high as 10^6/second to be used in this large-solid-angle detector, even with a poor duty cycle. The apparatus is especially suited to studies of electroproduction of ρ^0 and ϕ, and to inclusive studies in inelastic electron-proton interactions.

The coincidence experiments in which outgoing hadrons as well as the scattered electron are detected can provide severe tests of proposed models. For example, one can look for fast pions in the lab which are associated with the break up or "fragmentation" of the virtual photon. Much information about high-energy scattering has been learned from studying hadronic fragmentation. Photon fragmentation should be even more interesting because of the variable-mass q^2. Parton and Regge models of inclusive electroproduction predict that these single-particle distributions will exhibit Feynman-Yang scaling (limiting fragmentation) in addition to overall Bjorken scaling (function of ω rather than ν and q^2 separately). It will also be especially interesting to compare the fragmentation of these space-like virtual photons with the time-like virtual photons from e^+e^- annihilation at SPEAR. The multiplicity and quantum numbers of the fragments will bear directly on the existence and nature of the hypothetical partons. Polarization information can also be obtained from the coincidence experiments, since the polarization of the virtual photon can be controlled to some degree by the scattering kinematics.

It is also particularly interesting to measure the elastic and inelastic electroproduction of hadrons at large transverse momentum relative to the virtual photon direction. Here one probes the short-distance structure of the produced particle as well as the target nucleon, and detailed checks of parton-model predictions can be made. The cross sections for the large-transverse-momentum processes are predicted to be small and will require the high intensity RLA beam.

The ability to vary the photon mass in coincidence measurements also allows a useful probe into the nature of diffractive processes. The measurements of elastic and inelastic electroproduction of the vector meson are essential for answering such questions as the following:

(1) Do these channels contribute to scaling behavior?

(2) Are diffractive effects controlled solely by the minimum momentum transfer to the target?

(3) How does the transition between point-like behavior at large photon mass and hadron-like behavior in real photoproduction occur?

(4) Do virtual photons become more pointlike? Is there a "small photon" effect, which would be reflected in the variation of the diffraction pattern of the electroproduction process with photon mass?

(5) Can the transition region from photoproduction to deep electroproduction shed light on impact-parameter and geometric pictures of hadron interactions?

(6) Are there s-channel helicity conservation laws in the high photon mass regions?

(7) What is the range of validity of vector dominance and generalized vector dominance theories?

(8) What is the interrelation between Feynman-Yang (hadronic) scaling and Bjorken (scale-invariant) scaling?

At low q^2 studies of diffractive processes can of course also be carried out in the NAL lepton beams and can reach higher virtual photon energies.

These same theoretical questions are also confronted in comparing the behavior of virtual photoabsorption cross sections on nuclei with real photoabsorption. Experiments at SLAC and DESY have shown that "shadowing" of photon processes and in hadron-nucleus interactions is absent when the photon has $q^2 > 0.2\ \mathrm{GeV}^2$. Furthermore, sensitive measurements are needed for understanding this behavior and its dependence on photon mass and energy. Extending the range of these studies to higher energies as well as doing more detailed and accurate experimental studies using the improved RLA duty cycle at present SLAC energies will add importantly -- perhaps crucially -- to our understanding of the transition from real "hadronic" photons to virtual "point-like" ones.

There are higher order electromagnetic processes which will be exciting to measure at RLA. For example, the measurement of the inelastic wide-angle bremsstrahlung process $e + p \to e + \gamma +$ (anything) not only tests the time-like and space-like electron propagators at large invariant masses, but also gives a measurement of the virtual Compton inelastic amplitude. The interference of the Bethe-Heitler and Compton amplitudes, which is measured in the difference of electron and positron wide-angle inelastic bremsstrahlung, is related to the matrix element of the product of three electromagnetic currents. Measurements of this basic process and confirmation of the scaling laws predicted by the parton model can lead to a determination of parton charge. Measurements of the difference of electron and positron elastic wide-angle bremsstrahlung leads to a determination of the real part of the elastic Compton amplitude. Here one can check the validity of the fundamental Kramers-Kronig dispersion relation. The determination of the photon mass dependence and energy dependence of the virtual Compton amplitude (especially confirmation of energy-independent, and photon-mass independent, terms corresponding to local point-like two-photon interactions) is a critical test of parton and light-cone theories. All of these measurements are extremely difficult with the present SLAC duty cycle because of π^o backgrounds, but are expected to be feasible with the high duty cycle of RLA.

2. Photon physics

RLA will provide photon beams well suited to a wide variety of experiments. The properties of the photon beams available from the RLA depend on unique features of this particular accelerator, and are not likely to be duplicated elsewhere. The only parameter of interest which will be surpassed at any other accelerator is the photon energy. Although photon beams of considerably higher energy will be available at NAL, the much lower intensity available in these beams, along with their lack of polarization, will limit the work undertaken with them to studies of the unpolarized total cross section and a few of the larger cross section diffractive processes.

A. Photon beams

Before discussing the RLA photon experiments, a brief summary of the various RLA photon beams is in order. These beams are:

(1) Ordinary bremsstrahlung. In the high-energy mode, yields of a few $\times 10^9$ equivalent quanta per pulse (upwards of 10^{12} e.q. per second) are readily available. Presently, beams of this intensity are used only in End Station A at SLAC. The facilities available there, the three large focusing spectrometers and the pair spectrometer, will be adaptable to use with higher energy photon beams with little or no modification. For example, the present 20 GeV spectrometer could readily be adapted for use at 45 GeV by simply re-arranging the existing magnets and some of the shielding. The 1.6 GeV

spectrometer would clearly have the utility it presently has with no modification. Even higher intensity bremsstrahlung beams could be delivered to targets in ESA by bringing the electron beam into the end station, producing the bremsstrahlung there in a thick radiator, and continuing both beams through to Beam Dump East.

An excellent facility for conventional bremsstrahlung beams could be made for use with the high-duty-cycle or high-energy modes of operation. This would be accomplished by mounting a permanent target for bremsstrahlung production in the recirculating beam at all times. Calculations indicate that a target could be made thin enough so that losses to the recirculating beam would be negligible (less than 1%) while providing bremsstrahlung yields on the order of a few $\times 10^{11}$ e.q. per second. Alternatively, bremsstrahlung beams of a few $\times 10^{11}$ e.q. per second could be provided by stripping off a small portion of the recirculating beam on each turn.

(2) Bremsstrahlung polarized by coherent pair production. This technique has recently been developed into a practical facility by a group at SLAC. Basically, one attenuates one linear polarization state of the unpolarized beam more than the other. It is possible to produce a high polarization at the bremsstrahlung tip by this method, and thus to create the highest energy polarized photons of any technique. The beam is most useful with experimental apparatus or techniques which can be made insensitive to the large number of less strongly polarized, lower energy photons. An important point with this beam is that the cross-section difference responsible for the polarization increases linearly with energy. At 40 GeV, a beam of 40% polarization at the bremsstrahlung tip, with an intensity of 10^8 e.q. per pulse could be made with the graphite polarizer now in hand. Because of the attenuation necessary to produce the polarization, successful utilization of this method needs the high intensities available at RLA. This technique offers enough advantages that it will probably replace the use of uncollimated coherent bremsstrahlung for energies greater than about 16 GeV, though detailed studies would have to be undertaken in some specific instances.

(3) Highly collimated coherent bremsstrahlung. By collimation to angles notably smaller than the characteristic angle of m/E, the coherent bremsstrahlung spectrum from crystalline targets is significantly improved in two ways. First, the width of the coherent peak is significantly narrowed, and second, the incoherent bremsstrahlung is greatly reduced. SLAC has recently perfected a technique for producing the very thin (less than 80 microns) diamond targets necessary for this work, and has brought such a beam into experimental use

for the first time. This beam relies on both the high intensity and the excellent phase space of the linac for its performance. In particular the yields are directly related to the electron beam phase space. A helpful factor in going to higher energies is that the coherent cross section increases linearly with energy. Based on the performance of the existing beam, and making reasonable assumptions about the phase space of the 40 GeV RLA beam (see Table 5 in Section III), yields of 6×10^8 quanta per second at 22 GeV (± 5% width, 65% linear polarization) and 1.5×10^8 quanta per second at 30 GeV (± 3.5% width, 39% linear polarization) appear possible.

Furthermore, it may be possible to produce a crystalline radiator thin enough to allow continous placement in the recirculating beam, for high duty-cycle use.

(4) Highly collimated backscattered laser beams. This technique, previously brought to full utilization at SLAC, produces photon beams of very high polarization, with very narrow, background-free spikes as a spectrum. The yields from this process are very low, however, making them suited for use only with large-solid-angle detectors. Again, the yields are directly related to the electron-beam phase space. With the same reasonable assumptions about phase space noted above, it appears that the present ruby laser system could provide enough yield for a bubble chamber exposure. Very rapid advances in the areas of high average power, high repetition rate, and repetitively Q-switched YAG lasers give promise that linearly and circularly polarized photon beams might be practical from these systems at energies between 4 and about 24 GeV, again with yields suited for large-solid-angle detectors.

B. Photon beam experiments

There are a variety of photon-beam experimental problems which could be studied with RLA. (This list is not intended to be exhaustive.)

(1) Bubble chamber survey at 20 GeV. Using the ruby laser beam, an exposure of 10^6 pictures would yield 3×10^4 events, covering all topologies in a reasonably unbiased fashion. Such an exposure would give a good outline of the physics, and would undoubtedly be useful in planning future, more highly selective, experiments.

(2) Pseudoscalar meson photoproduction. In this work, and for vector-meson photoproduction as well, two points are worth stressing. First, due to the steep energy dependence of secondary-particle yields at BNL and CERN, most experiments with boson beams have been done at energies at or below

16 GeV, even though the primary energy at these machines is about 30 GeV. At SLAC, where photon experiments are often done at the maximum machine energy, the experiments are thus a good complement to the higher energy proton machines. Second, since the photon has two spin states, twice as many amplitudes are necessary to describe photoproduction process as would be required if it were produced by spinless bosons. However, since the photon can be polarized, useful information can be obtained which is not readily accessible to measurements of single-boson-induced reactions. For example, forward production of single scalar or pseudoscalar mesons with polarized photons leads directly to a separation of natural and unnatural parity t-channel exchange contributions. Similar separations for production by spinless bosons require the measurement of more than one reaction, with the concommitant systematic errors.

Pseudoscalar meson photoproduction studies have produced a wealth of new information and uncovered a number of still poorly understood phenomena. For example, there is the near constancy of $s^2 d\sigma/dt$, the approximate e^{-3t} falloff away from $t = 0$, and the dominance of natural parity exchange in the t-channel. These properties are common to all the measured reactions. To accommodate these features into contemporary theories or phenomenological models seems to be very difficult.

A study of these reactions at higher energy, especially with polarized photons, will be very interesting. With the new graphite-attenuated beam, it will be possible to study both the polarized photon asymmetry and the differential cross section in the same experiment out to a t of 1.5 $(GeV/c)^2$, at energies between 20 and 40 GeV. Larger momentum transfer studies could be made with unpolarized beams. With this facility it should also be possible to study backward photoproduction, where baryon exchange is presumably dominant, with polarized photons. This will be the first information of this type available.

With the aid of the high-duty-cycle mode of RLA, it will be possible to undertake double-correlation measurements where either one initial and one final spin, or both initial spins, are determined. Measurements of this type will be of considerable aid in studying the amplitudes which contribute to these processes. Present-day models are sophisticated enough to require this sort of information. The combination of high energy and high intensity of RLA in its low-duty-cycle mode makes it possible to pursue studies of very high momentum transfer inclusive photoproduction processes; these have become of great theoretical interest as a result of recent ISR results.

(3) Vector meson photoproduction. The observed vector-meson photoproduction cross sections decrease very slowly with photon energy. Measurements of these cross sections at higher energies, and in nuclei, provide a crucial test of models such as vector dominance.

The search for new vector mesons by their diffractive production by photons can also be extended. Higher energies relieve the complications that arise from minimum momentum transfer effects, which have been a bit troublesome in some of the present experiments. Since many of the final states from these reactions involve a number of particles, these experiments are "naturals" for the large-solid-angle detectors, combined with good duty cycle, sophisticated photon beams. Event rates of several per second seem achievable, and would represent a substantial increase in our knowledge of these particles.

In investigating diffractive problems where spin and helicity rules are of interest, photons play a unique role. In these forward processes, where photons resemble hadrons, they offer an opportunity to investigate polarization effects not accessible in hadron reactions. Thus, for example s-channel helicity conservation has been shown to be a prominent feature of rho, omega and phi photoproduction out to moderate momentum transfers. It will be of great importance to determine how far in t this behavior extends. If the present t dependence is maintained, exploration out to $t = 2\ (\mathrm{GeV}/c)^2$ can be done with RLA photon beams. Photoproduction of ϕ mesons is a unique reaction in which no ordinary Regge poles other than the Pomeron can contribute if exchange degeneracy holds. This reaction may provide interesting information about the Pomeron at low energies.

(4) Compton scattering. Elastic photon scattering experiments test the Regge hypothesis for the couplings to the nucleon and the photon as well as vector dominance. Present experiments at energies up to 18 GeV indicate some disagreement with current models. The real part of the Compton scattering amplitude can be measured by interference with the Bethe-Heitler amplitude. Both these experiments will profit from higher energies, and the high-duty-cycle mode of operation of RLA will allow extension of the angular distribution measurements into the higher momentum transfer region. The possible presence of fixed poles (i.e., amplitudes with energy dependence unrelated to t) in photoproduction and Compton scattering is of great interest. The light-cone and parton models predict fixed-pole behavior in the Compton amplitude but not in photoproduction of any hadron which is composite. For such

investigations one requires both more accurate low-energy data for the evaluation of sum rules and higher energy data to establish the asymptotic behavior. For large angles, parton models predict that the Compton amplitude is energy independent and has form-factor-like dependence on t. No such behavior is expected for large-angle ρ photoproduction. All of these tests are in the natural province of the high-duty-cycle RLA.

(5) Primakoff effect. The cross sections for this process grow with the fourth power of the photon energy. [The Primakoff peak, integrated over the small t range, grows like $\ln(s)$.] This situation, coupled with the fact that the polarized photon asymmetry for this process is nearly unity, will allow studies to be conducted at RLA.

(6) $q^2 = 0$ point. Measurements of any particular channel in photoproduction are important as a $q^2 = 0$ point for comparison with the electroproduction data for the same channel.

(7) Large-angle photon processes. Photoproduction at large angles can be an important probe of hadron structure at short distances. Parton models predict that the cross section at fixed energy and fixed but large center-of-mass production angle has the form $d\sigma/dt = s^{-N} f(\Theta_{cm})$, that is, a universal angular dependence independent of energy. The s-dependence can be related to the power-law fall-off of the form factors of the target proton and produced hadron. If the parton models are valid, then these large-angle processes obey the impulse approximation and involve a basic interaction at short distances, and the photon can display its point-like scale-invariant coupling. Comparison with large-angle electroproduction will also be of great interest. Since the cross sections for these basic processes fall so rapidly with energy, it is clear that the high-intensity RLA beams are essential.

Very inelastic scattering of real photons will also shed important new light on the constituent structure of both protons and photons. The inelastic photoproduction of hadrons at large transverse momentum is interesting as a test of the short-distance structure of the photon and the produced hadron. In certain parton models, the photon is predicted to behave in a completely point-like fashion, and new types of scaling laws arise. Such processes are also sensitive to the existence of "hard" parton-parton or gluon forces.

The very inelastic Compton effect, $\gamma + p \rightarrow \gamma + X$, at very large transverse momentum transfer may be observable, and its behavior can extend the ideas of the parton model to very virtual parton states in the proton. This will cast light on the validity of the model in this new application. It is predicted to be a large and measurable process at high energies.

(8) Mu-pair experiments. Mu-pair processes are of great interest in different kinematic regions: (a) low-mass muon pairs give information similar to inelastic Compton scattering, (b) experiments in which one energetic muon goes forward are an excellent vehicle for testing electrodynamics involving highly off-shell leptons, and (c) muon-pair experiments can be described as time-like lepton scattering processes similar to the Brookhaven (Lederman) experiments on the production of muon pairs from hadrons.

3. Hadron physics

RLA will also be a copious and effective source of secondary hadron beams, as previously demonstrated in Table 2. These yields are for secondaries in the range 10-40 GeV/c. While the improved duty cycle will allow some experiments with pions which cannot presently be done, the greatest interest will lie in the 25-40 GeV/c region. In this interval the duty cycle and intrinsic rf bunching of the primary electron beam are quite well suited to the use of rf separators for charged beams. Also, the variety of experiments will be extended over the present situation by the introduction of useful K^-, $\bar{p}$, and $\bar{n}$ beams. The neutral K_L^o and $\bar{n}$ beams at SLAC are exceptionally clean compared to those at proton accelerators since electroproduction is relatively free of neutron backgrounds. Reasonable momentum measurements of these neutrals can be made up to momenta of ~ 7 GeV/c by time-of-flight methods based on the intrinsically short rf bunches (10^{-11} sec) in the SLAC pulse.

The momentum interval 25-40 GeV/c is particularly important since it lies beyond the reach of the CERN-PS and the BNL-AGS proton synchrotrons. While the yields cited in Table 2 are lower than those expected at NAL (by a factor of 10-100 for 5×10^{12} protons/sec), the thrust of the NAL effort will rightly be focused on the higher energy phenomena. Furthermore, for reasonable cross sections the fluxes often exceed the capacity of data-handling systems. Recently considerable effort has been made at SLAC to develop very high volume data-acquisition systems (LASS) and the necessary computing facilities for reducing these data. In this area SLAC will be a valuable complementary facility to NAL as it now serves in relation to Brookhaven and CERN.

The interest in hadron beams in the 25-40 GeV/c momentum range is that they will extend our present knowledge of the energy dependence of specific final states, aid in the isolation of diffractive from exchange processes, and facilitate the search for new diffractively produced resonances, for exotic exchanges, and for new heavy mesons. Current theoretical ideas of duality and factorization have predictions in this energy range which will be tested. Furthermore, large center-of-mass angle scattering in two-body and quasi-two-body processes is a measure using hadronic probes of the innermost structure of nucleons. Comparison of the large-angle scattering for various initial and final states as a function of energy provides a useful supplement to the structural information obtained with electromagnetic probes. Other hadron experiments are discussed earlier in this section and in the following description of bubble chamber physics.

As noted above, for processes with reasonable cross sections, wire-chamber spectrometers with huge event-rate capabilities and large acceptances for high-mass resonances can be used quite profitably at SLAC. The large aperture solenoidal spectrometer (LASS) presently being built at SLAC can be used at these higher energies without extensive modification. The conventional dipole portion of this device is capable of measuring fast, forward particles to $\leq 0.5\%$ in momentum, while the solenoidal part measures the angles of all charged particles to high precision and the momenta of particles >3 GeV/c to a percent or two. It has a large acceptance over the full kinematic range of variables and is ideally suited to the study of bosons produced at the upper vertex or baryon resonances produced at the lower vertex. It is most effective for final states which do not involve neutral particles, but used in conjunction with neutron detectors or shower counters, LASS will be an effective tool for other final states as well. Data can be collected at rates up to 100 events/sec.

There are several experiments of an extended nature which require long running times but are nevertheless important. From past experience at proton machines, not many of these are completed per year, and SLAC-RLA could make significant contributions in this field. Examples are: polarization parameters in πp and Kp elastic scattering; detailed examination of multi-neutral final states; and low-cross-section states in πp and Kp interactions in the 5-10 GeV region. Examples of the latter that LASS could measure are backward processes, exotic exchanges, and large t processes. The good duty cycle will allow $\sim 2 \times 10^5$ π/sec intensities to be used so that backward

$\pi p \longrightarrow px$ processes which have 1 μb cross sections would yield 2500 events/hour/GeV^2, while large-t events in the same process having cross sections between 0.01 - 0.1 μb would still give 25-250 events/hour/GeV^2.

4. Bubble chamber physics

The high repetition rate of SLAC, its characteristically short pulses, and the availability of pulse-to-pulse beam switching have led to the development of a very productive bubble chamber program at SLAC in both the conventional and hybrid modes. In conventional usage, there have been a great many high statistics experiments, mostly in hadron physics but with a significant series of investigations in photoproduction as well.

In hybrid usage, there have been a number of unique applications developed at SLAC which have broadened the scope of the bubble chamber technique. Hybrid techniques of this sort at the RLA energies will not, for practical purposes, be attainable at other laboratories. In particular these are:

(1) Time-of-flight measurments of the momentum of neutral kaons, neutrons, and anti-neutrons by counters surrounding the chamber. (As mentioned above, these measurements rely on the rf bunching of the electron beam which is unique to SLAC.)

(2) Fast cycling (10-20 pps) of the large hydrogen chambers; the lights are flashed only when a very fast forward particle is observed and its momentum is measured by spark chambers placed behind the bubble chamber. (This and the following application both exploit the high repetition rate of SLAC.)

(3) Rapid-cycling chambers of target size (45-90 pulses per second and 30-60 cm long) with thin beam windows all around. When the lights are triggered by counter-spark chamber arrays, the chamber becomes a visible hydrogen or deuterium target.

Since the chamber has 4π geometry, many biases can be turned off for part of the experiment by running in an untriggered mode. A second feature, peculiar to SLAC, is that when the proposed system operates at 25-40 GeV/c in a hybrid mode, the number of beam particles per pulse acceptable to the bubble chamber (15-20) exceeds the number acceptable to a spark chamber (5-10); thus the bubble chamber as a target is more than matched to its counter-spark-chamber subsystems. As would be expected, most of the benefits to bubble chamber physics from this proposal will accrue at the higher energies.

Keeping these points in mind, one can foresee a large class of experiments in the 25-40 GeV range that can be done at SLAC in a highly competitive and perhaps unique manner. Among these are:

(1) Studies of energy dependence and differential cross sections for highly peripheral quasi-two-body reactions involving backward nucleon resonances. These are excellent experiments for the fast-cycling chambers; one such experiment has already been completed at 14 GeV using the SLAC 40-inch chamber.

(2) Studies similar to (1) except where the final state involves a backward hyperon resonance. These are particularly suited to the rapid cycling target chamber because of the short lifetime involved.

(3) Studies of nucleon-antinucleon resonances such as $R^+ \rightarrow \bar{n}p$ by triggering on a fast forward $\bar{n}$ in a reaction $\pi^+ p \rightarrow \bar{n}pp$.

(4) Studies of antilambda-proton elastic scattering by triggering on fast forward protons in $K^+X \rightarrow \bar{\Lambda}X'p$ and observing the $\bar{\Lambda}p$ scattering in the chamber.

(5) Studies of exotic exchanges by triggering on fast forward nucleons and looking in the chamber at backward-produced mesons. These studies would be especially effective for backward going K^{0}'s.

Conventional use of a 2-3 meter chamber (with good optics and high resolution) with its small demand (1-2%) on machine intensity, would also be useful for studies of high mass resonances and multiple-particle final states. Neon-hydrogen mixtures will extend these to states with several neutral π's. A chamber of this size with a field of 25-30 kG is quite capable of the resolution needed.

5. Streamer chamber physics

The SLAC streamer chamber has been used in a wide variety of experiments including photon, muon and meson beams. It has several advantages over the bubble chambers: it can be triggered more rapidly, auxiliary detectors can be easily installed around the chamber, and it can be triggered in a wide variety of conditions. In short, it is a very flexible tool for studying many classes of events whose usefulness will increase significantly with RLA.

The data-taking rates for the streamer chamber are generally limited by background because of the relatively long time constant of the chamber compared with the time width of the beam pulse. Lowering the beam intensity will reduce the instantaneous background rates, while increasing the number of pulses will provide higher data-taking rates. Low-energy high-duty-cycle experiments of the following type are possible with RLA:

(1) Interactions from a tagged photon beam or monocrystalline beam. Standard types of experiments will provide 10 to 30 times as much data as presently available from track chambers. Using very selective triggers RLA will provide about 100 times as many "special" events per microbarn as currently obtainable.

(2) The observation of hadron interactions is limited by the background of delta rays unless the target region is outside the chamber. RLA will provide about 50 times improvement in data rates for pion scattering.

(3) Radiative effects and corrections now limit inelastic electron scattering to a kinematic region (q^2, ν) smaller than that possible with muon beams. With the improved duty cycle, rates with electron beams 10-30 times greater than present SLAC muon-beam rates are possible.

The streamer chamber is not limited to low-energy experiments. External wire chambers can be installed around the basic equipment to increase the accuracy of the streamer chamber for high-momentum particles. Typical examples of this are high-energy photoproduction experiments with 10 times the statistics currently available; 30 to 40 GeV/c meson beams; and electron scattering yielding about 30,000 events at small angles but with large energy loss.

6. K^o decay physics

The present advantages of SLAC for K^o physics are the relative absence of neutron background (K^o/n ratio > 1 above 1 GeV) and time-of-flight information (accuracy $\pm 1/3$ nsec, giving useful momentum information up to about 6 or 7 GeV). The present disadvantage is the poor duty cycle, which results in a K^o flux limitation that is considerably below the capability of the machine.

It thus appears that the high-duty-cycle mode of RLA will offer the main advantages for K^o physics. At present, because of the number of sparks in the wire chambers, the flux of K^o's available from the SLAC accelerator is limited to a primary electron current of 3 or 4 milliamps. Even at this low current, the secondary beam has to be attenuated by about 4-5 interaction lengths. (It is preferable for reasons of accelerator operation and K^o/neutron ratio to run relatively high current with a large attenuator rather than low accelerator current and a small attenuator.) With the improved RLA duty cycle, a factor of 6-8 in K^o flux could be obtained by removing some absorber. Another factor of 3 could be obtained by increasing the electron current. Conceivably, another factor of 1.5 to 2 could be obtained by reducing the production angle from the present 3^o to 1.5 or 2^o. Thus the K^o flux could be increased by a factor of about 30. Since the duty cycle would increase by a factor of ≈ 120, the background spark problem would also be considerably reduced. These factors lead to an expected flux of about 5×10^7 accepted K^o decays/day for experiments which use the existing K^o spectrometer with the RLA accelerator running at 180 pps. This flux level, combined with a very large acceptance detection system, would enable one to reach meaningful levels for rare K^o decay modes.

C. Sample Data Rates Using Present SLAC Equipment with RLA

1. Single-arm spectrometers

With some modifications, the three single-arm spectrometers now used at SLAC can achieve the counting rates previously shown in Fig. 2 for inelastic e-p scattering. These spectrometers can remain in their present location in End Station A.

2. Electroproduction apparatus

A relatively simple apparatus using a superconducting flux-exclusion beam pipe, a large analyzing magnet, proportional chambers, hodoscopes and shower counters has been used to measure ρ^o electroproduction and single π inclusive processes at SLAC. A comparison of this experiment with the results that could be expected with RLA is shown below:

	SLAC Experiment	RLA Experiment
Running Time (hours)	200	200
Total No. of Electrons	1.3×10^{14}	1.4×10^{16}
Inclusive Events	200,000	200,000
$q^2 (GeV/c)^2$	0 - 6.0	3.0 - 12.0
$P_\perp^2 (GeV/c)^2$	0 - 1.0	0 - <1.0
Rho Production	3000	10,000
q^2	0 - 4.0	1.5 - 5.0

3. Large-angle solenoid spectrometer (LASS)

This apparatus, now under construction, is described in Report No. SLAC-152. It can be used with either the high-duty-cycle or high-energy mode of RLA and in electron, photon or hadron beams. The following are some counting rates that may be obtained:

(1) Inelastic electron scattering. Assuming 3.6×10^6 e^-/sec (superconducting tube and a one-meter LH_2 target) for the high-energy mode, and 2×10^8 e^-/sec for the low-energy, high-duty-cycle mode, then the rates shown in Table 3 should be achievable.

(2) Photoproduction. Assuming a one-meter LH_2 target and 3.6×10^5 quanta/sec for the high energy mode, and 3.6×10^7 quanta/sec for the low-energy high-duty-cycle mode of RLA, then the following rates should be achievable:

20 GeV (good duty cycle)	100 events/sec/μb
40 GeV (poor duty cycle)	1 event/sec/μb

Since photoproduction total cross sections vary from about 10 μb (ρ^o production) to $\sim$ .01 μb (single inelastic channel at 40 GeV) these rates are quite acceptable.

(3) Hadron interactions. Assuming a one-meter LH_2 target and the fluxes shown below, then the following rates should be achievable:

	π	Event Rate	K	Event Rate
20 GeV (good duty cycle)	2×10^5/sec	1000/sec/mb	2×10^3/sec	10/sec/mb
40 GeV (poor duty cycle)	10^3/sec	5/sec/mb	10^3/sec	5/sec/mb

The data-gathering capacity of LASS should be in the 50 - 100/sec range. For π beams at good duty cycle rates, cross sections as low as a fraction of a microbarn can be investigated.

4. Streamer chamber

The large streamer chamber now in regular operation at SLAC will benefit from the good duty cycle because its dead time of several microseconds (now just about matched to the pulse length of the linear accelerator) is short enough to take full advantage of the factor of $\sim$ 100 improvement. Thus all present experiments can be run at data rates $\sim$100 times larger. Typical rates expected with streamer chamber experiments at RLA are shown below.

TABLE 3

Inelastic Electron Scattering

Counting rates per hour* for various cuts in q^2, W variables using the LASS wire-chamber spectrometer.

E_e = 20 GeV (good duty cycle)

$W \geq$	2 GeV	3 GeV	4 GeV
$q^2 > 0.5$ GeV^2	390 K	230 K	110 K
$q^2 > 1.0$ GeV^2	160 K	100 K	50 K
$q^2 > 1.5$ GeV^2	85 K	55 K	30 K
$q^2 > 2.0$ GeV^2	40 K	35 K	15 K
$q^2 > 2.5$ GeV^2	30 K	25 K	12 K
$q^2 > 3.0$ GeV^2	20 K	15 K	10 K
$q^2 > 4.0$ GeV^2	10 K	10 K	5 K

E_e = 40 GeV (poor duty cycle)

$W \geq$	2 GeV	3 GeV	4 GeV
$q^2 > 0.5$ GeV^2	6 K	4.5 K	3.0 K
$q^2 > 1.0$ GeV^2	3 K	2.2 K	1.5 K
$q^2 > 1.5$ GeV^2	1.5 K	1.3 K	900
$q^2 > 2.0$ GeV^2	1.0 K	900	600
$q^2 > 2.5$ GeV^2	700	600	400
$q^2 > 3.0$ GeV^2	500	400	300
$q^2 > 4.0$ GeV^2	200	300	200

*Counting rates are limited by acceptable background rates, not by the current available.

(1) Hadron interactions. Assuming a 40 cm LH_2 target and the fluxes shown below, the following rates should be achievable:

	π Flux	Event Rate	K Flux	Event Rate
20 GeV (good duty cycle)	3.5×10^5/sec	500/sec/mb	10^4/sec	17/sec/mb
40 GeV (poor duty cycle)	3.5×10^3/sec	5/sec/mb	10^2/sec	0.17/sec/mb

(2) Photoproduction. The memory time of the streamer chamber is ~1.5 μsec. Assuming 15 e.q./1.5 μsec derived from a straight bremsstrahlung beam incident on a 40 cm LH_2 target, the following rates should be achievable:

	γ Flux	Event Rate
20 GeV (good duty cycle)	10^6 e.q./sec	100/sec/μb
40 GeV (poor duty cycle)	10^4 e.q./sec	1/sec/μb

With a tagged γ beam, these rates would be decreased by a factor of ~10.

5. Bubble chambers

SLAC now has a 40-inch and a 15-inch bubble chamber, both capable of having their lights triggered by auxiliary electronic systems. The 40-inch has a potential of 20 expansions/sec, and the 15-inch should go ~60/sec. Both have already operated successfully at half these rates. The chambers will not be able to take advantage of the high-duty-cycle mode of RLA, so the rates shown below are for the high-energy mode of RLA operation.

Using a downstream spectrometer for the momentum measurement of fast tracks, the effective length of the 40-inch chamber becomes 36 inches, while that of the 15-inch chamber is 9 inches. Assuming 15 particles/pulse into the chambers the following rates should be obtainable in the high-energy mode:

Chamber	Flux ($\pi^{\pm}$, $K^{\pm}$, $\bar{p}$, p)	Event Rate
40" (15 exp/sec)	300/sec	0.3/sec/mb
15" (60/sec)	1200/sec	0.3/sec/mb

Note: the 40-inch chamber has a thin exit window only at the downstream side, while the 15-inch chamber has a 360-degree thin beam window.

6. $\underline{K^o \text{ spectrometer}}$

A spectrometer which measures K^o decays in a K^o_L beam has been in operation at SLAC for some time. With RLA, an increase of the presently available flux by a factor of about 30 could be expected. With this enhanced flux (10^{10} K^o_L's per day into the spectrometer), and assuming a detection efficiency of 20%, one would observe a total of 10^7 decays/day. The rates for particular channels of interest are as follows:

$K^o_L \rightarrow 2\pi^o$: 5×10^4/day

$K^o_L \rightarrow$ 4 body: 5×10^3/day (assuming a branching ratio of 10^{-4})

$K^o \rightarrow 2\mu$: 0.3/day (assuming the unitarity value)

Thus the existing K^o spectrometer would be a very effective tool for use with RLA.

7. Improvements in Rates

All the numbers given above pertain to presently existing equipment with little or no modification. Gradual improvements and changes could readily increase these numbers. Eventually some new equipment, such as a 2 - 3 meter fast-cycling bubble chamber, or a new and larger streamer chamber, could improve some of the rates by an order of magnitude, especially at the higher energies.

II. GENERAL DESCRIPTION OF THE RECIRCULATING LINEAR ACCELERATOR

The general plan of the Recirculating Linear Accelerator (RLA) is illustrated in Fig. 4. A new beam from the injector is accelerated once through the existing SLAC linear accelerator to an energy of 20 GeV or less. This beam is then extracted from the accelerator and inflected into the 6.9 km long recirculator for 120 revolutions, which corresponds to one machine interpulse period of the linac (1/360 sec or 2.8 msec). Then, when the modulators have recharged and the klystron system is ready for the next rf pulse, the stored beam is extracted from the recirculator and reinserted into the linear accelerator for a second pass. The maximum beam energy is thus increased to 40 - 45 GeV by the second acceleration. As an alternate mode of operation, it is possible to use the recirculator as a "beam stretcher." In this mode, a fraction of the beam is "peeled off" and "spilled" into the beam switchyard and experimental areas every time the 1.6 μsec train of electrons approaches the east loop. Since the recirculating period is 23 μsec and the beam pulse is 1.6 μsec long, the resulting duty cycle is 7%.

Both the low-energy beam from the injector and the high-energy recirculated beam can be contained simultaneously in the two-mile accelerator so that the full repetition rate of 360 pulses per second can be retained in RLA. In this mode of operation, the reinjected high-energy beam bunches will merge with the newly injected first-pass bunches on the crests of the accelerating wave and pass together down the linac.

The recirculator proper consists of two 95-m-radius loops located at the ends of the 3-km-long accelerator and joined by two long straight sections. The beam is bent around the loops by an array of about 160 alternating-gradient magnets. The 30° reverse bends are used to connect the loops to the straight sections. The reverse bend systems consist of an array of quadrupoles and bending magnets which make it possible to adjust the isochronism of the entire recirculator to an unusually low value for a "circular" machine. The beam lines for the two long straight sections are located just above the linear accelerator tube in the existing housing.

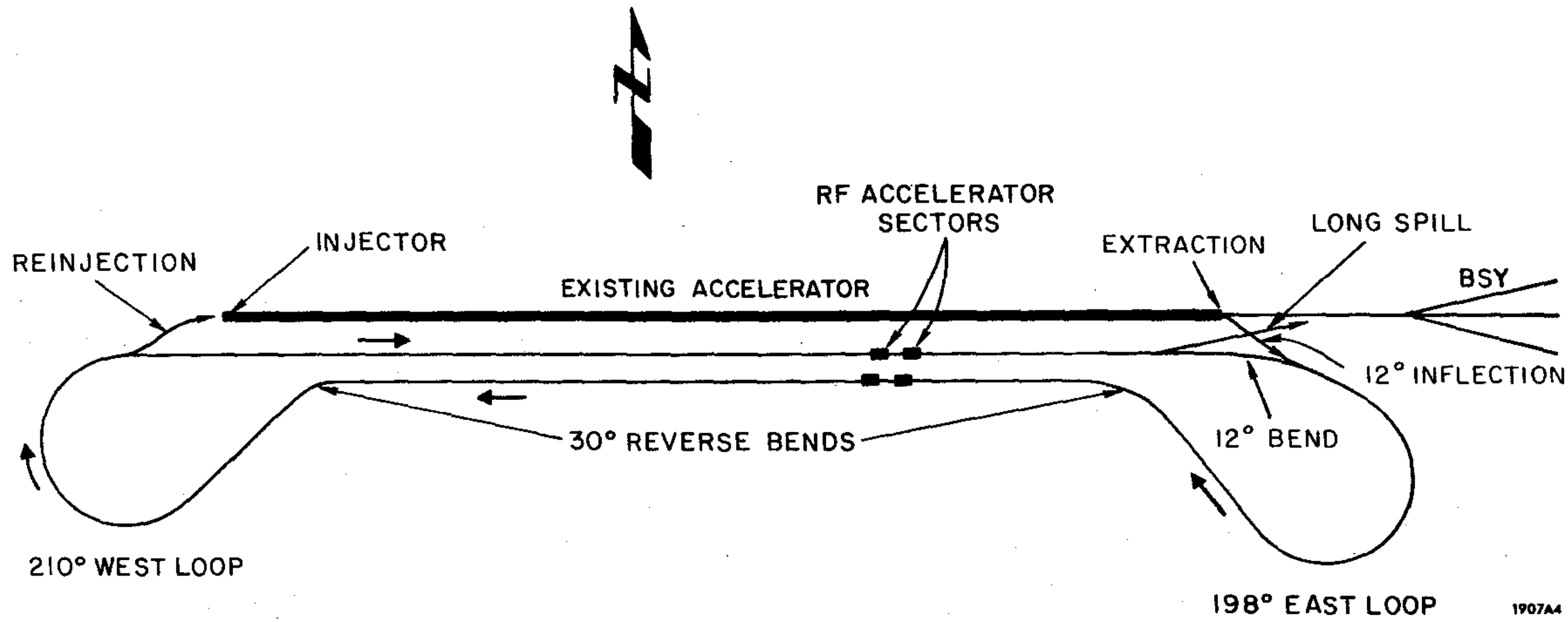

FIG. 4--Schematic of the Recirculating Linear Accelerator showing the major components and the general scheme of operation.

In the course of traveling around the recirculator, the stored electrons radiate away some of their energy as synchrotron radiation. For example, a 20 GeV electron radiates away about 200 MeV in one trip. The radiation process has several important consequences for the design of the recirculator. For one thing, a high-voltage radio-frequency accelerating system must be provided to restore this lost energy and, for another, the radiation is deposited in a vertically narrow band in the vacuum chamber causing both heating and outgassing which must be dealt with in a special manner. The radiation is of course quantized and thus subject to fluctuations which tend to expand the bunches of the beam in both the transverse and longitudinal dimensions. This tendency is opposed by radiation damping, which can be achieved in all three degrees of freedom by appropriate design of the lattice.

The chief requirement on the lattice of the RLA is that the distribution of particles in the six-dimensional phase space should not grow to a value greater than the acceptance of the linear accelerator during the storage interval of 1/360th of a second. The acceptance of the accelerator is limited by the requirement that a low-energy beam must be accelerated through the same structure. If the high-energy and the low-energy beams are to be accelerated together, which is a requirement for 360 pps operation of the RLA, then the acceptance for the high-energy beam is limited by the strength of the focusing system that will transport the low-energy beam. Extra focusing for the high-energy beam alone, in the form of pulsed quadrupole lenses, could be provided, but at the cost of limiting RLA operation to 180 pps. The present focusing system for the accelerator has a matched acceptance in both the horizontal and vertical planes of about $A = 0.3 \times 10^{-6}\ \pi$ meter-radians for a 17.5 GeV beam. This can be increased by adding more closely spaced quadrupole lenses, or by adding pulsed focusing, or both, up to an estimated $A = 0.6 \times 10^{-6}\ \pi$ meter-radians.

The longitudinal acceptance of the linear accelerator, i.e., the acceptance in phase spread and energy spread, is limited by the requirement that the final high-energy beam have a sufficiently narrow energy spread for efficient experimental use after its second traversal of the linac. For example, a range of $\pm 8^{\circ}$ in phase about the rf crest results in about 1% spread in energy gained on the second pass, which corresponds to a spread of about 0.5% in the final spectrum if the energy is doubled, neglecting the energy spread of the stored beam.

The operation of RLA is probably best understood by tracing the history of a bunch of electrons through the system and out to a target. The bunch is injected near the west end of the two-mile accelerator where it joins a bunch of high-energy electrons from the previous pulse which is just beginning its second and final trip down the accelerator. Consider the case in which the linear accelerator is capable of 25 GeV total acceleration from end to end, but in which injection takes place partway down the accelerator so that the first-acceleration output energy is 17.5 GeV, and the recirculator is set to that energy. The two combined beams reach the end of the accelerator with electrons of 42.5 GeV and 17.5 GeV. By a suitable magnetic beam transport system, the 42.5 GeV beam is directed into the beam switchyard (BSY) and transported through it to an experimental target. The 17.5 GeV beam, a 1.6 μsec train of bunches 1/3 nanosec apart, is bent 12° southward to the inflection system of the recirculator which includes as its final element a fast kicker magnet to place the trajectory of the incoming beam on the recirculator axis.

The bunches are now recirculating, losing 120 MeV to synchrotron radiation in each turn and gaining a like amount from the rf system. The rf-accelerator system is concentrated in sectors 21 and 22 of the main accelerator housing. There are sixteen accelerator structures planned for the RLA, eight of which would be in each line as the recirculating beam lines pass in opposite directions. The spaces between the accelerator sections are used to locate quadrupole focusing elements.

While the bunches are travelling around the recirculator, they will pass a slow extraction system which is capable of peeling out a small fraction of the electrons on each turn, removing them from the recirculator and directing them into the BSY for experimental use. As mentioned above, this process can increase the duty cycle by a factor of more than 100, namely to 7%. The long-duty-cycle beam energy is limited, of course, to the maximum storage energy, which will be approximately 20 GeV.

For achieving the highest possible energies with the same duty cycle as that of the present linac, the bunches are not peeled out (i.e., the slow extraction system is turned off) but are retained for 1/360th of a second, after which time another fast kicker deflects them into an extraction channel which removes them from the recirculator and reinserts them into the west end of the two-mile accelerator for their final acceleration to 42.5 GeV.

Typical performance goals for RLA are given in Table 4. They are generally consistent with the requirements of the anticipated particle physics program, which was described in the previous section. In the following sections, the Recirculating Linear Accelerator and its operation are described in more detail.

TABLE 4

Typical RLA Performance Goals

	High Energy Mode[1]		High Duty Cycle Mode	
Output Beam Energy (GeV)	41.5	44	17.5	19
Recirculating Beam Energy (GeV)	17.5	19	17.5	19
Peak Output Beam Current (mA)	24	10	.2	.1
No. of Electrons per Pulse $\left(\times 10^{11}\right)$	2.4	1	2.4	1
Duty Cycle (%)	0.06	0.06	7	7

(1) Parameters given assume the installation of 30 MW klystrons throughout the two-mile accelerator.

III. LATTICE, ORBITS, AND BEAM TRANSFERS

A. General

The design of the lattice is dominated by radiation effects on the stored electrons. The extent of the beam in transverse phase space at the end of the storage period depends primarily on the quantum-induced horizontal growth and on the radiation damping. To a lesser extent it also depends on the initial distribution in phase space and on the storage time. The asymptotic value of the quantum-induced size depends on the square of the energy. Since the storage period of 1/360 second is approximately the same as the damping period, the beam does not reach its asymptotic limit, and the energy dependence of the beam size is somewhat greater than E^2. At a given energy then, if the initial emittance from the accelerator is a constant $\left(\epsilon_i = 5.0 \times 10^{-8}\pi \text{ meter-radians has been assumed}\right)$ and if the storage time is given, the horizontal emittance at the time of reinjection into the linac depends on the quantum driving term and on the horizontal damping time constant. The vertical emittance depends on horizontal-vertical couplings, unintentional or intentional.

In order that the final transverse emittance of the reaccelerated beam can be maintained at approximately the level normally achieved in the SLAC two-mile accelerator, it is necessary to limit the emittance of the stored beam to a value only a factor of two or three larger than its initial emittance. To accomplish this, the main bending cells where most of the radiation effects take place are designed to give radial damping and to reduce the quantum effects to unusually low values for a ring of such radius. This is accomplished by combining rather short cells (8.3m long) with very strong focusing in the radial plane.

The final phase space as seen by the physics experimenter will be typically at least a factor of two smaller than the transverse phase space at reinsertion, because of adiabatic damping during reacceleration. Table 5 gives the expected phase space as a function of recirculating energy, assuming a doubling of RLA energy for the second acceleration.

TABLE 5

Phase Space Comparisons

Present SLAC Phase Space

Exceptionally well-tuned SLAC beam	$2.5 \times 10^{-8} \pi$ meter-radians
Assumed insertion phase space for RLA	$5.0 \times 10^{-8} \pi$ meter-radians
Assumed energy spread at insertion	$\pm$ 0.2%
Assumed bunch length at insertion	$\pm 3.0^{\circ}$

RLA Phase Space (All Emittances in Units of 10^{-8} π Meter-Radians)

Recirculating Energy (GeV)	17.5	20.0	25.0
Final Energy Range (GeV)	34-42	40-45	45-50
Emittance at Reinsertion	8.8	12.3	23.0
Horizontal Final Emittance	4.4	6.2	11.5
Vertical Final Emittance	2.5	2.5	2.5
Final Energy Spread (%)	$\pm$0.34	$\pm$0.36	$\pm$0.36

For discussing the details of the lattice and beam transfer systems, it is convenient to divide the machine into the following parts: main bends, reverse bends, long straight sections, 12-degree east bend and RLA injection system, and extraction and linac reinsertion system. See Fig. 5. The properties of the complete recirculator are summarized in Table 6.

B. Main Bend Cells

The alternating-gradient loop lattices are composed of 5° cells. Each cell consists of one focus magnet and one defocus magnet. The magnets are closely spaced to achieve a relatively high packing fraction in order to minimize synchrotron radiation losses. The bending rings have an average bending radius of 95 m, a value chosen to match the available site. High gradients are being contemplated to minimize transverse beam growth due to quantum fluctuations and to achieve radiation damping for vertical, horizontal and longitudinal motion. A magnet design and construction program is underway to assess the practicality of building such high-gradient magnets.

The principle parameters of the main bend cells are listed in Table 7. The fields are given for operation at 20 GeV although the magnets are being designed for eventual operation at 25 GeV.

It is convenient to think of the alternating gradient cells as beginning and ending in the middle of successive horizontal defocusing magnets. The extra half of a defocusing magnet at each end of the main bend array thus becomes part of the matching system to the reverse bends. See Fig. 6. Each main bend and each reverse bend is achromatic by itself. Thus, both energy dispersion and transverse optics must be considered in the matching problem. The energy (η-function) matching of the main bends is done by a single zero-gradient magnet which bends the beam by 3.125° and disperses it so that the quadrupole singlet which follows can properly focus the dispersed rays. Since each defocusing magnet bends by 3.75°, the sum of the 1.875° bend from the half of a defocusing magnet and 3.125° from the η-matching magnet contributes 5° total bend, just as in every regular cell.

The transverse (β-function) matching problem consists of properly adjusting the quadrupole lenses near the bend group to fit the beam to the size and divergence most natural for the next stage of the recirculator. The only special problems for the β-matching are those posed by the physical constraints

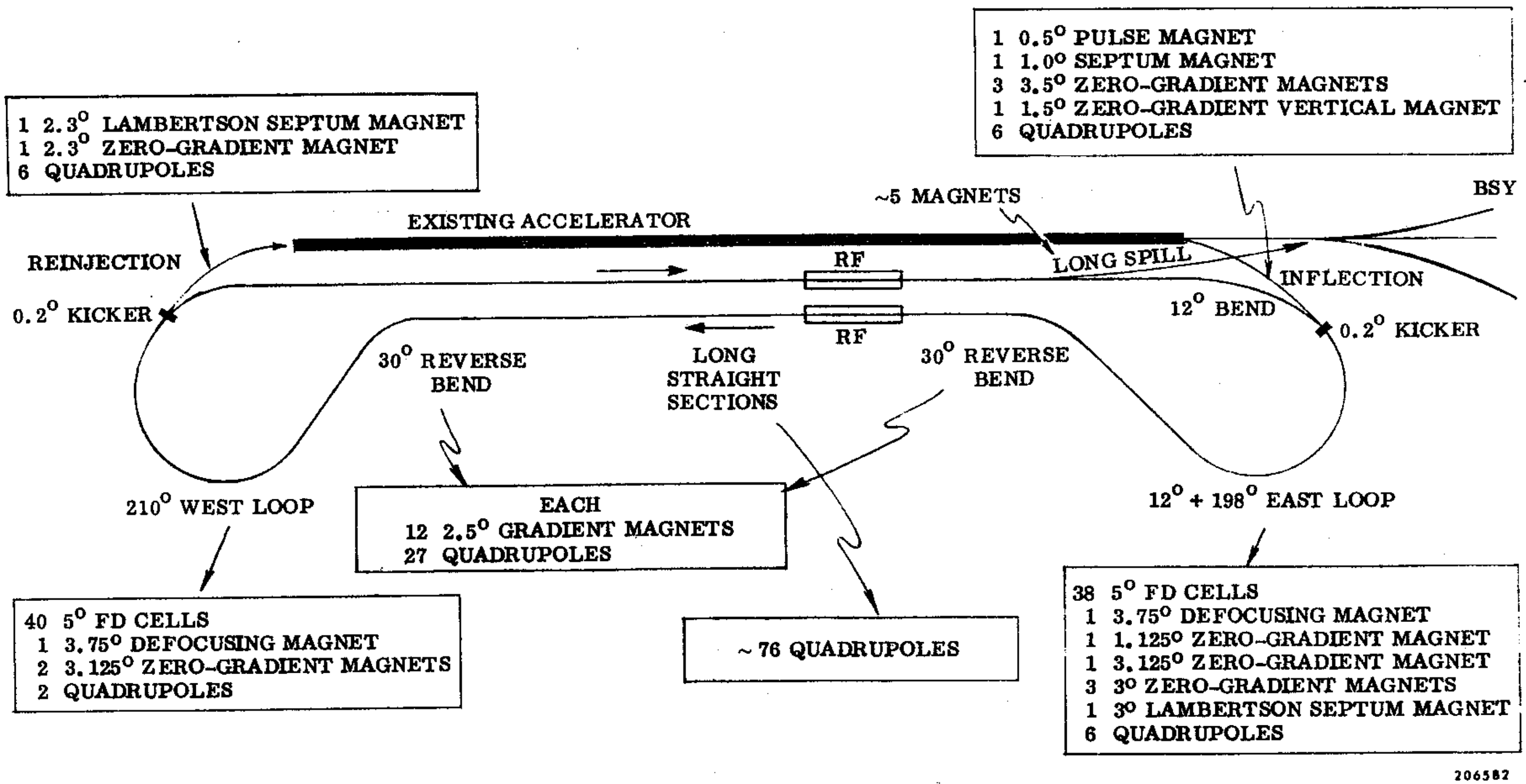

FIG. 5--Component parts of the RLA lattice.

TABLE 6

Transport Properties of the Complete Recirculator

Betatron Tune*	ν_x	ν_y
Main bends (78 cells)	29	8
Straight sections (15-1/2 cells)	3	3
Accelerator sections	3	3
Reverse bends	7	8
Miscellaneous**	7	4
Total	49	26

Beam Path Length		
East loop (incl. 12° bend and η-match)		406 m
West loop (incl. η-match)		359
East loop straight section		259
West loop straight section		244
Eastbound main tunnel		3080
Westbound main tunnel		2207
Reverse bends		408
Total	L	6963 m

Travel time around loop	t_0	23.21 μsec
Frequency around loop	f	43.08 kHz
Synchrotron harmonic	h	66,312
Momentum compaction	α	$(.5 \pm .5) \times 10^{-5}$
	αL	3.5 ± 3.5 cm

* Rounded to integers; total tunes adjustable over range of approximately $\pm$ 1.

** Contributions from η- and β-matching sections, 12° east-end bend, and loop straight sections.

TABLE 7

Main Bend Cell Parameters

Defocus Magnets:		
Number Required:	41 in west loop 39 in east loop	
Effective Length:	5.19 meters	(17.0 feet)
Bend Angle:	3.75^{o}	(0.0654 radians)
Bend Radius:	79.3 meters	
Guide Field:	8.412 kG at 20 GeV	
Gradient Length: (defined as $-\rho/n=B/(dB/d\rho)$)	-14.6 cm	
*Sextupole Term: (K_2)	$-0.00253\ cm^{-2}$	(~3.7% at 1.0 cm)
Focus Magnets:		
Number Required:	40 in west loop 38 in east loop	
Effective Length:	2.50 meters	(8.20 feet)
Bend Angle:	1.25^{o}	(0.0218 radians)
Bend Radius:	114.7 meters	
Guide Field:	5.82 kG at 20 GeV	
Gradient Length:	3.50 cm	
Sextupole Term: (K_2)	$0.0060\ cm^{-2}$	(2.1% at 1.0 cm)
Cell Parameters:		
Length of Cell:	8.29 meters	(27.19 feet)
Horizontal Phase Advance:	0.37 of 2π	
Vertical Phase Advance:	0.10 of 2π	
Maximum β_x:	16.0 meters	
Minimum β_x:	1.2 meters	
Maximum Dispersion, η_{max}:	0.254 meters	
Minimum Dispersion, η_{min}:	0.114 meters	
Maximum β_y:	24.4 meters	
Minimum β_y:	7.26 meters	

*Fields defined in TRANSPORT, Report No. SLAC-91, as $B = B_0\left(1 + \left(\frac{-n}{\rho}\right)\chi + K_2\chi^2\right)$ where χ is measured from the design orbit.

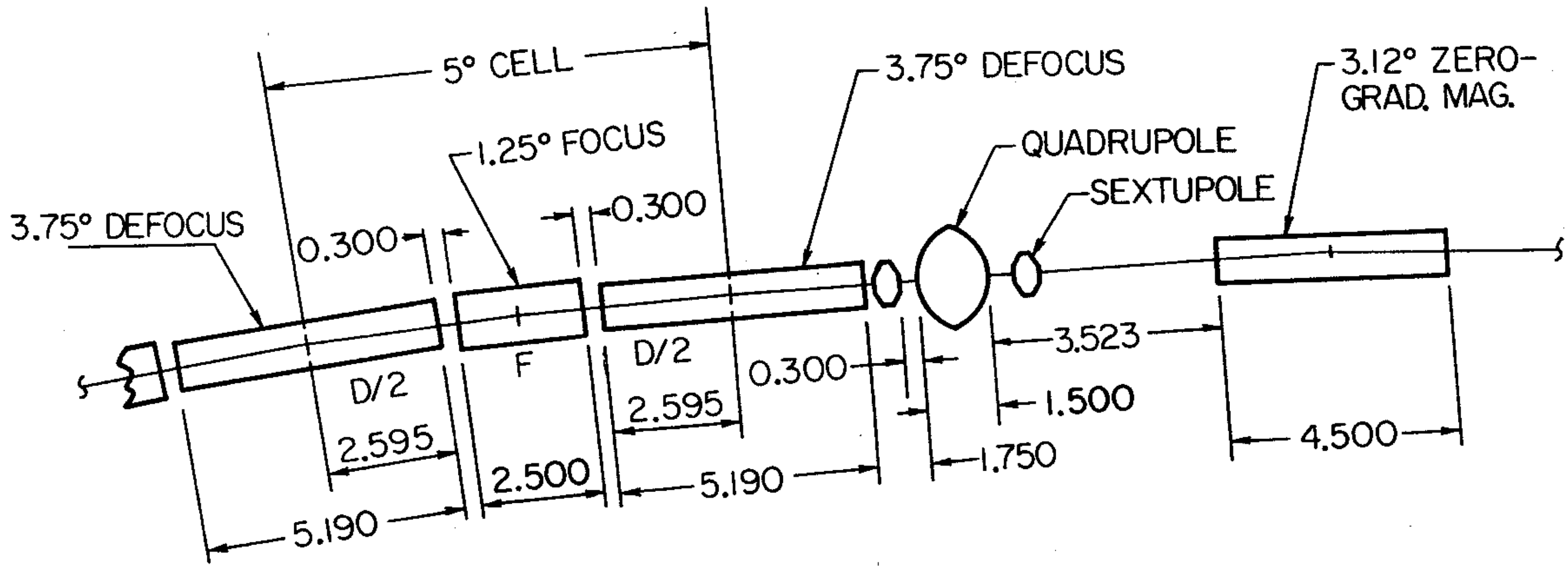

NOTE : Length in meters

2243A1

FIG. 6--Section of the main ring showing the η-matching section and one complete cell.

of the extraction and reinjection systems at the ends of the accelerator.

The choice of cell parameters is restricted by some practical limitations. The cells should be as long as possible to reduce the total number of magnets, but if the cells are too long, the betatron phase advance per cell becomes too great for stability. The individual magnets cannot be too long or mechanical problems will result in increased costs. The long defocusing magnets, which bend 3.75° and are 5.19 meters long, result from these considerations.

The focusing strength may also be limited by practical considerations of magnet design. It is possible that the magnet design study now underway will show that the gradients chosen here are too great. If it is necessary to use slightly less focusing, the resulting increase of the quantum driving term will cause the emittance of the recirculated beam to be somewhat greater. This would result in slightly higher beam losses on the second acceleration or, alternatively, the need for additional focusing at a somewhat lower energy. The effects are continuous and are in no way catastrophic. However, the gradients required for the cell with the characteristics defined in the way described above appear to be within the "state-of-the-art". Theoretical magnet design studies and tests of magnet models have been made to confirm the practicality of these designs.

The main bend magnets have a small second-order correction, i.e., sextupole term to minimize the chromaticity (tune shift as a function of energy). Most other circular accelerators have either added discrete sextupoles (e.g., SPEAR) or built sextupole corrections into their gradient magnets (e.g., Cornell) with the same criterion. In the other areas where the beam is dispersed (reverse bends, 12° bend, η-matching areas) discrete sextupole magnets will be installed to permit chromaticity correction in those areas and to allow for fine adjustment of the overall chromaticity of the recirculator.

In view of the critical importance of damping under certain conditions of operation, it is interesting to view the sextupole correction in a slightly different way: First one imagines that the beam is inserted into the RLA ring 1% low in energy, and that all proper matching and focusing adjustments have been made, including path-length adjustments. Then it follows that in the main bends, the beam will follow the η-function curve and will always be on the inside of the design orbit. Since it is in a higher field part of the defocus magnet (and a lower-field part of the focus magnet), it follows that the beam is more strongly bent in the defocus magnet. The result is more transverse damping and less longitudinal damping. Obviously, the opposite effect can be realized by adjusting the recirculator for lower energies than the linear accelerator is set to supply. This capability of adjusting the damping helps guarantee that adequate flexibility is incorporated in the RLA design. The sextupole correction that was defined above is the correction needed to make the betatron phase shift per cell independent of energy, and is precisely the same as is required to permit this method of adjustment of the damping function.

C. Long Straight Sections

The only parts of the recirculator that are relatively weakly focused are the two long straight sections located in the linear accelerator housing. For the most part, the focusing system in these sections consists of weak quadrupole singlets spaced 101.6 m apart, i.e., one per sector of the linac. The planned aperture of 2.8 cm radius inside the vacuum pipe has an acceptance of about 2.0×10^{-6} π meter-radian in both the horizontal and the vertical motion, which is seven times that of the linear accelerator. This system is modified in the regions of the rf-accelerating sections where the aperture is restricted to about 1 cm radius. In those regions, quad spacings are reduced to about 25 m so the acceptance is about one half that of the normal straight-section cells, but is still sufficient to avoid any significant losses if the recirculating beam is well steered.

D. Reverse Bends

The reverse-bend systems perform the double function of returning the beam to the accelerator housing, thus saving a great deal of tunnel building, and restoring the desired degree of isochronism to the beam. The isochronism provides adjustment for the momentum dilation parameter (α)("momentum compaction" in most literature) which is crucial to determining longitudinal stability and the resulting bunch length. The bending radii used in the reverse bends are nominally twice the radii in the main bends since there is no geographic limitation and the saving in synchrotron radiation more than compensates for some additional magnet costs. The reverse bends as shown in Fig. 7 consist of a total of 30° of bend in six 5° cells each consisting of two 2.5°

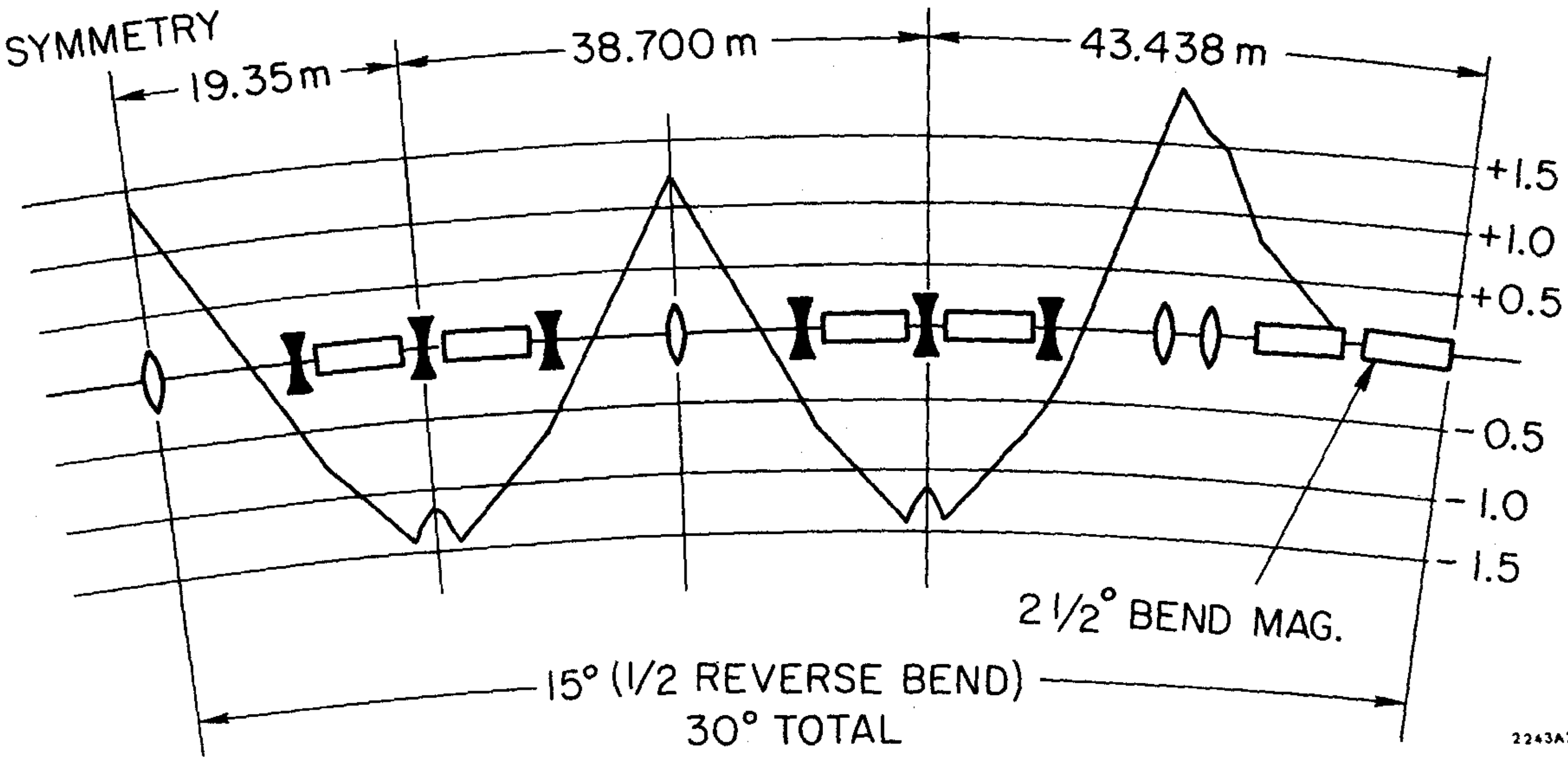

FIG. 7--Reverse-bend schematic showing one-half of the symmetrical system with a superimposed plot of the dispersion function $x(\delta p/p)$ in meters. Gradient magnets are used for all the bend magnets to provide additional horizontal damping.

gradient magnets. The first and last cells provide the dispersion necessary to permit the quadrupoles, Q11 and Q12, to focus the dispersed ray across the central orbit. Thus, the η function becomes negative so that the momentum dilation of the bunch is reduced as the beam goes through the four inner groups of two 2.5° gradient magnets. Where the η-function is negative, all the gradient magnets are set for horizontal focusing, which increases the horizontal damping. This reduces the amount of damping required from the main bends, thus easing magnet design problems in the main bend cells. In the main bends, the horizontal focusing magnets detract from the damping, which is why the cells are designed to have less bending in the horizontal focusing magnets and more in the defocusing magnets.

Table 8 lists the principal parameters of the magnets for the reverse bend systems.

TABLE 8

Reverse Bend Parameters

Number of Systems:	2	
Total Bend Angle:	30°	
Gradient Magnets		
Number Required:	12 each system	
Effective Length:	7.5 meters	(25 feet)
Bend Angle	2.5°	(.043 radians)
Guide Field:	3.88 kG at 20 GeV	
Bend Radius:	172 meters	
Gradient Length:	26.4 cm	
Quadrupoles		
Number Required:	19 each system	
Strength: (defined by $\int(dB/dx)d\ell$)	225 kG maximum at 20 GeV	

E. 12° East Bend and Inflection

The east end of the accelerator housing is also a special region for the RLA. Instead of the single 3.125° magnet used at each of the other three ends of the main bends, at the east end there is first a group of zero-gradient magnets which bend through a total angle of 12° and then a 1.125° magnet. Quadrupoles are interspersed, and a final η-matching quadrupole makes a final adjustment of the dispersion into the main-bend array. Other quadrupole doublets within the 12°-bend group contribute to the β-matching of the beam from the long drift line to the main bend. The low-energy extracted beam from the linear accelerator is inflected into the RLA through a short group of magnets also totaling 12° in bend angle. The two beam lines come together, as shown in Fig. 8, through a 3° Lambertson septum magnet which is the last 3° of the 12° bend. The inflection beam passes through the low-field region of the septum at an angle of 0.2° inclination to the recirculator plane. After both beams have passed through the 1.125° magnet, the inflection beam is deflected vertically by 0.2° by the pulsed kicker magnet so that it is aligned in the RLA plane. (The Lambertson septum magnet is so called because of its similarity to magnets called by that name at NAL and used in the extraction system there.)

There are several special problems associated with the design of the two intersecting 12° bends. Both beam lines must be matched into the recirculator through the common 1.125° bend and the following quadrupole. The inflection beam line from the end of the accelerator must initially separate the high-energy (45 GeV) beam from the low-energy beam which is to be inserted into the RLA. It must then make the 12° bend while still inside the accelerator housing in order to get through the wall before hitting an extra thick area of wall in the beam switchyard. The difference in path length between the recirculator path and the reinjection-inflection path must be an integral multiple of the rf wavelengths in length. For 360 pps operation, the reinjected beam must be in phase with the rf wave that is accelerating the new low-energy beam in the linac. Thus the path through the linear accelerator must also be an integral number of rf wavelengths long. The difference in the two paths, which includes the small contribution from the west end (a few centimeters), is designed to be 21 cm (or 2 wavelengths). A convenient means of adjusting the difference, if this should be needed, is by moving a pair of adjacent bending magnets toward or

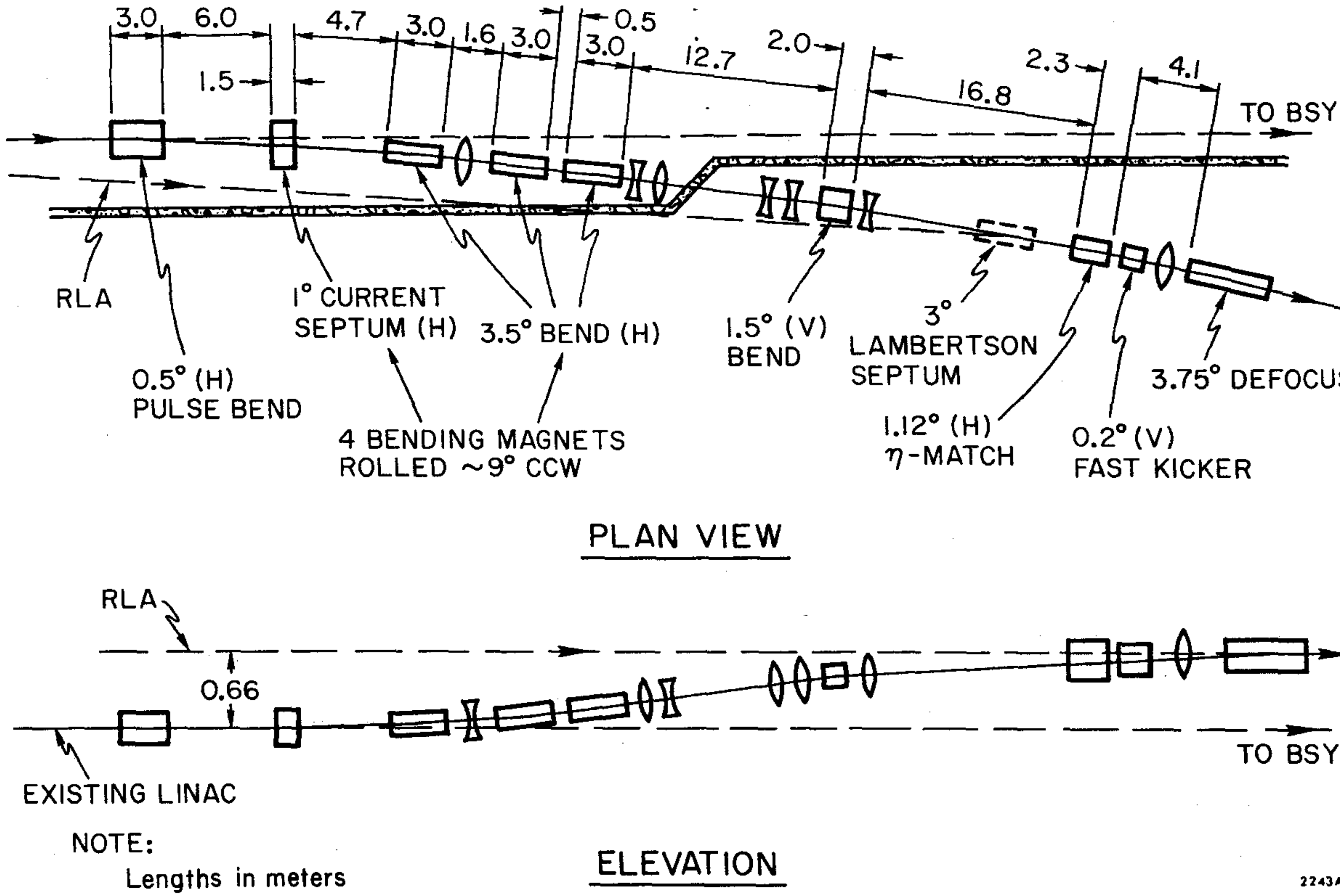

FIG. 8--Inflection system used to fill the recirculator from the two-mile accelerator.

away from each other so as to leave the common vertex unaffected. This is not a very sensitive adjustment, i.e., very small changes in path length result from rather gross changes in magnet position. Thus the alignment tolerances are not affected.

F. Reinjection (West End)

The reinjection system is shown schematically in Fig. 9. At the end of the 2.8 msec storage period, the fast pulsed kicker magnet deflects the beam horizontally by 0.2° to the strong-field side of a Lambertson septum magnet rotated through 90° so that it bends vertically. In it the beam is deflected by approximately 2.3° down toward the linac injector through another bending magnet which realigns the beam with the accelerator axis. Focusing to match the beam to the accelerator transport system is provided by quadrupole lenses. There is a small residual vertical dispersion in the resulting beam because there is not enough room to make a completely achromatic system.

Both the high-energy beam and the newly injected beam must be transported through the accelerator simultaneously. However, if the linear accelerator is operating at a peak energy gain of 25 GeV, and if the RLA is recirculating a 20 GeV beam, then 360 pps operation is possible only if the new linac beam is injected at or near sector six. This permits increased focusing in the first six sectors and delays the critical β-matching until the reinserted beam has gained another 5 GeV.

G. Zero-gradient Bending Magnets and Quadrupoles

The detailed specifications for the zero-gradient magnets will not be made until after an attempt has been made to reduce the number of different types of magnets. For example, the 3.125° η-matching magnets (3 required) and the 3.0° magnets in the 12° bend will probably be the same design. There will have to be some special magnets such as the two Lambertson septum magnets and the short, high field 3° magnets on the insertion line.

A similar attempt will be made to reduce the number of types of quadrupoles. The studies made so far show the need for at least two specific types of quadrupole lenses. One is the weak lens used for focusing in the long drift lines. A prototype quadrupole that is of an inexpensive and novel design has been tested and judged suitable for this purpose, and other even less expensive designs are being considered. In special cases where an

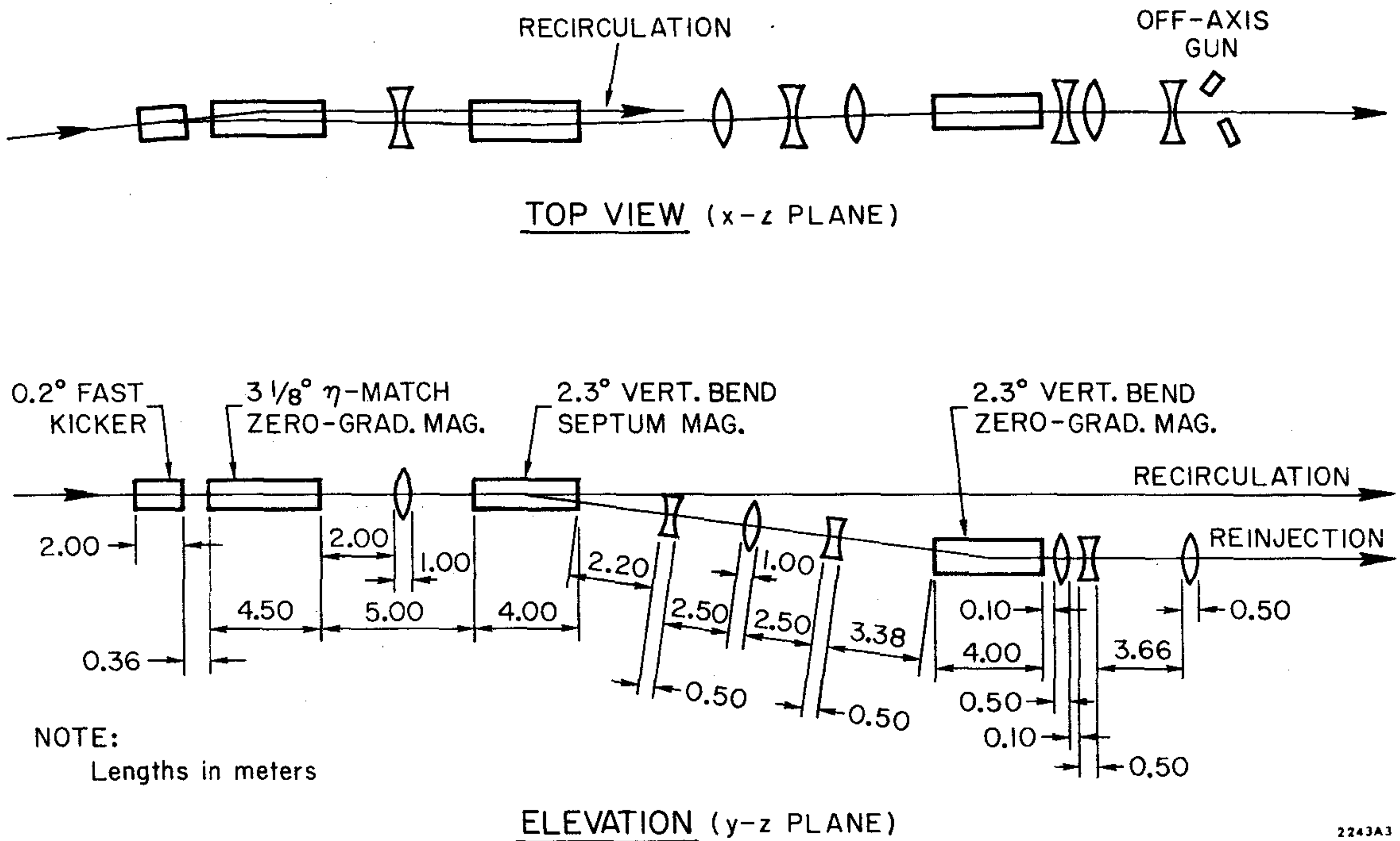

FIG. 9--The system used to reinject the beam from the recirculator back into the two-mile accelerator.

effective strength of about twice the normal strength of these long focal length quadrupoles is needed, it may well prove to be less expensive to install a tandem pair in series than to produce a small number of another design. The second type of quadrupole that will be needed in some quantity is one which is often required in quadrupole doublets. These are quadrupoles of moderate strength that could be constructed with about one meter effective length.

The entries in Table 9 of miscellaneous zero-gradient bending magnets and quadrupoles are for the maximum values for each type. The economics of providing a smaller or greater number of types will be studied later.

H. Independent Magnet Controls

The number of power supplies and independent set points required for RLA depends in part on the geographic layout and, in part, on the variety of functions that need to be controlled. In Table 10 the following assumptions have been made:

1. All supplies and controls for the east main bend are carried separately from their counterparts in the west main bend. If control setpoints were to be combined between east and west, the number of controls could be reduced by about four.

2. The two reverse bends are counted as one system; all individual controls operate in both areas.

3. The eastbound and westbound linear accelerator sections are identical and are combined as one system. The focus and defocus quadrupoles in the accelerator sections are on separate controls to permit tune adjustment of the entire RLA.

4. All long-drift-line quads (focus and defocus, east and west) are in series.

5. All ten quadrupoles in the 12-degree bend area of the each loop are on separate controls. Since these control at most six beam-optics functions, it may be possible to reduce this count by four after further study.

6. Each oblique drift line contains seven independent quadrupoles to satisfy four beam-dynamics functions. It may be possible to reduce the number of controls by three in each line after further study.

7. The septum magnets at each end are on separate power supplies.

8. Magnets of three different designs in each main bend are assumed

TABLE 9

Zero Gradient Magnets and Quadrupole Lenses

Zero Gradient Magnets

1) Description: 3° low field

Strength: (given as $\int B d\ell$) 36 kG-meters maximum at 20 GeV

Number Required: 7
(three in η-match, three in 12° bend, one in reinjection)

2) Description: 3° Lambertson Septum

Strength: 36 kG-meters at 20 GeV

Number Required: 2
(one in reinjection, one in 12° bend)

3) Description: 3° high field (short magnets)

Strength: 36 kG-meters at 20 GeV

Number Required: 9
(three insertion, one in east η-match, three in extraction, two in long spill line)

4) Description: 0.2° fast Kicker

Strength: 2 kG-meters maximum at 20 GeV

Number Required: 2
(one in insertion, one in reinjection)

5) Description: 1° current sheet septum

Strength: 9 kG-meters maximum at 20 GeV

Number Required: one in insertion

6) Description: 2° C-magnet

Strength: 18 kG-meters at 20 GeV

Number Required: one in insertion

Quadrupole Lenses

1) Description: small, weak focusing

Aperture: 6 cm

Strength: 10 kG maximum at 20 GeV

Number Required: ~ 100

2) Description: strong focusing

Aperture: 6 cm

Strength: 200 kG maximum at 20 GeV

Number Required: ~ 74 including reverse bends

TABLE 10

Independent Magnet Controls

Item	No. of Controls	Area	Type	Description
1	1	West bend	Main bend	40 focus, 41 defocus, 2 zero-grad series
2	2	West match	Sextupoles	2 sextupoles each end of bend
3	1	West match	Quadrupole	2 η-match quads
4	4	West match	Quadrupoles	4 singlets, match loop to straight section
5	2	Reinjection	Bends	2 bend magnets
6	4	Reinjection	Quadrupoles	4 quads - match to linear accelerator
7	1	Long straight	Quadrupoles	All small quads, both lines
8	4	Accelerator	Quadrupoles	4 quads -match into accel. structure both ways
9	4	Accelerator	Quadrupoles	4 quads - match out of accel. structure both ways
10	2	Accelerator	Quadrupoles	6 focus and 4 defocus - separate control
11	8	East 12^o	Quadrupoles	10 quad singlets
12	2	East 12^o	Bend	4 3^o zero-grad magnets
13	2	East 12^o	Sextupole	2 sextupoles in 12^o bend
14	5	Inflection	Bends	5 kinds of bend magnets
15	4	Inflection	Quadrupoles	4 singlets
16	1	East bend	Main Bend	38 focus, 39 defocus, 2 zero-grad series
17	2	East bend	Quadrupoles	2 η-match quads
18	2	East bend	Sextupoles	2 sextupoles on south end of east loop
19	7	East oblique	Quadrupoles	7 singlets
20	1	Reverse bends	Bends	12 magnets in each bend - all in series
21	6	Reverse bends	Quadrupoles	6 sets of 2 to 4 quads - both bends
22	4	West straight	Quadrupoles	4 singlets, match E.R.B. to straight section
23	4	West straight	Quadrupoles	4 singlets, match straight section to W.R.B.
24	7	West oblique	Quadrupoles	7 singlets
TOTAL	80			

to be in series; that is, focus, defocus, and zero-gradient magnets must be designed to operate in series.

I. Aperture, Steering and Tolerances

In establishing apertures for the RLA, a somewhat different approach has been used from that customarily used for synchrotrons and storage rings. The magnet system is not pulsed; it is static at the operating energy and driven by well-regulated dc power supplies. Furthermore, unlike the case of an accumulating electron storage ring, injected electrons are placed directly on or near the axis so that no extra aperture is needed for intentional betatron and synchrotron oscillations associated with the accumulation process.

For RLA, the apertures in different parts of the recirculator were established with reference primarily to maximum beam size, magnet economics, construction problems, vacuum-pumping problems and the like, but with less concern for magnet fabrication and position tolerances. Horizontal and vertical beam steering will be provided at intervals and locations around the recirculator based on reasonable assumptions about these tolerances and, with the aid of the beam-position monitoring system, which will be indexed directly to the magnets, the beam will be steered through the structure and made to close upon itself to establish a satisfactory equilibrium orbit. This procedure requires that the extent in phase space of the input beam be small compared to all apertures, that the definition in phase space of the input beam be established with high precision relative to the acceptance of the ideal (unperturbed) machine, and that the resolution of the beam-position monitors be similarly high. It is believed that these conditions can be met without exorbitant effort or cost.

Normal seismic disturbances will not require resteering. Support structures will be designed to keep the frequency at which resteering will be necessary within reasonable bounds. Tolerable pulse-to-pulse "jitter" of the incoming beam will be studied.

The total storage period of 120 turns is unusually short in terms of the build-up of betatron amplitudes attributable to higher order nonlinearities in the guide field. It may be possible therefore to build magnets with higher multipole content than would be allowable for storage rings. This possibility will be studied by computer simulation.

IV. MAGNET SYSTEM

A. General

The RLA magnet development work has been primarily directed towards solving those engineering problems which are independent of the exact magnetic field design. The main bend magnets will be required in the largest quantity, represent a large investment, and require in one case a high gradient and in the other a long magnet. They are therefore the first ones being investigated.

B. Defocus Magnet

The defocus magnet appears to present the most difficult fabrication problems. It will be approximately 5 meters long and requires a fairly large field gradient. Because of the length and the field gradient, this magnet will be curved to the 79.3-meter bend radius. Laminated construction appears to be desirable, because it will allow stacking on a curve, allows mixing of the steel, and can produce the desired magnet cross section very precisely, especially in a 'C' magnet. The 'C' configuration is preferred because it allows the vacuum chamber to be inserted after the magnet has been completely fabricated and measured.

The lattice parameters indicate a pole shape for the defocus magnet as shown in Fig. 10. The gap is sufficiently large to allow for a 14 mm high-beam operations region and approximately 4-mm-thick vacuum chamber walls. The C configuration with a minimum gap of about 26 mm does not allow a double-pancake coil package to be inserted into the coil slot, so that the coils will have to be inserted one layer at a time.

In order to arrive at a suitable fabrication technique, the following several questions must be answered:

1. How to stack on a radius, maintain a high packing factor and minimize distortions?
2. How to secure the laminations: one to another or to a common fixture?
3. How to support the completed magnet?
4. How to fabricate the magnet coils when the gap will only clear one layer?
5. How to measure the field?

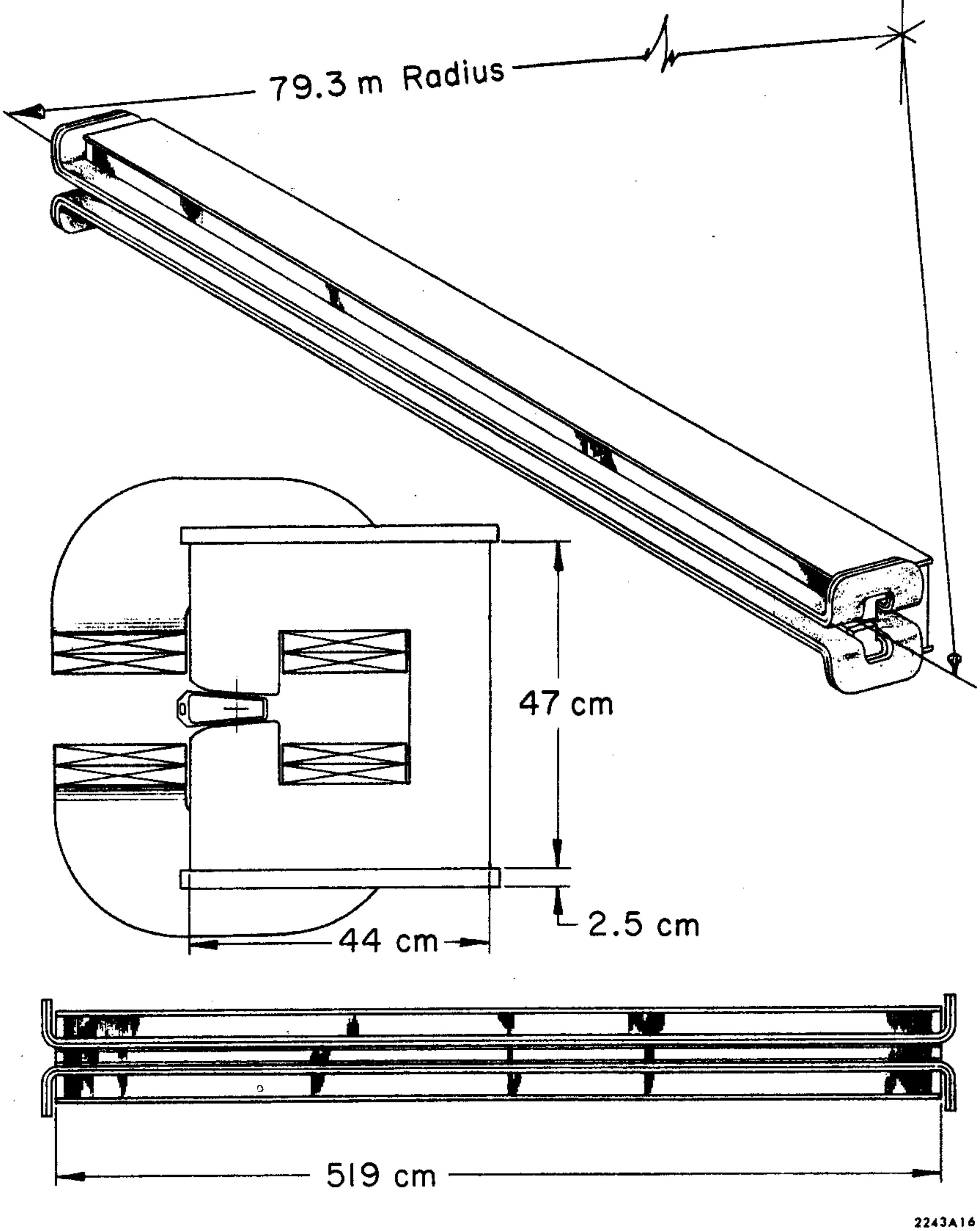

FIG. 10--Defocus magnet assembly.

The model of the defocusing magnets is designed to test the effectiveness of the proposed solutions to the above questions.

C. Focus Magnet

The focus magnet will essentially be a half quadrupole, as shown in Fig. 11. It will also be a laminated magnet. The beam operating region is 10 mm high. The minimum gap will be 24 mm, again requiring the coils to be installed one layer at a time. Some of the basic problems present in the defocus magnet are also present here, although the shorter length simplifies support and alignment. The large gradient will require tighter tolerance on stacking. An additional problem is that the vacuum chamber will be captured by the image plane which is required to terminate the field. The major effort for this magnet has been in the development of pole profiles which give predictable fields over the desired volume.

A study has been made to determine how accurately the fields can be predicted by the use of computer programs. Detailed magnetic measurements have been compared with the calculated fields for two magnets. The first, a laminated half quadrupole, was found to have residual magnetic fields in the image plane which was split on the mid plane. Additional measurements on one-half of a quadrupole confirmed that the image plane must not be split. The sextupole component was found to be a strong function of the image plane position. Agreement between measurement and prediction was good.

The design of the RLA lattice is such that an unusually large fraction of the beam path in the bending loops is occupied by magnets. Figure 12 illustrates the close magnet spacing and shows a beam-position monitor installed in one of the short drift spaces.

D. Other Magnets

Preliminary analysis of several other magnets has begun. Approximate dimensions for a Lambertson-type septum magnet to be used in the reinjection system have been determined. Early analysis of the reverse-bend magnet indicated a cross section like that shown in Fig. 13. This magnet is somewhat longer than the defocus magnet, but is expected to be no more difficult to fabricate. Fabrication techniques developed for the defocusing magnet will also be applicable to the reverse-bend magnet.

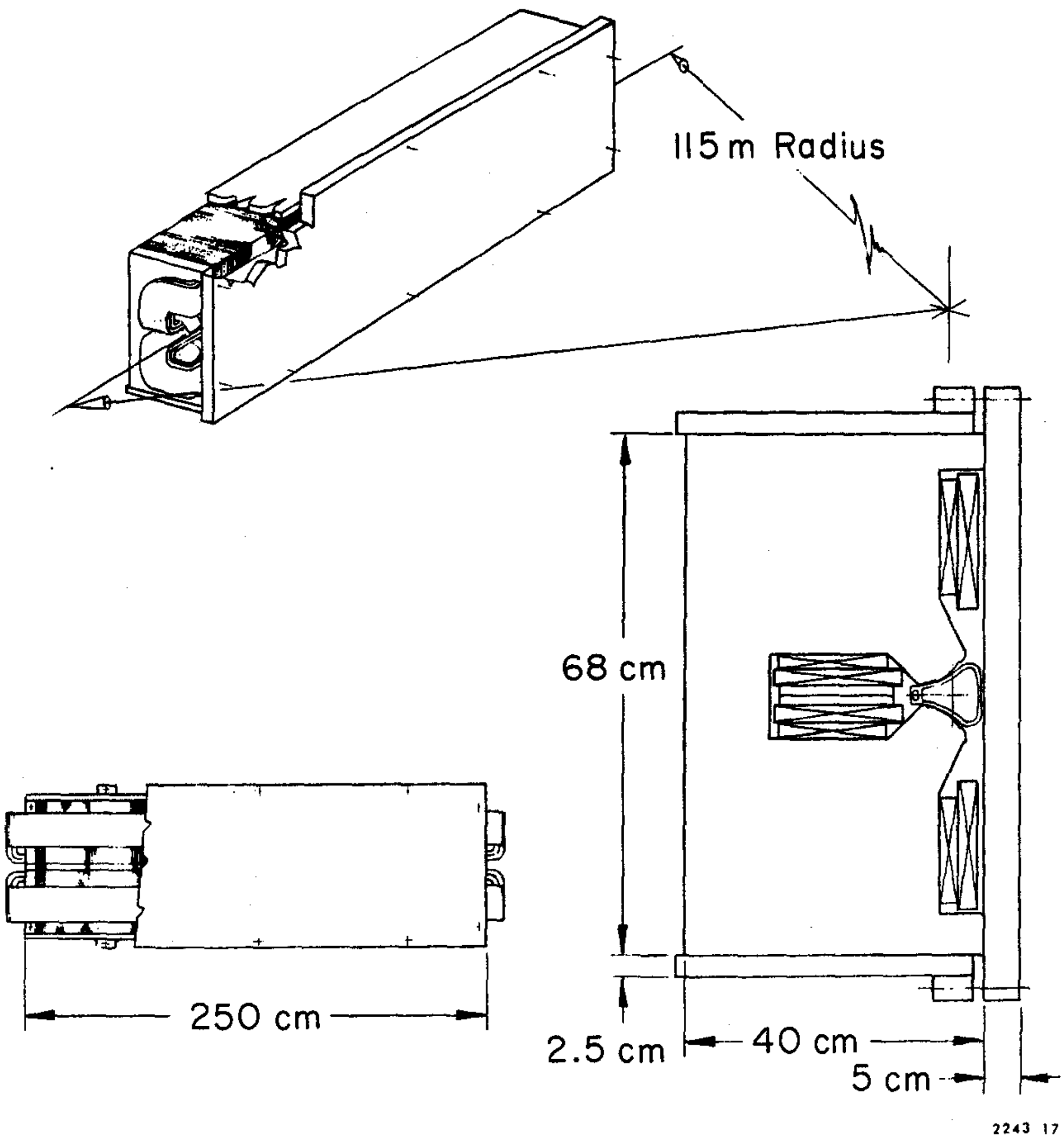

FIG. 11--Focus magnet assembly.

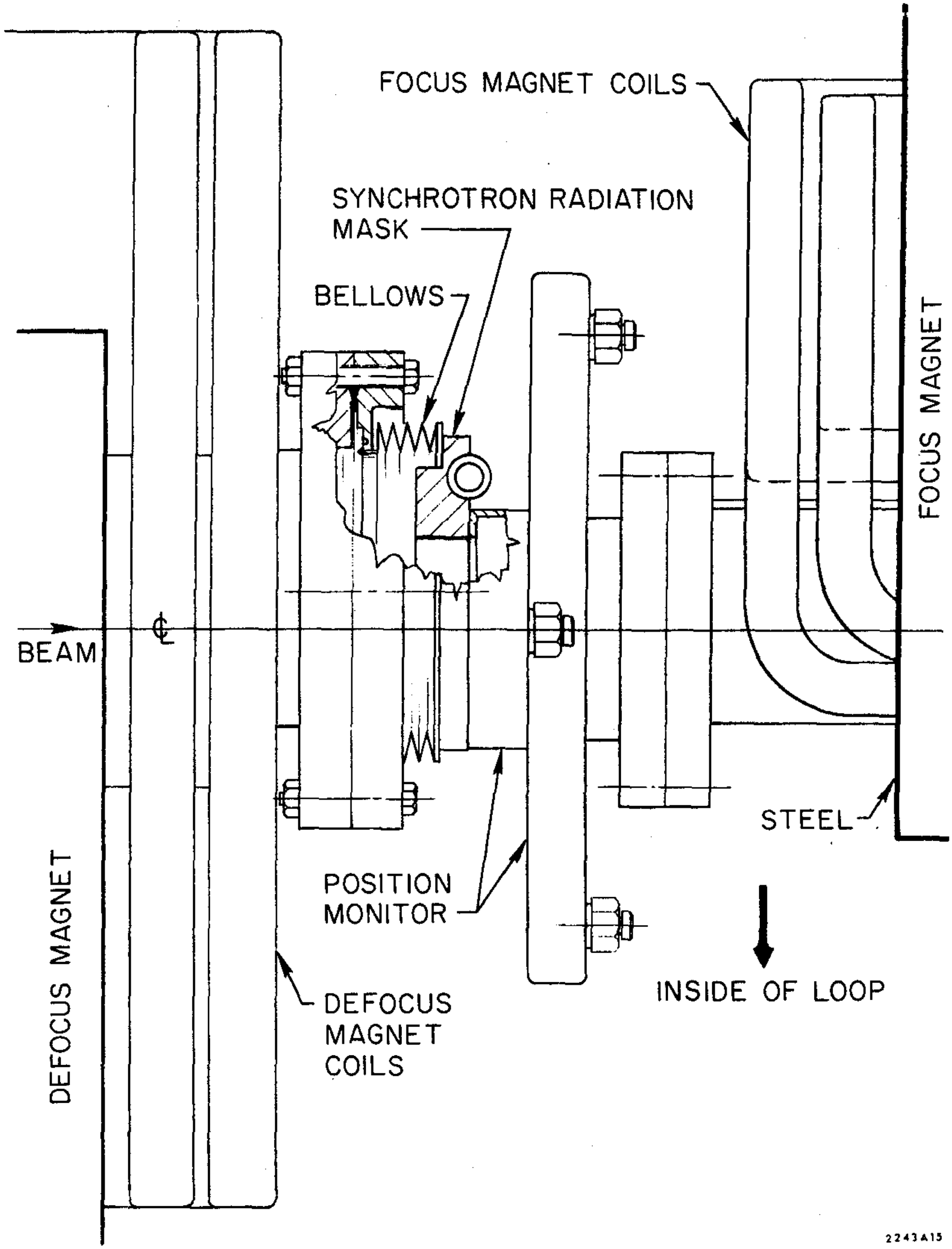

FIG. 12--Plan view of a beam-position monitor installed in one of the bending loops. The distance between the adjacent magnet coils, 20 cm, is typical of the short drift spaces that characterize the RLA lattice.

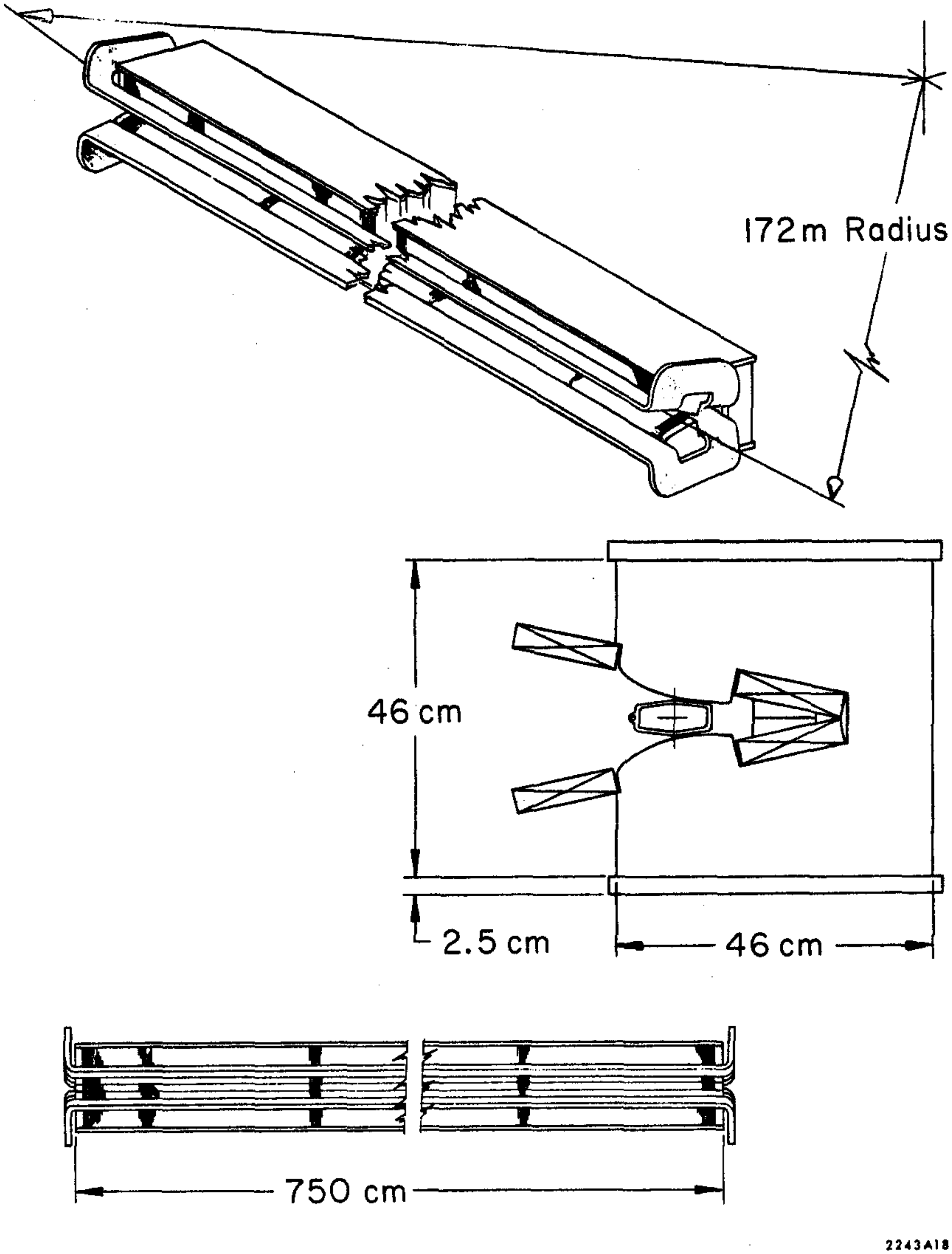

FIG. 13--Reverse bend magnet assembly.

E. Magnetic Measurements

There are two main requirements for the magnetic measurements program to meet: (1) To verify that the design and fabrication process is correct and capable of repeatably producing magnets with the field specifications that are required. (2) To maintain quality control during production.

The first requirement can be met by the detailed analysis of the amplitudes of the various multipole fields. Techniques for measuring and analyzing fields in this way have been in use at SLAC for several years. The equipment, which for the most part already exists, has recently been augmented by the addition of a small control computer which also can do some elementary data reduction. The effectiveness of this system will be verified during the testing period for the model magnets described above.

The second requirement, that of testing each magnet during a production run, will use the same instruments and control computer as are developed for the detail measurements. It is expected that it will be adequate to determine that the multipole amplitudes fall into acceptable ranges for a representative set of levels of magnet excitation. Such tests should require only about four hours per magnet using the computer control system.

The multipoles will be determined from a Fourier analysis of the signal from a rotating coil. The length of the coil determines how much of the magnet length is being "integrated" at each position. Short coils are essentially spot sampling devices. Medium-length coils are most useful in integrating the end effects of a magnet. Full-length coils measure all of the components at one time, but have to be bent very accurately to follow the curve of the bending magnet.

F. Support and Alignment

The recirculating beam elevation is defined to within very narrow limits by clearance requirements in the existing accelerator housing. Because of the proximity of the west loop to the SLAC boundary, it is desirable to place the west loop housing as low as possible and to keep the housing radius as small as possible. Thus the bend magnets will be located in the upper outside corner of the seven-by-eight-foot housing. Placing the magnets high in the housing allows the magnets to be hung from the ceiling, leaving additional floor space open. The additional floor space will be helpful especially during installation when there will be transporting, welding, and vacuum equipment in the housing. For uniformity, the magnets will be hung in the same way in both the west and east loop housings. The proposed cross section of the loop housings is shown in Fig. 14.

Consideration is being given to mounting loop magnets in pairs on a common girder. Pre-aligning the magnets on a girder in the shop could reduce the installation and alignment time required in housing. Laminated magnet construction may require the use of a support structure. A girder could conveniently satisfy this requirement.

Supporting heavy weights from the ceiling is only feasible where a cast-in-place structure with sufficient reinforcing can be built, such as where cut-and-cover construction is planned. Within precast pipe or lined tunnel sections, only light loads, such as the beam pipe, can be supported from the ceiling. Magnets and any other heavy equipment will have to be supported from the floor. Therefore, within the reverse-bend and diagonal tunnels, the method of support will depend on the local housing construction method.

All components which must be precisely aligned will have external fiducials from which the components' position and rotations can be accurately determined. For the laminated magnets these fiducials will be notches located accurately with respect to the poles; the notches will be punched into the laminations at the same time the pole profiles are punched. Every effort will be made to build fiducials into components at fabrication. There will undoubtedly still be some components which will require the installation of fiducials such as tooling balls in the shop.

In order that the west loop housing can be made with the least disturbance to the surroundings, the plane of the loop is tipped down toward the south by 4%. This allows the housing nearly to follow the local terrain. The east loop will also be sloped for uniformity and to minimize horizontal-to-vertical mode coupling. Thus the entire RLA loop lies in a single plane.

Alignment observations will be made with the aid of special tooling which will precisely position alignment targets with respect to fiducials. Either optical or laser alignment tooling will be used to observe the targets. An adjustable bubble level, similar to one used on the present accelerator, will be used to observe roll (rotation about the beam axis).

Alignment tolerances for the RLA have been calculated and are within the normal state of the art for beam transport systems. The calculations include

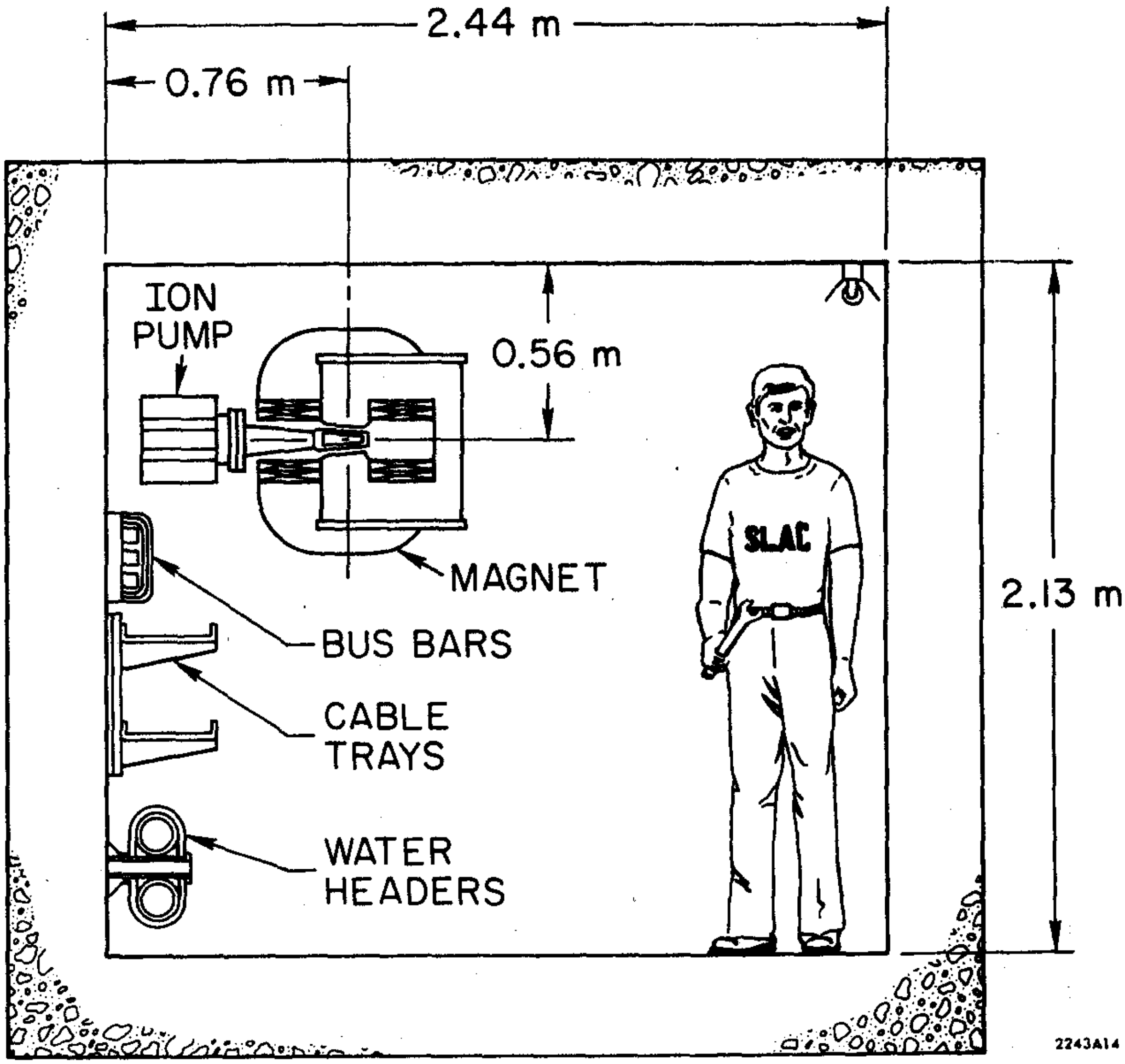

FIG. 14--RLA main loop cross section.

the assumption that local steering will be provided.

G. DC Magnet Power Supplies

The RLA loop will require dc power to about 420 magnets, including the approximately 90 small quadrupole magnets and steering magnets, but excluding the magnets in the SLAC beam switchyard. Total power consumption for the dc magnets will be just under 5 MW, with the 158 east and west loop F and D magnets alone accounting for about 3 MW.

Many combinations of magnets will be operated in series. This is true not only for the F and D magnets in each of the two loops, but also for many of the more than 140 quadrupoles included in the above magnet count. The proposed power systems envision series operation of groups of magnets wherever practical. This will be done even for groups of magnets that operate at slightly dissimilar currents, the plan being to set the power supply for the magnet requiring the largest current and to install remotely controllable bypass current shunts around those magnets that require reduced currents. The RLA magnets are being designed for relatively low voltage drop across each magnet, so a transistorized current-bypass shunt of relatively modest size can be used, provided the power supply size is appropriate and the magnets which are to be operated in series are selected carefully. The practical limitations on just how far this scheme of operating magnets in series should be carried are determined by the distances between magnets and by the amount of current to be bypassed. If the distances are ignored as in Table 10, the RLA could be built using a minimum of 80 separately controlled magnet current systems. The actual scheme proposed here has been chosen as a reasonable compromise from the point of view of power-supply size and type, and distance between magnets. This scheme will require about 110 separate magnet current-control circuits, energized by approximately 54 power supplies in combination with 56 current bypass shunts. This count does not include the 50 small steering magnets and the 40 small quadrupole magnet circuits along the straight sections.

Three separate groups of dc magnet power supplies were considered in arriving at the requirements for RLA, as follows:

1. Power Supplies for the F and D Magnets

The present magnet designs call for a current of 1705 A in the D magnets and 1537 A in the F magnets. (A redesign so that all magnets would operate at the same current would not appreciably change the power supply cost provided the required regulation accuracy and the total power did not change.) Four separate large power supplies will be used for four magnet groups, two in the east loop and two in the west loop. A single large power supply will energize all the magnets of the same type in each loop.

The proposed system will use four similar power supplies rated at 800 kW each (1750 A at 450 V dc), and supplied by a 4160-volt ac primary. A common circuit breaker will be used to energize the two supplies in each loop. The power supplies will use SCR's as the controlling elements in water-cooled rectifier-bridge assemblies. In many of their details these power supplies will be similar to other large power supplies now in use at SLAC. Each power supply will be current-regulated and individually adjustable with a remote-controlled digital-to-analog converter. The power supplies will be housed in two buildings, one near the end of each of the two main bends. Water-cooled aluminum bus bars will be used to connect magnets of the same circuit in series, and a magnet and personnel protection system will be included.

2. Medium-Size Power Supplies

The word "medium" is used here to denote all the dc magnet power supplies larger than 1 kW, except for the four 800-kW power supplies referred to above. Included are all the power supplies needed to energize the reverse-bend magnets, the inflection and reinjection bend magnets, and all quadrupole magnets in the loops. This amounts to 173 magnets energized from approximately 50 different power supplies, ranging in power from 10 kW to 350 kW each. Although the total power required by these medium-size power supplies is only about 2 MW, they represent about 2/3 of the total cost for dc power supplies, because of the large number of relatively small units that need to be individually controlled and because only limited standardization is possible.

The number and types of medium-size power supplies are shown in the following list. These are all power supplies that will be energized from the 480-volt primary power source and will be water-cooled except perhaps for the 10 kW units.

Type of Power Supply	Use	Quantity
350 kW, 200 V, 1750 A dc	Reverse bends	2
50 kW, 70 V, 700 A dc	Quadrupoles	23
10 kW, 33 V, 300 A dc	Quadrupoles	19
Misc. supplies, about 50 kW each	Inflection & Reinjection bends	6
	TOTAL	50

The reverse-bend magnets in each loop, east and west, will all be connected in series, and will require one separately controlled 350 kW power supply for each loop.

The 114 quadrupole magnets require currents that vary between about 90 and 690 amperes. It is desirable to try and limit the number of different types of power supplies in the interest of standardization. An adequate choice seems to be the two sizes indicated for quadrupoles in the above list, where the 50 kW power supplies are intended for quadrupoles that require 300 to 700 amp, and the 10 kW power supplies are intended for quadrupoles that require less than 300 amp. The voltage chosen is such that a fairly simple magnet and personnel safety system can be used. The power supplies will be located either in the SLAC klystron gallery as close as possible to the magnets to which they are connected, or else in the power supply building which also houses the main loop F and D power supplies. Interconnection between these magnets and their power supplies will be done using air-cooled cable.

Typically, each power supply will energize between three and four series-connected magnets. Wherever practical only quadrupole magnets that have to run at the same current will be connected in series. For about 56 of the magnet circuits it will be necessary to use controllable current-bypass shunts. Choice of which magnets to connect in series determines the amount of current that needs to be bypassed. It is typically only about 20 A, although the extreme value is about 110 A. The quadrupole magnets are low voltage, so that a transistor-controlled current bypass shunt is a convenient and desirable choice. It has been assumed that about 60 similar current bypass shunts would be built and installed, each rated at 1000 watt, 20 volt, 50 amp. These will all be current-regulated and individually adjustable with remotely controlled digital-to-analog converters.

There are about 6 to 10 bending magnets which have not yet been designed but for which it is estimated that conventional 0.1% current-controlled power supplies rated at about 50 kW each would be required.

3. Small Power Supplies

Along the straight section of RLA there will be two quadrupoles in every sector, one for each beam direction. In addition, there will be approximately 50 steering magnets distributed around RLA. These are relatively small magnets, requiring typically not more than 100 watts each. The quadrupole magnets are all designed to run at the same current, about 19 A. From the point of view of cost there seems to be a fairly even tradeoff between the alternative of using 50 small (200 watt) individually controlled quadrupole power supplies located near the corresponding magnets, or one or two larger power supplies feeding many magnets that are series-connected over the 2-mile accelerator length. The tentative decision is to use the small individual supplies, one per magnet, and each separately controlled. When the final design is made, a single large power supply or a few large units may yet be found to be a preferable alternative.

Although the steering magnets have not yet been designed, it is expected that the typical requirement will be for power supplies rated about 300 watts, ± 15 volts at 20 A. All steering-magnet power supplies need to have reversible output, and must be continuously controllable down to zero current. It is estimated that about 50 such separately controlled steering supplies will be required.

4. Current Control and Readout

As mentioned above, all power supplies and bypass shunts will be built so that the output voltage of a D/A converter will be used to control a magnet-current setpoint. Exclusive of the straight-section quadrupoles and steering magnets, a total of at least 110 D/A converters will be required, one each located near or at a power supply or bypass shunt.

For magnet-current readout it is proposed to use transductors of a type for which there has been good experience at SLAC. In addition to giving an output signal that is isolated from the magnet circuit, transductors have the advantage that an output signal of a few volts is easily obtained, thus simplifying measuring problems. With the possible exception of the straight-section quadrupoles and the steering magnets, it is proposed that all magnet-current measurements be obtained from transductors. These transductors will be independent of the current-readout devices used in the power supplies themselves, i.e., those devices that are part of the feedback-control system of each power supply. An independent check on the accuracy and stability of the readout values can thus be made easily.

V. VACUUM SYSTEM

A. System Requirements

The entire recirculating structure may be divided into four separate vacuum systems, namely those for (1) the long straight sections enclosed within the accelerator housing, (2) the circular loop sections at each end of the two-mile accelerator, (3) the reverse-bend systems which serve to join the first two sections listed into a closed structure, and (4) the two sectors of rf accelerating structure used to compensate for synchrotron radiation losses.

The requirements on the vacuum system are imposed by the acceptable beam loss due to residual gas and by the vacuum quality needed by the two-mile accelerator which is connected at both ends to the RLA. An arbitrary criterion of 5×10^{-7} Torr for the average pressure has been established for the RLA vacuum system as being consistent with both of the above requirements. This value is also low enough to assure good lifetime for the ion pumps in the RLA vacuum system.

With the exception of the two end regions where the beam passes between the recirculator and the accelerator, the accelerator vacuum system and the RLA vacuum system will be independent. This will help minimize difficulties in diagnostics and maintenance of both systems, minimize present system alterations and down time, and minimize the likelihood as well as a consequences of human operational error.

In the regions of the recirculator where the beam of stored electrons is bent, the vacuum requirements are dominated by the phenomenon of synchrotron-radiation-induced gas desorption. When synchrotron-radiation photons strike the inside of the vacuum chamber wall, photoelectrons are emitted which, upon leaving or re-entering the wall, may desorb gas molecules attached to the surface. It is planned to make the vacuum chamber in the curved parts of RLA of aluminum. An estimate of the rate at which the desorption process will take place at RLA beam energies can be made by extrapolating the measured rates in the SLAC storage ring SPEAR (which has an aluminum chamber and which operates at beam energies up to 2.6 GeV) to higher energy. Analysis of SPEAR measurements is underway but is not yet complete. The chambers and pumping systems described in this section are based on preliminary results of this analysis.

Three practical methods which can be used to pump the recirculator: turbomolecular pump, diffusion pump, and sputter-ion pump systems. The least expensive method is the use of sputter-ion pumps. This is partly becuase there are some ion-pump power supplies presently on hand at SLAC and partly because such pumps may be purchased in very small sizes. Small pump size is a requirement for minimum cost because the small cross section of the chamber limits the length of chamber which each pump can evacuate. Reliability and low maintenance of ion pump systems, as well as comparative immunity to radiation fields, are additional advantages over the other forms of pumping. Lastly, in the event of power failure, ion pumps become passive volumes whereas the other systems would require the additional expense of automatic valves to protect the recirculator vacuum system.

B. Straight Sections

The following conclusions have been reached about the vacuum system for the long straight sections. Assuming a given average pressure requirement and total system length, then

(a) The least expensive configuration in terms of pumping requirements and tubing costs for the straight sections is the one with the smallest diameter.

(b) The minimum diameter of the tubing is determined by beam "stay clear" considerations.

(c) The optimum configuration appears to be one of stainless steel tubing with an inside diameter of about 5.6 cm. Ion pumps with speeds of $\sim$20 liter/sec will be distributed along this tubing at intervals of 100 meters.

A schematic representation of a typical straight, four-sector-long, parallel manifold system is given in Fig. 15. This configuration is followed everywhere except for the locations of the two sectors ($\sim$200 meters) of rf accelerator structure used to compensate for synchrotron radiation losses in the recirculator (see Fig. 16) and at the ends of the accelerator where only one recirculator beam (eastbound) remains in the housing. The in-line vacuum valves shown in the figure are manually operated. Lead or indium seats will be used in these valves to reduce the required sealing forces.

It will be necessary to evacuate the straight drift sections to a pressure of 10^{-4} Torr prior to starting the ion pumps during initial installation

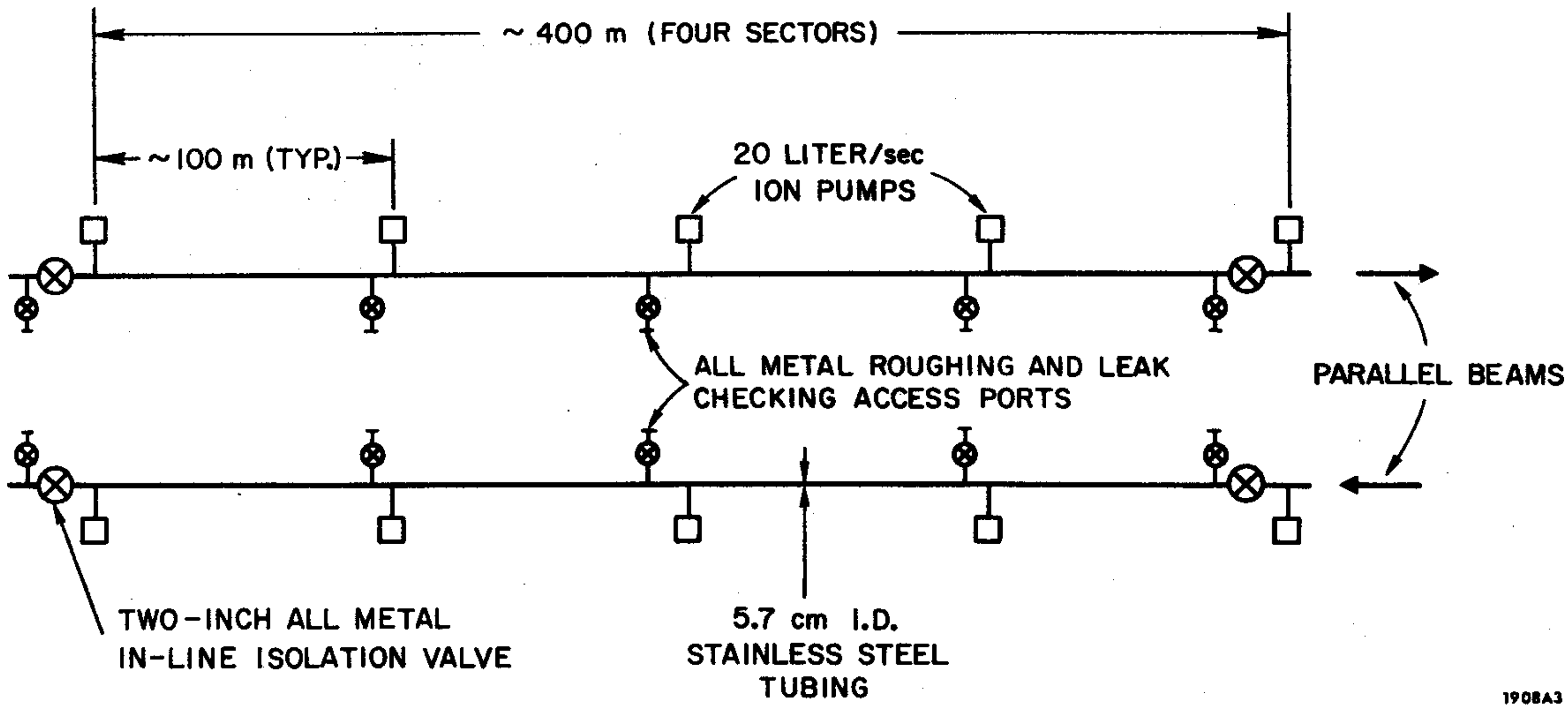

FIG. 15--Schematic representation of a typical section of parallel-beam vacuum system extending through four accelerator sectors.

and when maintenance requires venting portions of the drift pipe to a controlled atmosphere. Provisions must also be made to isolate the straight drift sections into shorter segments which will permit partial system venting for maintenance operations and will allow evacuation, leak checking, and complete preparation of sections of reasonable length during the construction phase. The all-metal valves serve this purpose.

C. Circular Loop Sections

Calculations indicate that synchrotron radiation losses will range up to 550 watts of beam power per meter of the main bend loops at the initial design conditions. As a conservative estimate, it is assumed that all of this power will be dissipated in the wall of the vacuum envelope. Because of better heat dissipation, lower gas desorption, and cost considerations, aluminum is probably the best material to select for such structures. An extruded water-cooled aluminum vacuum envelope of cross section similar to that used in SPEAR is preferred. Approximate shapes of the cross sections of the chamber are given in Figs. 10, 11, and 13 in the previous section. As shown in these figures, different envelope configurations must be used in the different types of bending magnets.

Heat-transfer design of the bending-magnet vacuum envelope will be such as to permit approximately three times the synchrotron radiation power dissipation noted above. Such power densities are possible in the event of an expanded RLA rf system. Calculations show that at the highest expected power dissipation level, the synchrotron radiation must be incident on a water-cooled wall. Where there are discontinuities in the vacuum chamber wall, such as between a defocus and a focus magnet vacuum chamber, masks will be provided.

Ion pumps with speeds of 50 liter/sec will be used to pump the bending-magnet vacuum chambers. Calculations based on preliminary analysis of gas-desorption experiments conducted in SPEAR indicate that one such pump per cell will be adequate to maintain the required average pressure. An extra port will be provided in each cell to permit the number of pumps per cell to be increased to two and thus to handle gas loads greater than presently anticipated in case the extrapolation of SPEAR desorption data from 2.5 GeV to 20 GeV proves wrong.

D. Reverse Bends

An extruded water-cooled aluminum vacuum chamber will also be required wherever bending magnets exist in the reverse bends. For purposes of standardizing hardware, manifolding, and ion pumps, 5. cm I.D. stainless steel tubing will be used wherever bending magnets do not exist in the diagonal sections. One 50 liter/sec ion pump and a spare pumping port will be located on the reverse-bend vacuum chambers in a manner similar to that in the circular loop sections. The short straight sections between magnets will be pumped by 20 liter/sec pumps.

E. RF Vacuum System

High-duty-cycle rf tests simulating RLA conditions were recently conducted on a standard 3-m-long accelerator section and rf load. These tests indicated that a pumping speed of approximately 25 liter/sec will be required to pump each load and section. As applied to RLA, this pumping will be accomplished through the use of a parallel vacuum manifold in the accelerator tunnel similar to that used in the present accelerator. Pumping at both ends of each 3-m accelerator section will be accomplished through the rf waveguide feeding the successive sections and coupled to this parallel vacuum manifold. However, unlike the present system, ion pumps will be located in the accelerator housing. A single 150 liter/sec ion pump will be used with each group of four accelerator sections and associated waveguide.

Small appendage pumps will be located in the klystron gallery to pump the waveguide in the region of each RLA klystron. To assure minimum down time to both RLA and the linear accelerator and to minimize exposure of the vacuum system to possible contamination, rf valves will be used to seal off the waveguide each time a klystron is replaced. System venting and subsequent roughing on replacing klystrons will be accomplished through small roughing valves located near each klystron output waveguide.

VI. RADIO-FREQUENCY ACCELERATING SYSTEM

A. General

A particle circulating in the RLA radiates away a substantial amount of energy as synchrotron radiation loss; a 20 GeV electron, for example, loses 206 MeV on each turn. Because of this radiation, a radio-frequency accelerating system of considerable size and complexity is required. This system must supply an accelerating voltage, not only to make up the radiation loss but also to supply an overvoltage to provide phase focusing so as to contain the spread in energies and phases of the stored particles and maintain sufficient quantum lifetime. In general, in the design of a storage ring, a low radio-frequency is usually chosen because of the lower overvoltage ratio required for adequate quantum lifetime. However, in the case of the RLA, the additional requirement is imposed that the S-Band (2856 MHz) bunch structure of the beam be preserved in order that the beam can be reaccelerated in the two-mile linac, so an S-band accelerating system must be used. The frequency of 2856 MHz corresponds to a harmonic number of 66312. In order to keep the bunch length short enough for reacceleration, the RLA lattice has been designed to make the trajectories of particles with differing energies nearly isochronous. In other words, the momentum compaction coefficient is very small, as was discussed in Section III. This measure results in modest overvoltage demands. For example, at a recirculating energy of 17.5 GeV, the radiation loss per turn is 121 MeV, and a peak rf voltage of 140 MeV per turn gives a more-than-adequate quantum lifetime of 44 seconds.

The use of such a high-frequencysystem has a significant advantage over the use of the lower frequency systems more common in existing synchrotrons in that the filling time of the structure is short compared to the time between passages of the beam pulse. This fact permits the use of a pulsed rf system with an 11% duty cycle. At frequencies below 500 MHz, filling times are of the order of or greater than the time between passages and pulsed operation becomes unattractive.

The accelerating structures chosen for RLA are exactly the same as those used in the two-mile linac. They are powered by high-duty-cycle (11%) klystrons designed and constructed at SLAC especially for this application. Thirty-two 3-meter-long constant-gradient sections are located in the eastbound straight section of RLA and 32 in the westbound straight section. Their locations are indicated in Fig. 4 in Section II of this report. Each sector of accelerating structure is made up of eight "girders". Successive girders are located alternately in the westbound and eastbound beam lines as indicated in Figs. 16 and 21. This arrangement, in which the accelerating structures for the westbound and eastbound beams are interlaced, provides for a 12-meter drift space between each girder to accommodate focusing magnets and beam monitoring equipment. The accelerator sections for the RLA rf system will be supported by brackets attached to the existing accelerator support girders. The capacity of the existing support jacks is adequate to carry the added load even in the case of the westbound accelerator which is 60 cm off center as shown in Fig. 16.

Each girder (4 accelerator sections) is driven by one klystron with a peak power capability of 500 kW and an average power capability of 55 kW. The development of these tubes and their associated modulators will be described later in this section.

A convenient way to characterize the capabilities of the proposed rf system is by means of the "load line" diagram, Fig. 17. This diagram refers to operation at constant input power. The stored current induces a back voltage on the structure which lowers the net available energy gain per turn. Thus the more current that is stored, the lower is the maximum energy at which it can be stored. The highly nonlinear relationship between the two alternative abscissa scales reflects the fact that the synchronous energy gain per turn varies as the fourth power of the recirculating beam energy.

Phase stability occurs in RLA with the electron bunches on the falling side of the rf wave, just as in any synchrotron operating above transition energy. The larger the synchronous phase angle, the stronger the phase focusing becomes, but also the greater is the peak rf voltage that must be supplied. The synchrotron phase oscillations which result from quantum fluctuations in electron energy tend to be smaller in amplitude as the bunches are phased further off crest, resulting in a shorter bunch length at the time of reinjection back into the main accelerator. Equally important, larger synchronous phase angles (off crest) result in longer quantum lifetimes.

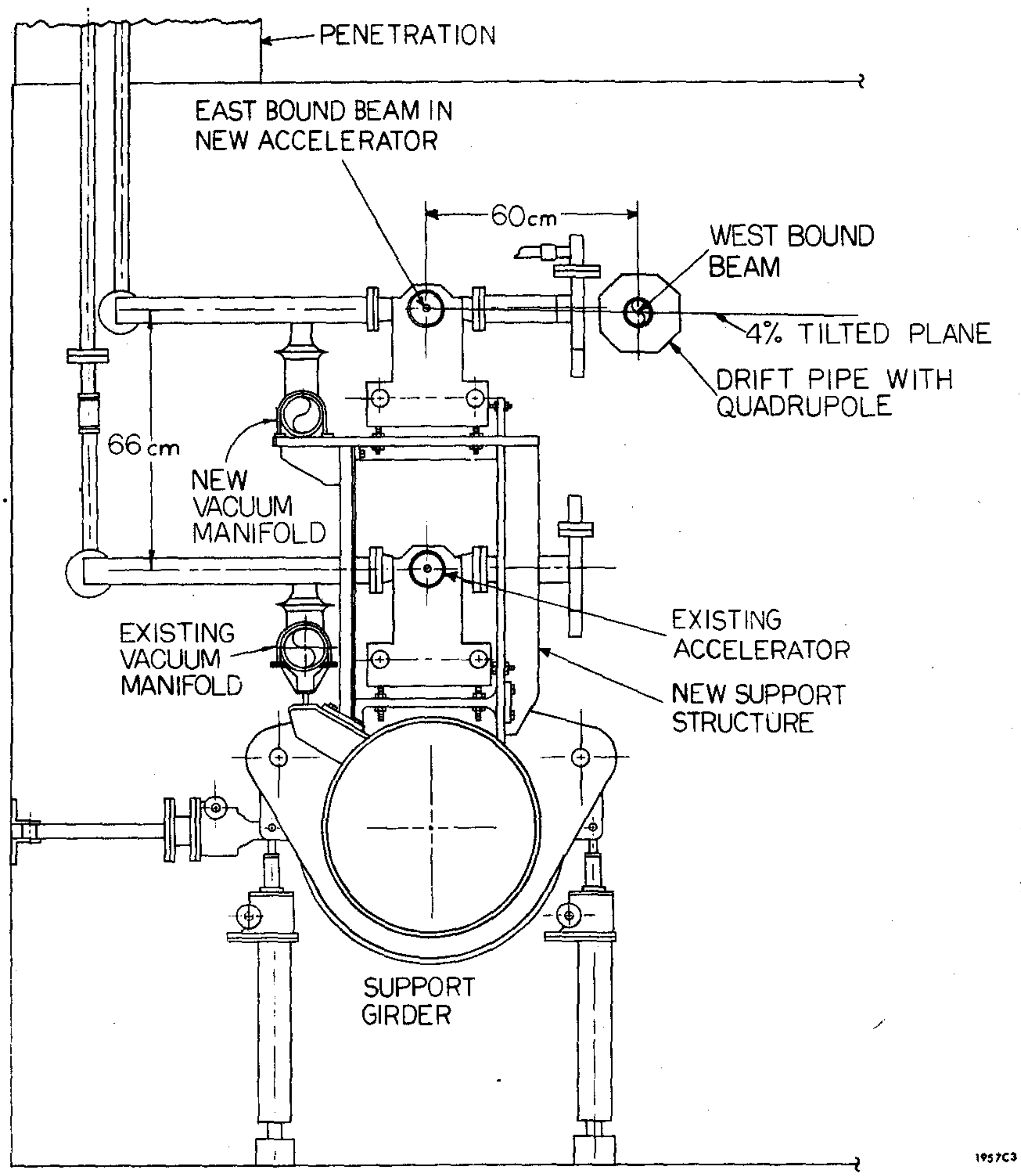

FIG. 16--Cross-sectional view of the accelerator housing showing the existing SLAC accelerator, the new accelerating structure planned for RLA (eastbound beam), and the RLA return-loop beam pipe (westbound beam).

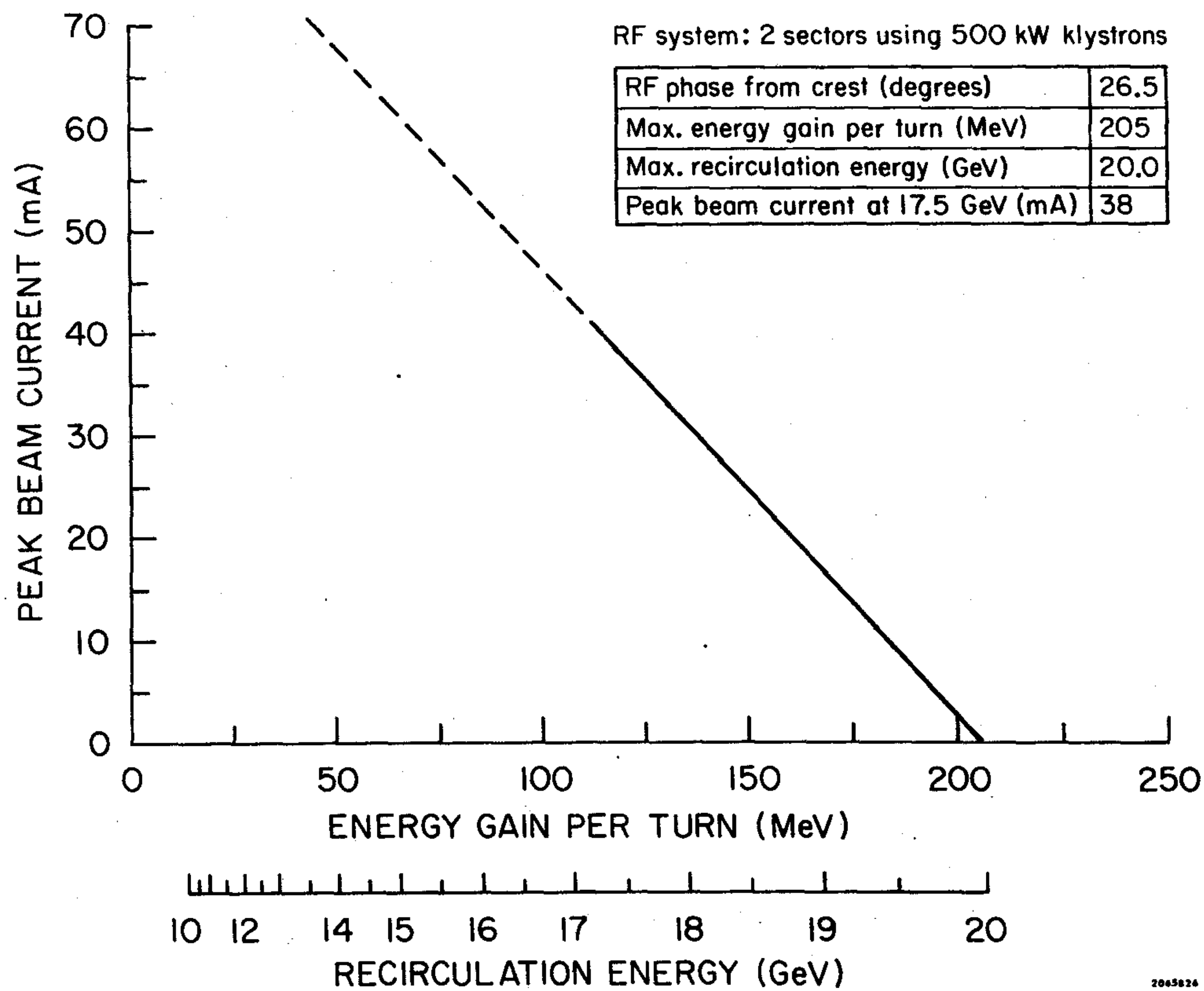

FIG. 17--Load-line diagram for the RLA rf system showing the peak recirculating current as a function of recirculation energy.

The amplitude and frequency of the phase oscillations also depend on the momentum compaction parameter α; a lower value of α results in phase oscillations of a lower frequency and smaller amplitude, and again in a shorter quantum-induced bunch length upon reinjection into the two-mile linac. These relationships are illustrated in Table 11 for beam energies of 17.5 and 20.0 GeV, assuming a magnet lattice design as discussed in Sec. III. In this table, ϕ_s is the synchronous phase angle; the column labeled "rf bucket" gives the maximum half energy spread that can be accepted by RLA; the final column gives the final half-energy spread after reacceleration, taking into account the effect of the bunch length and energy spread at reinjection and on final acceleration. Values for α are taken to be 10^{-4} and 10^{-5}, which probably represents the feasible range of α for RLA. The advantages of operations at a small value of α are clearly seen.

The peak voltage available from the rf system (unloaded) is about 230 MV. At 20 GeV, the figures in Table 11 show that a low current can be recirculated at a synchronous phase angle of 116.5°, with adequate rf bucket size, quantum lifetime, and final energy spread. At 17.5 GeV, a peak rf voltage of 140 MV is needed to recirculate a beam with acceptable values for these same parameters. The difference between this voltage and the total peak available rf voltage (230 - 140 = 90 MV) is, roughly speaking, available to accelerate a beam current having an induced beam loading voltage equal to this same value. For two sectors of SLAC structure, the induced beam loading voltage is 2.37 MV/mA. Thus at 17.5 GeV one can expect to recirculate a peak current on the order of $90 \div 2.37 = 38$ mA. This calculation of beam current assumes a simple model for beam-loading compensation in which some of the klystrons are used to establish a net cavity voltage at a given phase angle with respect to the incoming beam, and the remaining klystrons, phased in opposition to the induced beam voltage, are used to compensate for beam loading. During the transient-beam-loading period, this second group of klystrons can be switched on at the proper rate, as a function of time, to compensate closely for the changing induced beam voltage. This method of beam-loading compensation is illustrated by the vector diagram in Fig. 18a. It may, however, prove more effective to turn all of the klystrons on at once, and to vary the phase angle θ, of the component of the cavity voltage produced by the klystrons in order to

TABLE 11

A. Longitudinal Beam Parameters at 20 GeV. Radiation loss, 205.8 MeV/turn. Initial bunch length and energy spread, $\pm 3^{o}$ and $\pm$ 0.20%, respectively

Peak RF (MV)	ϕ_s (degrees)	Synch. Freq. (per turn)	RF Bucket (%)	Bunch Length (degrees)	Quantum Life (msec)	Final Energy Spread (%)
Momentum compaction, $\alpha = 10^{-4}$; synchrotron damping time, 2.1 msec.						
220	110.7	0.065	0.41	10.4	4.9	0.83
230	116.5	0.074	0.60	9.2	3.6×10^{1}	0.65
240	121.0	0.082	0.77	8.6	5.5×10^{2}	0.56
250	124.6	0.088	0.92	8.0	1.3×10^{4}	0.50
Momentum compaction, $\alpha = 10^{-5}$; synchrotron damping time, 2.9 msec.						
220	110.7	0.020	1.28	3.8	1.6×10^{7}	0.15
230	116.5	0.023	1.89	3.3	4.2×10^{16}	0.13
240	121.0	0.026	2.43	3.1	1.1×10^{28}	0.13
250	124.6	0.027	2.92	2.9	8.1×10^{40}	0.12

B. Longitudinal Beam Parameters at 17.5 GeV. Radiation loss, 120.6 MeV/turn. Initial bunch length and energy spread, $\pm 3^{o}$ and $\pm$ 0.20%, respectively

Peak RF (MV)	ϕ_s (degrees)	Synch. Freq. (per turn)	RF Bucket (%)	Bunch Length (degrees)	Quantum Life (msec)	Final Energy Spread (%)
Momentum compaction, $\alpha = 10^{-4}$; synchrotron damping time, 3.1 msec.						
130	111.9	0.054	0.36	9.8	8.1	0.74
140	120.5	0.066	0.61	8.3	3.2×10^{2}	0.53
150	126.5	0.074	0.82	7.6	5.0×10^{4}	0.44
160	131.1	0.080	1.01	7.1	1.7×10^{7}	0.39
Momentum compaction, $\alpha = 10^{-5}$; synchrotron damping time, 4.3 msec.						
130	111.9	0.017	1.14	3.7	5.2×10^{7}	0.14
140	120.5	0.021	1.94	3.2	2.7×10^{23}	0.12
150	126.5	0.023	2.61	3.0	1.4×10^{43}	0.12
160	131.1	0.025	3.20	2.8	3.5×10^{65}	0.11

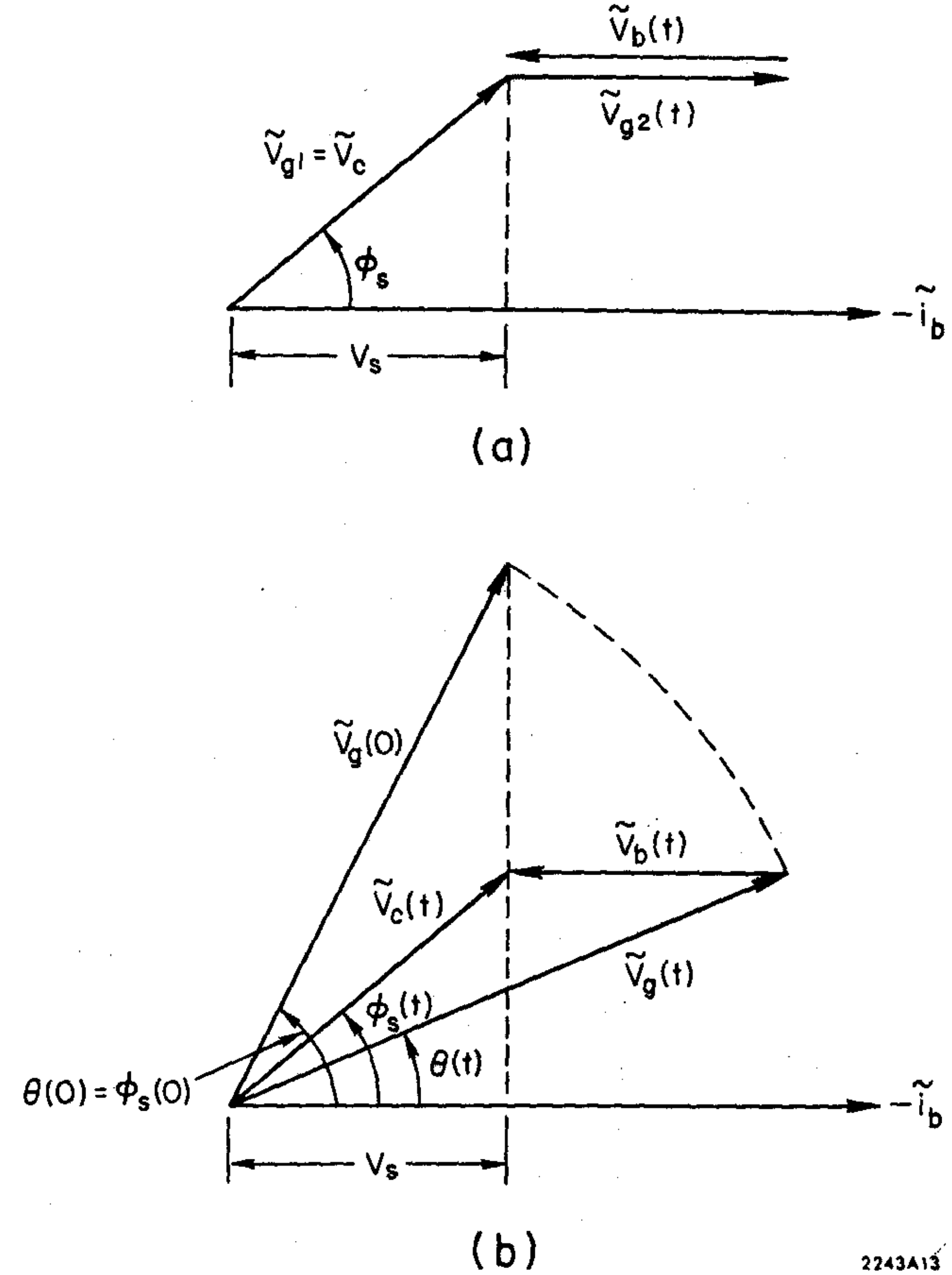

FIG. 18--A comparison of two possible methods for transient beam-loading compensation with RLA. (a) Some of the klystrons are used to produce a time-varying voltage $V_{g2}(t)$ which is approximately equal and opposite to the beam-induced voltage $V_b(t)$. Here $\tilde{V}_c$ is the net cavity voltage, and $eV_s = e|\tilde{V}_c| \cos \theta_s$ is the synchronous energy gain per turn. (b) The phase $\theta(t)$ of the klystron-produced voltage V_g is varied during the beam pulse. Since $|\tilde{V}_g| = |\tilde{V}_{g1}| + |\tilde{V}_{g2}| > |\tilde{V}_{g1} + \tilde{V}_{g2}|$, somewhat more current can be accelerated by this method for a given final synchronous phase angle.

achieve a constant synchronous energy gain during the transient loading period. This method of beam-loading compensation is illustrated in Fig. 18b. In this way about 10% more beam current can be accelerated than by the previous method. In order to produce the proper time variation in the phase of the accelerating wave, the phase of the input drive to the klystrons must be properly programmed as a function of time. Detailed calculations are in progress to exploit this method of transient beam-loading compensation.

B. 220 kW Klystron Development

In 1971 an effort was initiated at SLAC to develop a very high repetition rate klystron suitable for use on the RLA rf system. At that time, the tentative design of RLA called for an rf system using 16 klystrons, each supplying a peak power of 220 kW and an average power of 24 kW. It appeared that the design goals for a klystron suitable for RLA as then proposed could be achieved by modifying the existing SLAC sub-booster klystron. Computer calculations indicated that the efficiency of this tube could be increased substantially by increasing the drift length between the second and third cavities. The gain requirement for RLA use would be met by adding an additional cavity. Because of the high repetition rate and duty cycle, it was not expected that an oxide cathode could provide the desired long life and reliability. Work was therefore started to replace the oxide cathode with a dispenser cathode.

A series of three tubes was designed and tested, the last of which operated successfully at a peak output power of 237 kW with an efficiency of 53%. In the meantime, however, design changes in RLA made it appear desirable to redirect the klystron development effort toward a tube capable of 500 kW peak power, which is described in the next section.

C. 500 kW Klystron

The basic design parameters for this tube are listed in Table 12. Other important klystron requirements and characteristics relevant to RLA design, such as the maximum allowable load pressure (10^{-7} Torr) and the phase change ($13^{\circ}/\%$) as a function of beam voltage, are given in technical specifications PS-701-145-00-RI, SLAC 50055 Klystron, SLAC Klystron Department, December 1972.

During the shakedown of RLA, and at the beginning of each cycle, it may be desirable to operate at a reduced peak power level. For this reason the RLA tube will be designed to operate stably down to a level of 220 kW. Klystron operating parameters for this power output level are given in the referenced specifications.

Table 12

500 kW Klystron Design Parameters

		Objective		Acceptance	
	Units	Max.	Min.	Max.	Min.
Operating frequency	MHz	2856.1	2855.9	2856.1	2855.9
Peak beam voltage	kV	46	--	50	--
Peak beam current	A	20.8	18.8	23.5	21.2
Average beam current	A	2.95	--	3.45	--
Perveance	$A/V^{3/2}$	2.1	1.9	2.1	1.9
Peak input beam power	MW	0.957	0.865	1.175	1.065
Beam voltage pulse length	μsec	3.3	--	3.4	--
Pulse repetition frequency	pps	43,000	--	43,000	--
Average input beam power	kW	136	--	173	--
Duty cycle, beam power	%	14.2	--	14.7	--
RF pulse length	μsec	2.6	2.5	2.6	2.5
Peak drive power	W	5	--	5	--
Peak rf output power	kW	--	500	--	500
Average rf output power	kW	65	55	65	55
Duty cycle, rf	%	13.0	11.0	13.0	11.0
Gain	db	--	50	--	50
Efficiency	%	--	52	--	43

In the desire for long operating life, one major area of concern in the design of this tube is the rf output window. The average output power (up to 65 kW) exceeds by about a factor of two the power capability of the present SLAC klystron window. A window redesign is in progress using beryllia, which has a significantly higher thermal conductivity than the alumina ceramic used at present. Tests of the window design at RLA power levels and repetition rate are planned using a resonant ring driven by an existing 220 kW tube.

D. Modulators

The RLA modulator must supply pulsed power to the 500 kW klystron described in the previous section. The most severe design requirement imposed on the modulator is the high repetition rate of 43,085 pps, which allows only about 23 μsec between successive pulses. The use of fast-recovery high-voltage devices and circuitry is indicated. Silicon-controlled rectifiers and thyratrons can be eliminated because of their slow recovery time. Vacuum tubes are clearly the only reasonable switching devices because they require no recovery time. In the case of vacuum tubes, switching speed is mainly determined by current-carrying capability, distributed and inter-electrode capacitances, and circuit impedances.

A floating-deck type of circuit, as shown in Fig. 19, was chosen because of its inherent high-speed capability and good efficiency. It is more difficult to design such a modulator so that it can be safely serviced, but it is worth the effort to eliminate the requirement for a high frequency pulse transformer. The circuit is shown in Fig. 19. The input ac power to all 16 RLA modulators is supplied by an induction-voltage regulator capable of a voltage range of 3300V - 5000 V about a nominal voltage of 4160 V. The nominal input voltage of 4160 V is stepped up to 34 kV line-to-line by the main high-voltage transformer, and rectified in a 3-phase full-wave bridge. It is filtered by an LC filter consisting of a 20 henry choke and a 0.68 microfarad capacitor. The capacitor also acts as a storage capacitor to supply the 23 amperes (max) peak current to the klystron during the pulse. The main switch tube (V_1) is normally cut-off. During the pulse its grid is driven to near zero voltage by the on-board driver, held at that voltage for 3 microseconds, and then returned to cut-off voltage. Thus a maximum voltage pulse of 50 kV is produced across the klystron. Taking into account a voltage drop of about 10% across the switch tube, the induction voltage regulator can control the dc high voltage over a range of 36-55 kV, which corresponds to a pulse voltage of 33-50 kV across the klystron.

The main switch tube is an Eimac Y-676 with a 100 kW plate dissipation rating. While the expected plate dissipation for RLA usage is only 15 kW maximum, this tube was chosen because of its 25-ampere current-carrying capability with negative voltage on its grid, and because of its 75-kV hold-off capability. Since the grid is always negative, the driver requirements during the pulse flattop are low, and the on-board driver can be relatively simple and small. Also, since the switch tube is a tetrode, it has fairly constant current characteristics which tend to hold the klystron voltage constant in spite of ac-line voltage variations. The 13-ohm resistor between the klystron and the main switch tube serves to reduce the energy dissipated in the klystron to

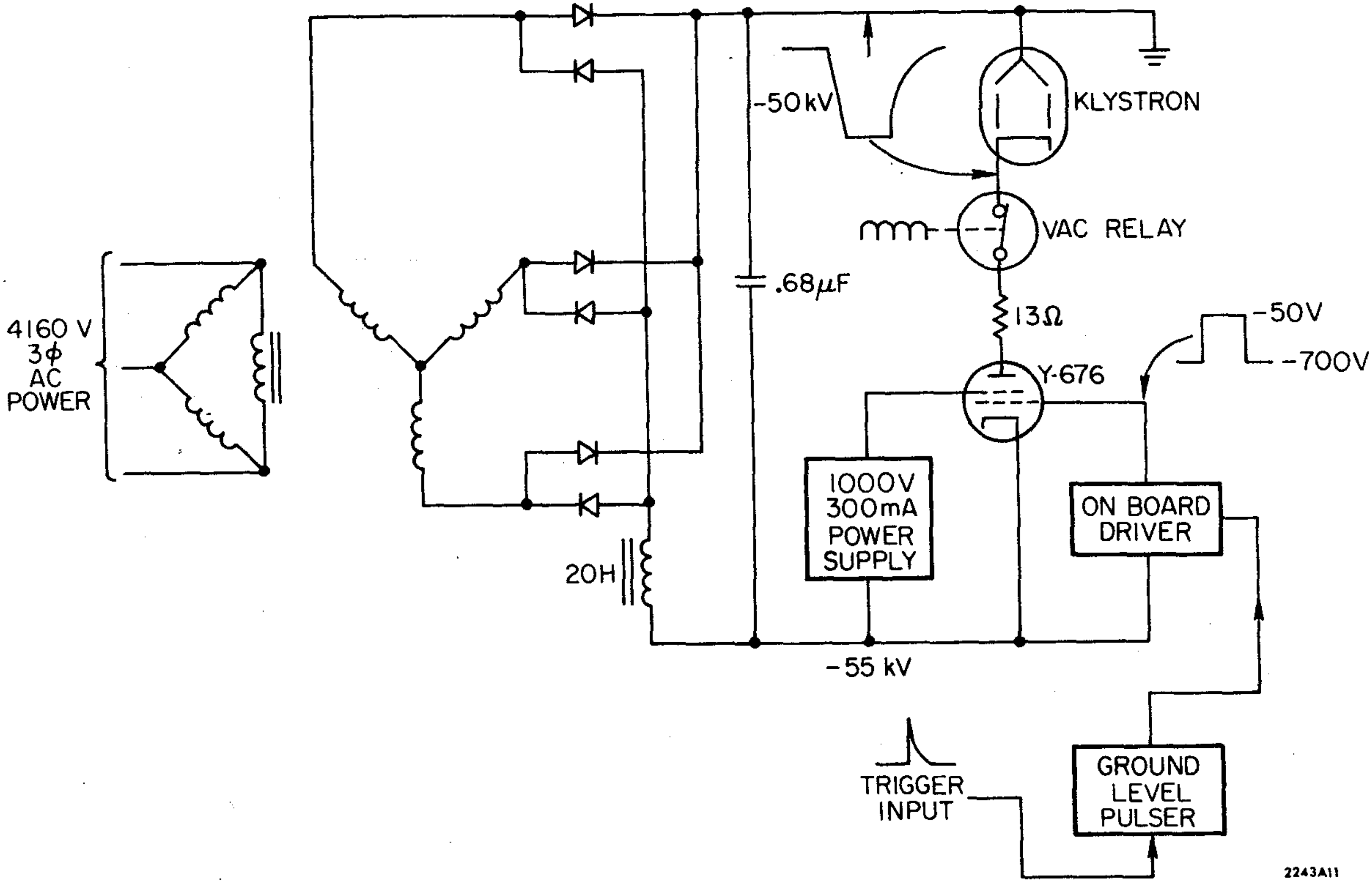

FIG. 19--Simplified circuit diagram of the 1.1 MW RLA modulator.

10 joules in the event of simultaneous arcs in the switch tube and klystron.

A simplified schematic diagram of the on-board driver is shown in Fig. 20. The driver delivers a 650-volt pulse to the main switch-tube grid with a 3 microsecond flattop and 100 nanosecond rise and fall times. Briefly, the circuit operates as follows. A trigger from the accelerator trigger system is fed to the low-level pulser (at ground level). This pulser produces an output pulse which is coupled to the floating pulse generator, which in turn puts out a square pulse of variable duration into the grid circuits of 8 paralleled pentodes. The grid of the final switch tube is connected in parallel with the bootstrapped load resistor of these 8 tubes. One of the problems in a modulator of this type is the possibility of bias shifts in RC coupling circuits due to the high duty cycle. Therefore, direct coupling is employed throughout.

A prototype modulator has already been built for the 220 kW klystron and is undergoing tests and minor modifications at the present time. Initial results are very encouraging. The rise time is about 0.5 μsec, and the fall time is about 1.5 μsec. The fall time is much longer than the rise time because the klystron capacitance must be discharged through the klystron resistance, which rises with decreasing voltage, while at the same time the switch tube is cut off. The flattop is 2.5 μsec, but it can easily be varied to produce any width within the capability of the power supply. The on-board driver is so stable that any repetition rate below the design value of 43,000 pulses per second may be used without any change in the output pulse shape, and repetition rates as high as 110,000 pulses per second have been achieved with maximum pulse widths of one microsecond.

In initial tests, a droop of about 2% over the flat top of the pulse has been encountered. This will be eliminated by appropriate shaping of the drive pulse to the switch tube. There are also plans to add pulse height regulation to this modulator, using a circuit which compares the output pulse height with a dc reference voltage, producing a difference voltage which then controls the voltage drop across the switch tube.

E. The Klystron Drive System

The proposed drive system for the RLA klystrons is closely analogous to the existing SLAC system, in which high-power rf pulses are transmitted

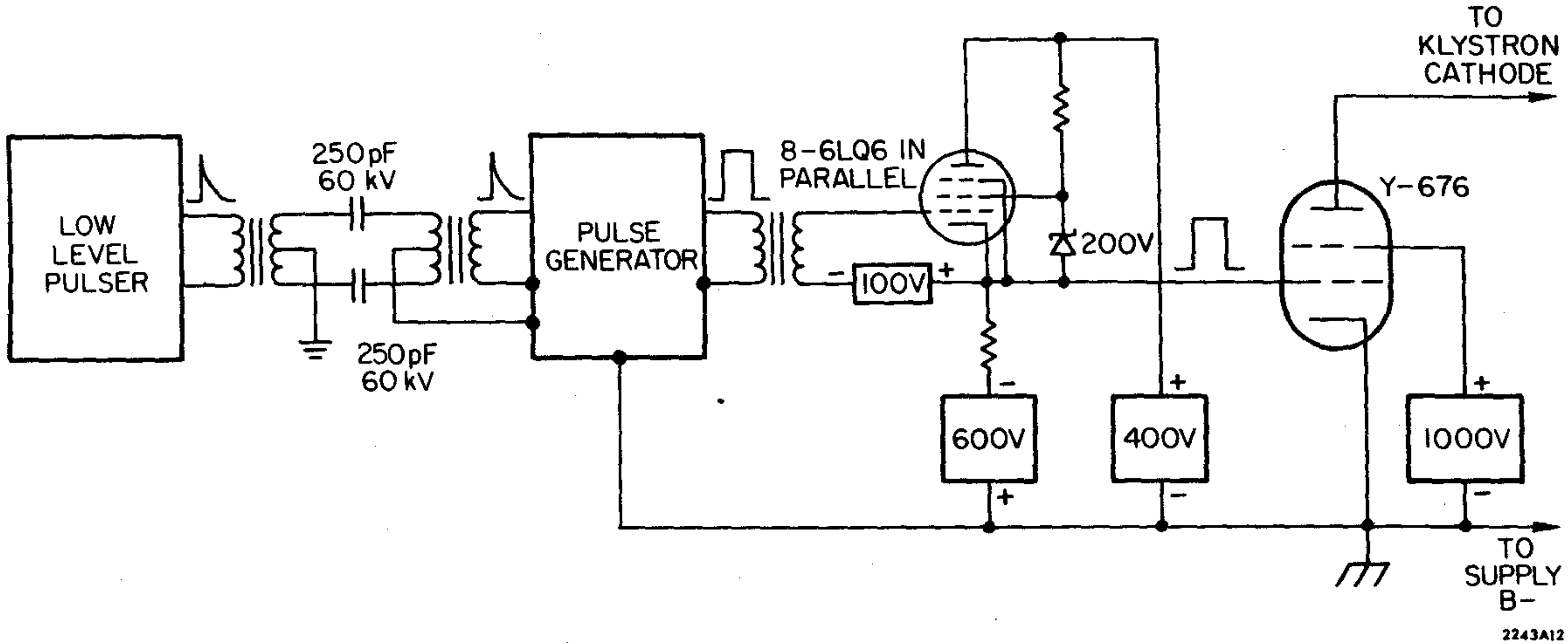

FIG. 20--Driver circuit for the RLA modulator.

along coaxial sub-drive lines and coupled off to drive the accelerator klystrons without further preamplification. However, pulse-timing problems, which arise because of the opposite directions of travel of the two beams and the time taken to traverse the east loop, make it more convenient to consider two separate sub-drive lines for RLA. The proposed system is shown in Fig. 21. An additional coupler is placed between the varactor multiplier and the phasing reference coupler in Sector 22. The 2856 MHz CW signal from the new coupler passes through a phase shifter ϕ_s (the function of this phase shifter will be described in the following section), a PIN diode modulator and a transistor preamplifier to a 1 kW CW klystron amplifier. The modulator output is a train of pulse pairs. As with the present SLAC machine, klystrons in the "accelerate" mode are triggered to amplify the first rf pulse in each pair. The second, "standby" pulse is available for phasing and maintenance. Each pulse is 2.5 microseconds long, and the pulse separation is adjustable for each of the two sub-drive lines. The pulse-pair repetition rate is 43 kHz.

The output of the 1 kW klystron is transmitted along a rigid coaxial sub-drive line (the same design as used on the present machine) which runs almost to the end of Sector 22. This line (the west-east sub-drive line) feeds RLA klystrons 21-1, 21-3, 21-5, 21-7, 22-1, 22-3, 22-5, and 22-7. The maximum end-of-life drive requirement of the RLA klystrons has been specified as 10 W. Assuming 1 db minimum loss in each of the components (level-set attenuator, phase-shifter, and isolator) preceding each klystron, and adding the known insertion losses of the cable system plus an additional 3 db safety factor, results in an input power requirement of 950 W.

A second, almost identical, sub-drive-line system originates with an additional coupler following the varactor multiplier in Sector 23. This system drives the even-numbered RLA klystrons, accelerating the westbound beam beginning with 22-8 and ending at 21-2.

The designs of the sub-drive line couplers, and the isolators and attenuators preceding the klystrons, will probably be similar to the ones on the existing machine. The attenuators will comprise two series elements, one manually controlled to set the klystron drive to saturation, the other automatically inserted during recycling to protect the rf windows. However, the klystron phase-shifters will be a PIN-diode incremental type controlled by digital logic, rather than the motor-driven Fox type now in use. Use of

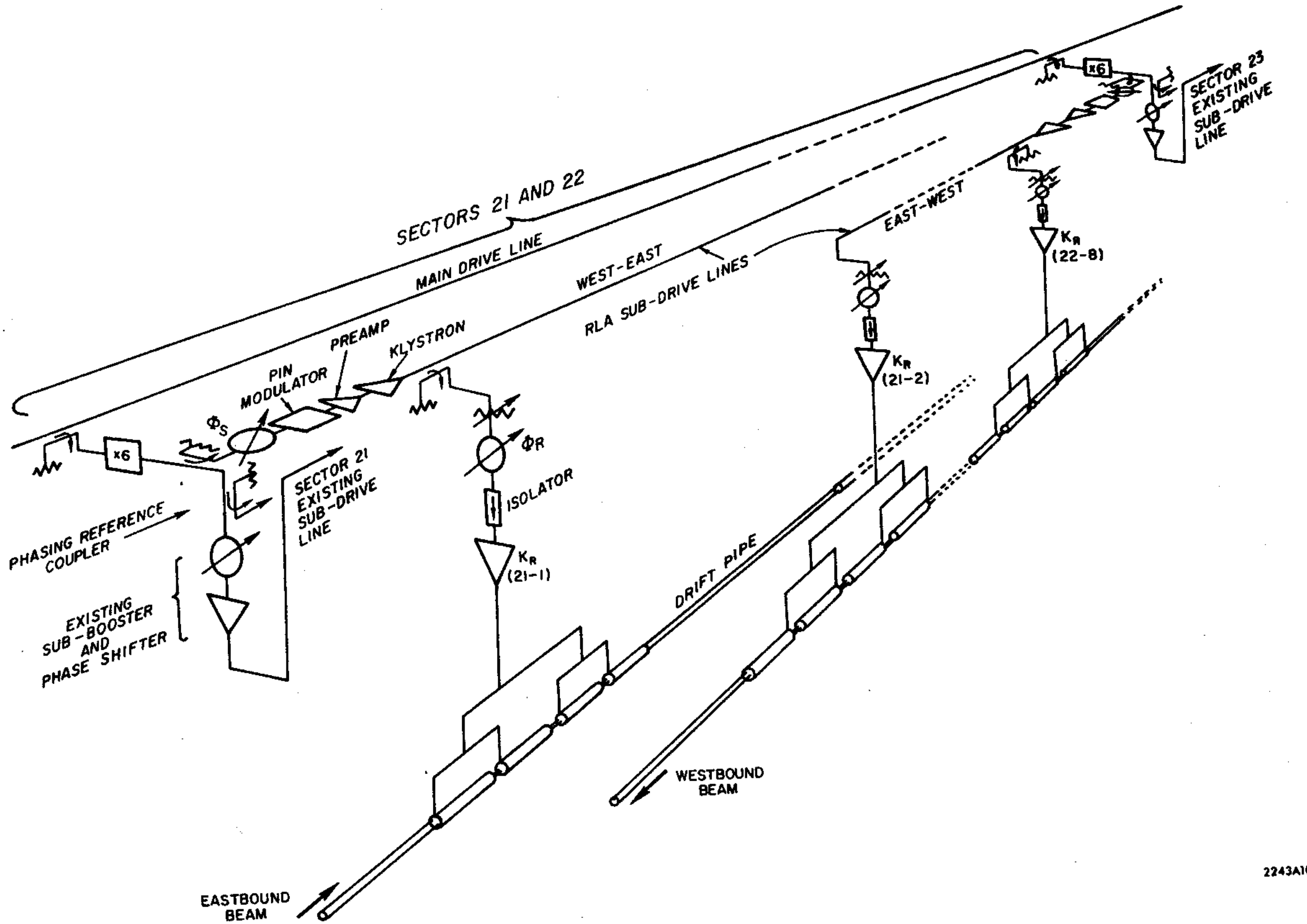

FIG. 21--RLA drive system schematic.

the PIN-diode type of phase-shifter will make possible the rapid changes in phase during the beam pulse which will be required to compensate for beam loading.

The rf drive system described above is a "high-power" system requiring expensive, low-loss coaxial sub-drive lines to keep the input power requirement within reasonable bounds. An alternative system, in which rf power in the milliwatt range is distributed using small semi-rigid cables and microstrip couplers, would be very attractive if 10-watt, 40 db-gain, S-band transistor amplifiers were comfortably within the state-of-the-art. This is not the case at the time of writing, but developments are being watched.

F. <u>The Klystron Phasing System</u>

The klystron phasing system must be capable of performing the following five functions:

1. Setting the phase of the klystrons fed by each sub-drive line so that they act together to produce maximum acceleration.

2. Adjusting the relative phase between the two halves of the rf system fed by the two sub-drive lines.

3. Setting to synchronous phase.

4. Making fast phase changes during the beam pulse to compensate for beam loading.

5. Providing for the possibility of feedback control of phase oscillations.

The first three functions will be discussed in this section. Beam-loading compensation has been discussed previously. With regard to the fifth function, it has not been determined whether a feedback system for providing additional damping of phase oscillations will be needed for RLA. However, two cavities (or short sections of traveling-wave structure) should be provided at the location of the rf system, one in the eastbound and one in the westbound beam line, which can serve as pick-ups to sense the beam phase for this purpose if required.

The problem of lining up klystron phases within each of the two subsystems is similar to the problem of phasing the present SLAC machine. Figure 22 illustrates a conceptually simple system for coupling the RLA accelerator into the present automatic phasing system for the main accelerator. Duplicating exactly the monitoring equipment used on the present accelerator,

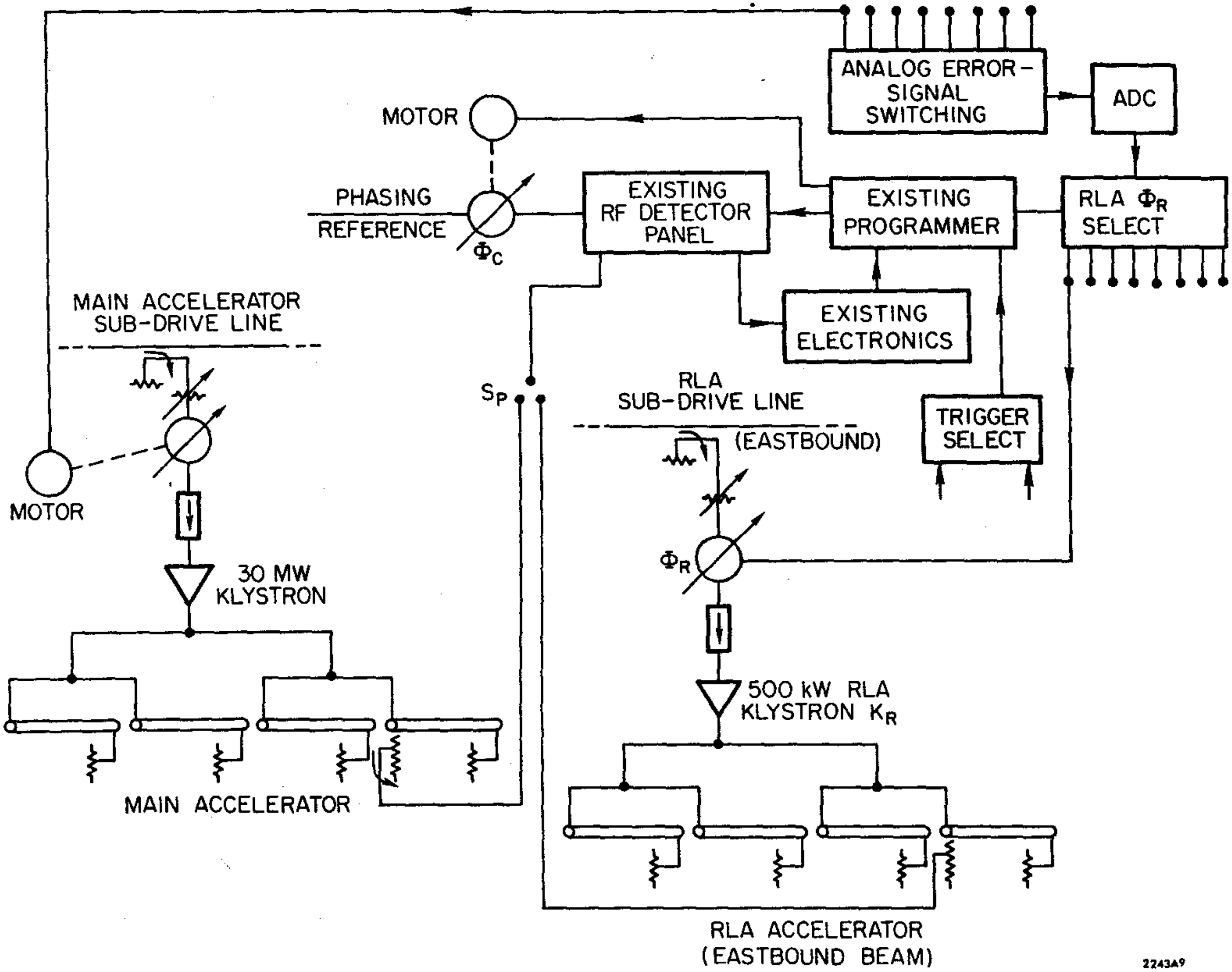

FIG. 22--RLA phasing system schematic.

a 20-db coupler is inserted between one 10-foot section and its load on each girder. The output of the coupler is connected to a coaxial cable which runs up the penetration containing the existing phasing cable. Above the penetration, the present connector is replaced by an electromechanical or PIN-diode switch, S_p, permitting either the main accelerator signal or the RLA signal to be selected for transmission to an rf detector panel in the sector above. Switch S_p must be capable of handling relatively high peak rf powers (20 to 40 kW) from the main accelerator, and must provide on the order of 80 db isolation between the two channels.

Normal phasing of the main accelerator can proceed when the S_p switches connect the rf-detector panel to the existing system.* When it is required to phase the RLA, the S_p's are thrown to connect the new system, and various changes are made in the phasing programmer logic:

1. New triggers compatible with RLA accelerator and standby timing are switched in.

2. When phasing the klystrons, the 2-phase ac motor signal (proportional to the phasing error) is switched to an A/D converter, the output of which is selected to drive the digital phase-shifter ϕ_R in front of the appropriate klystron.

3. When phasing the westbound beam, the programmer selects only the even-numbered klystrons in sequence for phasing and leaves the odd-numbered stations on accelerate. The converse holds for phasing the eastbound beam.

The system outlined above probably represents the most economical way of realizing an automatic phasing mechanism for RLA since it makes maximum use of existing equipment. However, in doing so it also inherits the disadvantages of the present system, notably thermionic diode balancing problems and slow operation caused by extensive use of electromechanical rf switches, telephone-type relays and motor-driven phase-shifters. In addition, sharing the system with the main accelerator may pose operational problems, e.g., phase comparison for feedback purposes, as mentioned above, would have to be discontinued while Sectors 21 and 22 of the main accelerator were being phased. The economic feasibility of an entirely separate, all solid-state system will be investigated.

Setting to synchronous phase angle can be accomplished in two ways,

---

*For a detailed description of the present phasing system, see Chapter 12 of R. B. Neal, ed., The Stanford Two-Mile Accelerator, W. A. Benjamin, Inc., New York, 1968.

either by introducing a fixed phase off-set into each of the individual klystron phase shifters (ϕ_R in Fig. 22) or by introducing the phase off-set into the two phase shifters ϕ_S (Fig. 21). As mentioned previously, the klystron phase-shifters ϕ_R will also be used for fast (intra-pulse) beam-loading compensation. They may, in addition, be programmed to compensate for changes in phase between eastbound and westbound beams which might occur with shifts in the position of the equilibrium orbit. However, it may be more convenient to make this phase adjustment with ϕ_S in the westbound sub-drive line.

G. High-power Waveguide Components

At present it is expected that the waveguide system which transmits rf power from the 500 kW klystrons located in the klystron gallery to the accelerating structure in the tunnel below will be similar to the system used on the present accelerator. The major components in the high-power waveguide system are: a directional coupler (model A coupler) used to monitor the klystron output power, a waveguide vacuum valve which allows vacuum to be maintained when a klystron is changed, a power divider (3-db short-slot hybrid) with associated load, transverse waveguide runs (1.5 m and 4.6 m) to neighboring penetrations, vertical runs (10.7 m each) through the two penetrations into the accelerator housing, two more power dividers with loads, and waveguide runs (averaging 2.4 m each) to the four input accelerator couplers.

The first decision to be made with respect to the high power waveguide system is whether it is to be evacuated or gas pressurized. At present, the prevailing opinion is that the factors in favor of an evacuated system outweigh the factors favoring a pressurized system. Klystron life is expected to be greater with an evacuated system, since a klystron can continue to run even after a window develops a crack. A second window would be required near the accelerator input coupler in a pressurized system, and the consequences of a window failure in this location can be severe.

Other changes in the RLA waveguide system as compared to the present system are being considered. For example, a savings could be effected by eliminating the waveguide valve, although this would mean that a klystron could not be changed until a down time at the end of a machine-operation cycle.

The present opinion is that the potential savings would not be sufficient to justify the loss in running time at top RLA energy (it has been estimated that the rf system would be down by one klystron about half the time). The possibility of using extruded aluminum wave guide in place of the copper waveguide with brazed-on cooling channel, as used in the present system, is also being investigated. Because there are 38 m of waveguide per klystron, the potential savings are considerable. However, the problem of providing reliable high vacuum flanges for use with the aluminum guide may be difficult and expensive, largely offsetting the savings achieved on the waveguide itself.

It is important that the high-power waveguide components, in particular the waveguide vacuum valve, be tested under RLA conditions of repetition rate and peak and average power as soon as possible. Tests at power levels exceeding the RLA values will be carried out using a resonant ring coupled to the existing 220 kW klystron. Tests on a resonant ring are helpful but not conclusive, however, because the resonant properties of the ring cause the power flow to drop whenever losses increase, and because sharp transients are eliminated. When a prototype of the 500 kW RLA klystron is available, tests on waveguide components can be made using the direct output of the higher power klystron.

VII. INSTRUMENTATION AND CONTROL

A. General

Many of the sub-systems in the RLA complex are similar to existing accelerator components, and for this reason the same general approach will often be used for control. The differences are significant, however, and will surely modify the design schemes in detail.

The existing accelerator control system was originally designed in the early 1960's for manual operation. Nevertheless, both because eventual computer control was envisaged and because of the length of the machine, most of the status and control signals are multiplexed; changeover to a "fully computerized" control system which takes advantage of this fact is in process. Many of the design decisions forced in this situation are not those one might make if the system were to be built from scratch today. The basic data-collection scheme for RLA will therefore be a fresh design, and will take full advantage of today's technology. All operational display and control of RLA will be accomplished through a computer system which will be added to the existing PDP-9/SDS 925 system. The exact form of this system is yet to be determined, but it is probable that the basic "man/machine interface" will be through the SDS 925 in the SLAC Main Control Center (MCC), using extensions and modifications to the existing touch panel system. Except for possible high-speed signals from beam monitors which cannot be adequately pre-processed for computer display, all monitor and status signals will be presented to the operator through the computer display system.

RLA is faced with the same data-collection problem as the accelerator: it is simply too long for a single central data-collection point to be practical. Unlike the linac, however, RLA tends to have its data sources concentrated in the loops at the "ends, and so it is reasonable to consider a few data-collection centers, each consisting of a data collector, concentrator, and transmission facility to the point of control (MCC).

Since the design of the data-collection system affects strongly the design of the data sources, it is necessary to come to a working decision as early as possible. It has been assumed in this report that there will be five data centers, located at sectors 1, 4, 21, 27 and 30. These correspond to the west loop, west reverse bends, RLA accelerator system, east reverse bends, and east loop, respectively. A mini-computer may be used at each of these locations as part of the data-collection center. See Fig. 23 for a block diagram of the proposed system.

In addition to the data-collection and display electronics common to all systems, the control system includes instrumentation and control for the following systems:

- RF System
- Magnet Power Supplies
- Beam Monitoring and Display
- Machine Protection Interlocks
- Personnel Protection Interlocks
- Trigger and Timing Equipment
- Vacuum System Monitors

Each of these will be discussed in turn.

B. RF System Controls

Included here are status monitoring and control of the new high repe-repetition rate modulators, the rf drive and phasing system, possible feedback systems to control synchrotron oscillations, controls for beam-loading compensation, and miscellaneous rf system status signals.

From a control standpoint it is not expected that the modulators will be substantially different from the present klystron modulators, and essentially the same control approach is feasible. The rf drive for the klystrons will be provided through sub-boosters in the gallery. Two methods of providing klystron drive have been proposed; one is closely analogous to the existing system used in the linac, wherein high power pulses from a sub-booster klystron are transmitted via coaxial cable directly to the tubes. In the other, CW power from the linac's 476 MHz drive line is multiplied to 2856 MHz, and pulse-modulated and amplified locally by high-frequency transistor amplifiers at each klystron. The second scheme has the advantage of not requiring sub-booster klystrons and allowing the phase shifters to work at lower power levels, but it depends primarily on the availability and cost of suitable power transistors for use at these frequencies. Neither of these schemes presents any unusual design difficulties in the control system, which, while differing in detail, will be similar in either case to the existing systems for the linac. Two sub-drive lines would

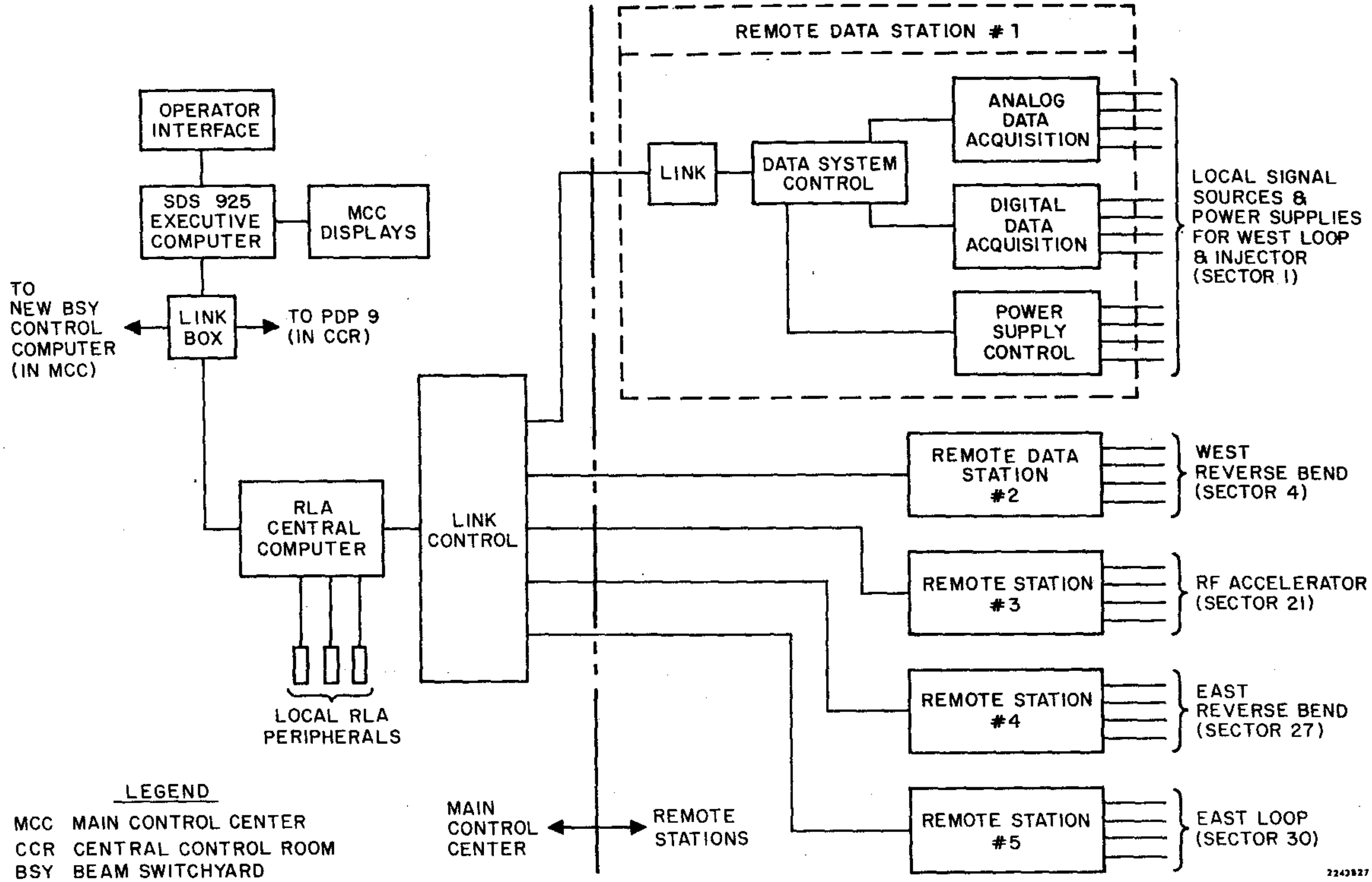

FIG. 23--Block diagram of the RLA instrumentation and control system.

be desirable, one for the east-bound and one for the west-bound beams. The rf drive to the klystrons (in either the CW or pulsed system) will consist of pulse pairs, each 2.5 microseconds long, the pairs repeating at 43 kHz, the revolution frequency of the beam in RLA. One of the pulses in the pair will provide accelerate pulse drive to the rf system and the other "standby" rf power. The "standby" or "non-accelerate" pulse can be used for phasing or maintenance purposes.

It is assumed that the phasing system will be similar in concept to the existing system for the accelerator, with the following exceptions. First, the availability of electronic phase shifters make them a logical choice over the presently used mechanical units from both cost and reliability considerations. Secondly, with electronic phase shifters, it is possible to use a single phase shifter for each klystron for all functions, i.e., setting the synchronous phase, beam-loading compensation, compensation for changes in phase between the east-bound and west-bound beams when the frequency of the entire machine is adjusted to make the loop an integral number of rf wavelengths, and feedback to control phase oscillations (if needed). Obviously, if complications in the control system warrant it, separate phase shifters can be added to accomplish any of these functions.

C. Magnet Power Supply Controls

The power supplies for the RLA magnets will be housed in shelters at each loop and in the gallery where space is available. See Section IV for a discussion of the separate power supplies required. As with other power supplies at SLAC, each power supply will contain a high-speed analog regulation loop, and set-point control of this loop will be accomplished by providing an adjustable reference voltage to this loop. Since control at a rate exceeding about 10% per second is not required for RLA, incremental controls (raise/lower) will be satisfactory. The major advantage of incremental controls is in the simplicity and uniformity of the resulting interface to the control system, and it is intended that the same type of interface signals will be usable for all supplies. The exact number of power supplies to be controlled cannot be determined until final details of the magnet system are worked out, but the approximate number assumed is 180, including main lattice magnets (bends, quads, sextupoles, etc.), pulsed magnets, matching magnets, septa, trim supplies, and beam-guidance power supplies.

The computer system will monitor all magnet currents and make periodic adjustments as required because of drift in the power supply, operation request, or basic control program sequencing. It is expected that all power supplies will be computer controlled. In addition to set-point control of the power supply output, those supplies required to turn on and off or reverse during normal operation of RLA will have these functions also computer controlled. The status of all power supplies will be brought to the MCC through the data system.

D. Beam Monitoring and Display

Beam monitors presently proposed for RLA include monitors to measure beam position, profile, current, and bunch length. In addition, a monitor to indicate instantaneous phase for synchrotron oscillation feedback has been proposed. The basic measurement technique of the last four have not been chosen, but it is probable that observation of the synchrotron light or a residual gas ionization monitor will be used for profile monitoring, a magnetic (toroid) monitor for beam-current pickup, and some sort of rf cavity for bunch length and phase pickup. Since there will only be a few (at most three) of each of these, the decision is not critical.

Beam-position monitoring, on the other hand, will be required frequently around the machine, particularly during commissioning and after alterations when the beam may get lost around the recirculator. The exact number of monitors required has now been fixed, but a number between 150 and 170 independent operating monitors has been estimated. As a result, the position monitors must be low in cost, reliable, and require as little bandwidth as possible in transmission back to the nearest data-collection point. Note that these remarks apply as much to the electronics used to process the raw signals from the monitor as to the monitor itself.

With these points in mind, several monitors were investigated: the "SPEAR" type (an electrostatic monitor with button electrodes), the "SLAC" type (a resonant cavity monitor using three resonant cavities), an amplitude-sensitive non-resonant microwave monitor, and a phase-sensitive non-resonant microwave monitor. The SPEAR-type monitor responds to frequency components in the 300-1000 MHz region; the low-frequency cutoff results from the need to terminate the electrodes into transmission line, and the high-frequency limit is set by the response of the signal-processing electronics. Because the linac pulse contains very little energy in this spectral region, the monitor is quite insensitive.* On the other hand, the SLAC-type monitor exhibits great sensitivity to the linac beam, both because of the "gain" due to resonance and because there is considerable energy available at 2856 MHz in the beam itself. However, their high cost (approx. $15,000 ea., including processing electronics) and large dimensions preclude their use in RLA.

Active consideration is presently being given to the microwave non-resonant monitors. The amplitude-sensing type in principle requires less electronics near the monitor; while the phase-sensing variety provides direct position readout (independent of beam intensity) and somewhat greater sensitivity at the expense of more complex electronics. Although both are being evaluated for use in RLA, the present weight of opinion is in favor of the phase-sensing type, which is described below.

The beam, bunched at 2856 MHz, passes through two apertured waveguides placed together in the form of a cross, as shown in Fig. 24. The bunches induce time-varying electromagnetic fields in each waveguide, which propagate outward, predominately in the TE_{10} mode, to matched waveguide-to-coaxial line transitions, symmetrically placed in the waveguides.

When the beam is on the system axis, mechanical symmetry causes the two horizontal (x) output signals to have the same phase. Similarly, the vertical (y) outputs are in phase. A beam-displacement δs in the x or y direction results in a differential phase shift $\delta\phi = (4\pi\delta s)/\lambda_g$, where λ_g is the effective guide wavelength appropriately modified by the presence of the aperture.

A local oscillator and mixer heterodynes the resulting signal to 15 MHz, and differential phase information is transformed into an analog position signal by a 15 MHz IF phase detector circuit. The required microwave circuits (local oscillator, power dividers and mixers) can be built on microstrip as an integrated circuit with the phase detector (which is a commercially available integrated circuit).

*Other "video frequency" monitors (such as loops or striplines) suffer from the same defect; split toroidal-type monitors were ruled out because of their inherent structural complexity.

RLA BEAM POSITION MONITOR SCHEMATIC

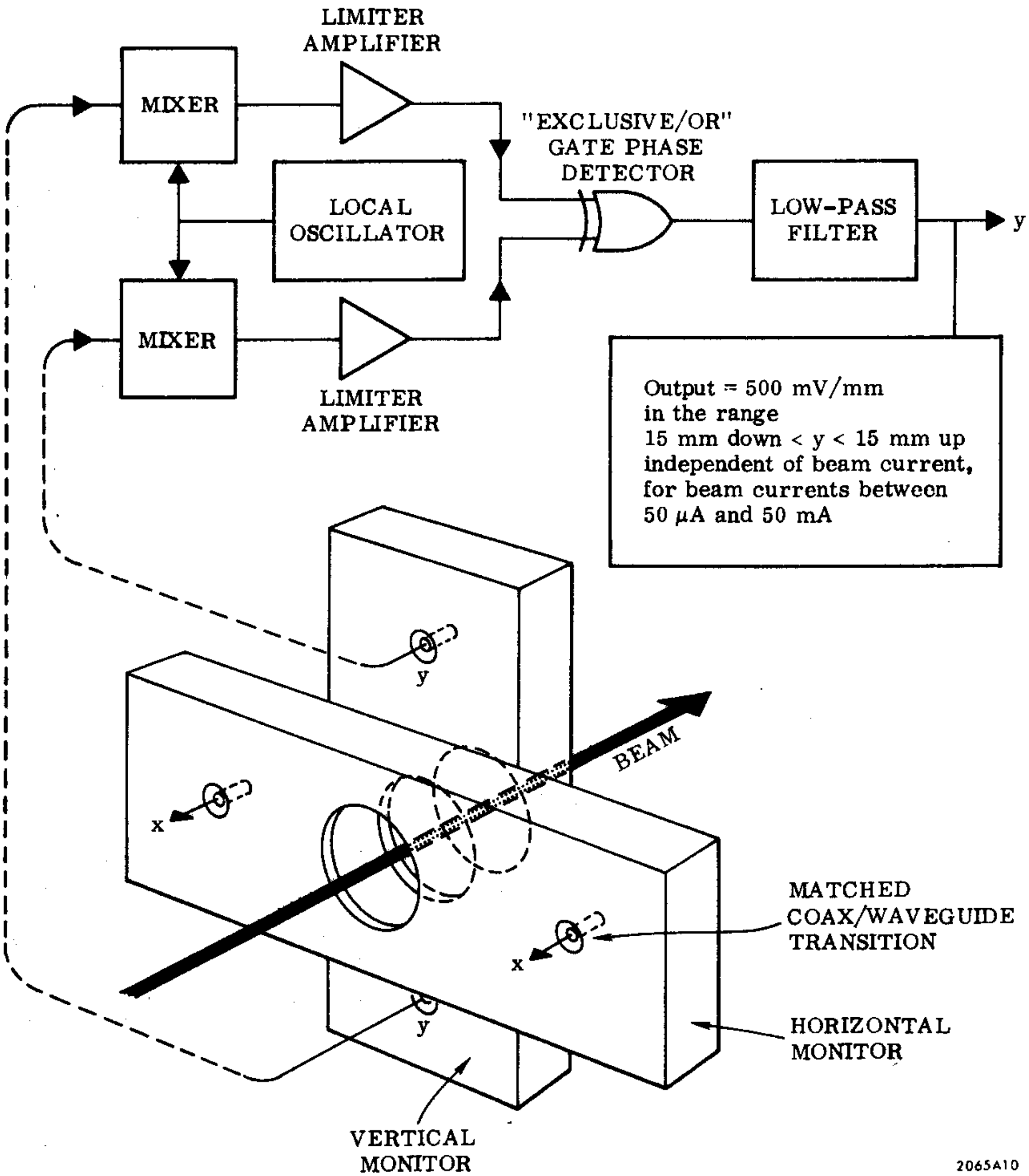

FIG. 24--The beam-position monitor planned for RLA.

The system is attractive largely by virture of the limiter amplifiers which produce clipped, amplified IF waves forms without phase distortion. The filtered output of the phase detector is independent of beam current over a large range, typically at least 1000:1. The theoretical power flow induced in a standard S-band waveguide by a well-bunched beam passing through small apertures in the broad walls is 180 $\mu W/mA^2$. Using half-height waveguide with 3.8 cm diameter apertures and rather diffuse electron beam, an induced power of 35 $\mu W/mA^2$ has been measured. Assuming reasonable cable and mixer losses, a useful beam-current range of 50 μA to 50 mA can be expected for the monitor. The large ratio of aperture diameter to waveguide height results in the effective guide wavelength being close to the free-space wavelength in the center of the aperture. This results in a phase shift of 7 degrees per millimeter of beam displacement, which translates to a final output analog signal of 700 mV/mm. This progressively decreases to 500 mV/mm for displacement greater than 1 cm from the system axis. There is no significant cross-talk between the x and y channels. The monitor cross can be made of aluminum or any material which is compatible with the rest of the beam vacuum envelope. A suitable rf coaxial vacuum feedthrough is being developed.

At present it appears that there is no need for turn-by-turn position display, and that an average of all turns results in an acceptable display. For initial tuning where the beam does not get stored, the signal is averaged over several successively injected pulses. The major advantage in signal-averaging apart from potential signal-to-noise improvements is a sharp reduction in the bandwidth required in transmission back to the data-collection facility. The resulting display is an average of beam position (the equilibrium orbit if many turns are averaged) versus azimuthal position around the recirculator. Final signal processing (including correction for inherent monitor nonlinearities) and display will be accomplished by the computer system.

E. Machine Protection Interlocks

Protection from damage to equipment due to loss of cooling water or other required services will be provided as required in each sub-system. For example, thermal detectors on magnets and other devices requiring air or water cooling will be interlocked with the corresponding power supply and will be considered part of that power-supply system. A PLIC system (long ion chamber) will be provided as an interlock against beam loss. The loop vacuum chamber will be water cooled to dissipate the heating due to synchrotron radiation. Since the beam itself is the heat source in this case, loss of cooling water to components intercepting synchrotron radiation requires beam shut-off. Under normal circumstances an injection interlock will suffice, since the "stored" beam is ejected after 120 turns. However, at the vacuum pressure expected in RLA, failure of the ejection equipment could result in the beam being stored for several seconds, perhaps minutes. Because of this, and the fact that a water vacuum leak would be so serious, momentary interruption of the rf system is proposed. This guarantees loss of any stored beam.

F. Personnel Protection

The personnel protection system must be expanded to provide controlled access to the new loop housings. Four access points per loop must be interlocked (two external access points and one or two accesses from the existing housing). Other manways will be interlocked for emergency exit only. The control logic to permit such access will be similar to the logic which controls entry to the beam switchyard and the SLAC accelerator.

The present beam shut-off system turns off all beams when excessive radiation is detected in uncontrolled areas. It is not yet known what modifications to this system may be required. The new requirements for the beam-containment system demand clearer specification of the new beam paths to be used in the switchyard and experimental areas.

As to site security, the present system must be expanded to monitor a larger perimeter and/or several isolated power-supply buildings. Telephone service will be provided only at normal entry points. The existing service channels will be extended into the new housings. The existing accelerator housing and gallery public address system will be extended into the new housing and power-supply buildings.

G. Trigger and Timing Equipment

Construction of RLA will involve basic changes in the tirggering of the entire SLAC accelerator. Until now, the basic clock for the accelerator was derived from the incoming powerline frequency; a six-phase clock at 360 Hz was created in CCR and transmitted to the injector to create the pulses on the main trigger line, which triggers both the injector and the klystron modulator However, it will be necessary when RLA is in operation to make the time between pulses on the main trigger line an integral number of revolutions of the stored beam in the recirculator. The accurancy required in this relationship between the two "clocks" is high; the re-inserted beam must fit the linac rf envelope to a fraction of a pulse length (say approx. 100 nsec). As a consequence, the entire accelerator must be synchronized to the RLA beam instead of the power line. Since much of the equipment designed at SLAC over the past ten years depends upon the approximate synchronism between the trigger line and the power line, it is proposed to retain this relationship to the extent possible. In the final system, the trigger pulses will be generated by the following method. A clock which pulses at the revolution frequency of RLA will be generated by dividing the 476 MHz main drive line signal by one sixth of the harmonic number of the RLA recirculator (the main drive-line signal is one-sixth of the rf frequency). This requires that the harmonic number of RLA be evenly divisible by six. This clock will be compared with the present 360 Hz signal from CCR, and the first revolution clock pulse after the 360 Hz power-line-related clock pulse will be used as a trigger. The resulting trigger pulse will "walk-across" the power line until it has drifted 23 μsec (one revolution period) from one of its extreme positions and then snap back to the other extreme position. Each time the snap occurs, the recirculated beam will execute one extra (or one fewer, depending upon the exact timing relationship) revolution. The present lattice design predicts a path length of about 6962.7 meters, corresponding to a harmonic number of 66,312 and a revolution period of 23.2 μsec. The ratio of this period to 1/360 second is 119.68, and so the beam will circulate 119 times for about once every three pulses and 120 times twice in three. The snap, which therefore occurs every three beam pulses (approximately 120 times per second), is one revolution period, or 23.21 μsec. Investigations are in process to find where in the accelerator complex this might necessitate modification of any existing equipment.

The trigger pulse referred to above would produce the "1 msec pretrigger"; additional scaling of the 43 kHz clock would then produce the main trigger a fixed number of revolutions later.

The revolution clock will also be used to generate RLA klystron-modulator triggers, and for gating beam-monitoring equipment (if necessary). A suitable method of distribution of the clock signal has not been chosen, but local trigger electronics will be required whenever triggers are needed at the revolution frequency. Trigger countdown will also be needed for the modulators to "run-in" new klystron tubes at repetition rates below 43 kHz. Extension of the existing 360 Hz system for inflection and re-insertion will also be required.

H. Vacuum System Monitors

Remote monitoring of pressure in the loop will be provided through the data-collection system as required. Status and control of valves and other vacuum equipment will be handled in the same way as in the present accelerator. No special problems are expected in this area.

VIII. BEAM SWITCHYARD AND SLOW EXTRACTION

A. General

The beam definition and beam-transport systems for the various modes of operation for RLA will be discussed briefly in this section. The term "low energy" will be used to mean a beam which has been accelerated in a single pass and thus has an energy of 20 to 25 GeV or less. "High energy" refers to a beam which has been recirculated and then accelerated a second time to an energy greater than 20 to 25 GeV. Included as points of interest are: (1) the injection into the beam switchyard (BSY) of the high-energy, low-duty-cycle beam and, because of proximity, the injection into RLA of the simultaneously accelerated low-energy, low-duty-cycle beam; (2) the two extraction systems presently being considered for the generation of the low-energy, high-duty-cycle beam; (3) modifications to the BSY itself.

B. The Injection System into RLA and the Beam Switchyard

At the end of Sector 30 in the main accelerator, the electron beam (low energy, high energy, or both) will pass through a magnetic system capable of deflecting the low-energy beam 0.5 degree to the south. This system will use the 5 existing BSY pulsed magnets bending 0.1 degree each to transport the low-energy beam through a septum magnet, a dc bending magnet system (15 degrees total bend), and finally a fast kicker magnet for injection into the east loop of RLA. This dc magnet system shown in Fig. 25, will contain enough quadrupole magnets to match the phase space from the accelerator to RLA.

While the low-energy beam is deflected 0.5 degree towards RLA, the accompanying high-energy beam is deflected through a smaller angle and misses the field region of the septum magnet mentioned above. The actual angle of deflection of the high-energy beam will of course depend on the ratio of the two beam energies present in the system. After the high-energy beam clears the components in the injection system leading to RLA, it passes into a series of 12 pulsed magnets (PM-10 through PM-21 in Fig. 25). This group of magnets pulses the beam into the various switchyard beam lines in much the same way as the present BSY pulsed magnets operate. The system will now be examined on a step-by-step basis.

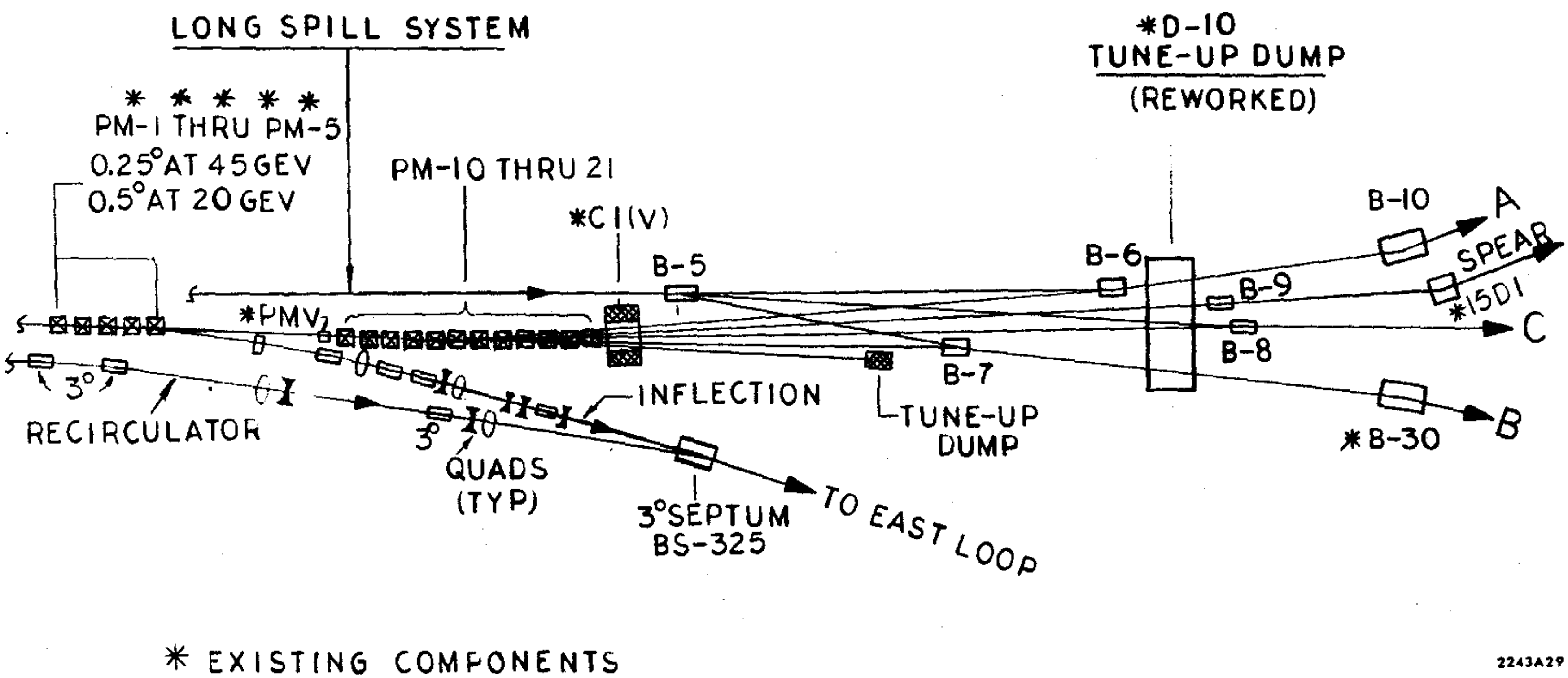

FIG. 25--The RLA beam-transfer system.

With the second pulsed-magnet group, PM-10 through PM-21, turned off, the high-energy beam passes undeflected through the pulsed magnets to a tune-up dump located further downstream. A set of spectrum foils placed just ahead of the dump allows the operator to set the energy of the beam to within approximately one percent of the desired energy. Knowing which spectrum foil was hit (determined by the setting of the magnet group injecting into RLA and the actual energy of the high-energy beam) enables the operator to define the position of the beam at the vertex of the second pulsed magnet group. This pulsed magnet group can then be set to direct the beam to one of the vertex points in the dc magnets B-6 through B-9 which direct beams to the existing A, B, SPEAR and C beam lines.

The scheme described above requires that the "common beam" area of the BSY be modified. Some new equipment, notably pulsed magnets and associated power supplies, will be necessary to handle the higher energy electron beam. An effort will be made to use reworked and relocated existing equipment wherever possible. The present plan places only one restriction on the pulse-to-pulse compatibility of the various beams from RLA; because only five power supplies will be installed to power the five pulsed magnets, it will not be possible to interlace, on a pulse-to-pulse basis, a high-electron beam with a low-energy positron beam, or a high-energy positron beam with a low-energy electron beam. Should this flexibility become necessary in the future, a few additional power supplies are all that would be required. Other than this restriction, the pulse-to-pulse compatibility of beams from RLA (including the 1.5 GeV SPEAR positron and electron beams) will be the same as at present.

C. Low-Energy, Conventional Slow-Spill System

Two methods have been considered for producing a conventional flat spill from RLA. Since the recirculating beam will make approximately 120 revolutions in the 2.8 msec period between accelerator pulses, a conventional spill system will extract approximately 1/120 of the amplitude of the beam pulse on each revolution. The two methods that have been considered involve the use of a stochastic process, such as Coulomb scattering, or a nonlinear magnetic perturbation.

Results of computer-simulation studies of many versions of both methods indicate that a satisfactory slow spill could probably be obtained using either method. The magnetic method appears to have some advantages: e.g., no enlargement of the phase area and hence no extra loss of beam in the recirculator.

However, preliminary beam-optical designs have been made for slow-extraction systems which could accommodate the use of either method. Present plans call for a system to be installed in the east-bound straight section of the recirculator, probably in the vicinity of Sectors 25 or 26 of the main accelerator.

A satisfactory magnetic perturbation for slow-spill purposes is the field produced by a pair of conductors carrying equal and opposite currents running parallel to the electron beam axis and separated vertically by a distance somewhat less than the initial beam diameter (a bifilar loop), as shown in Fig. 26. The basic idea is to sweep the electron beam horizontally toward the perturbation at a controlled rate. On each turn of the beam around the recirculator the perturbation deflects a small part of the beam, mainly in the vertical plane, and sends that part past the thin septum of a dc electrostatic deflector and into a long extraction channel. The remainder of the beam passes symmetrically through an identical but cancelling perturbation and reenters the recirculator "unperturbed". The process continues until all of the beam is finally ejected. The spill rate may be controlled more or less arbitrarily by controlling the horizontal deflection rate. Calculations show that a uniform deflection rate gives a nearly uniform spill rate.

Results calculated for the magnetic method indicate $\gtrsim$ 95 percent extraction efficiency for a septum thickness equal to 1 percent of the initial beam diameter. Losses are mainly on the septum with minor losses on the pipe walls in the vicinity of the perturbation. For the stochastic method the highest calculated efficiencies were also $\gtrsim$ 95 percent with comparable losses on the septum and on apertures in the recirculator where the latter losses result from the enlarged phase area caused by the Coulomb scattering.

The fact that the phase area of the ejected beam is substantially reduced compared with that of the recirculating beam may prove to be useful in certain applications. With the magnetic method the reduction is by a factor 1/3 in y, ϕ and x (not in θ). With the stochastic method the reduction is almost the same in y and ϕ (vertical plane) but in both x and θ the phase area is increased somewhat.

The extracted beam will be transported to the BSY through standard beam pipe and periodic magnetic steering and focusing elements, and will pass to the north of the vertical collimator, as shown in Fig. 25. For the initial installation, a dc magnet will be provided in the long-spill beam to kick the beam into either the A, B, or C beam lines, or into the tune-up dump for

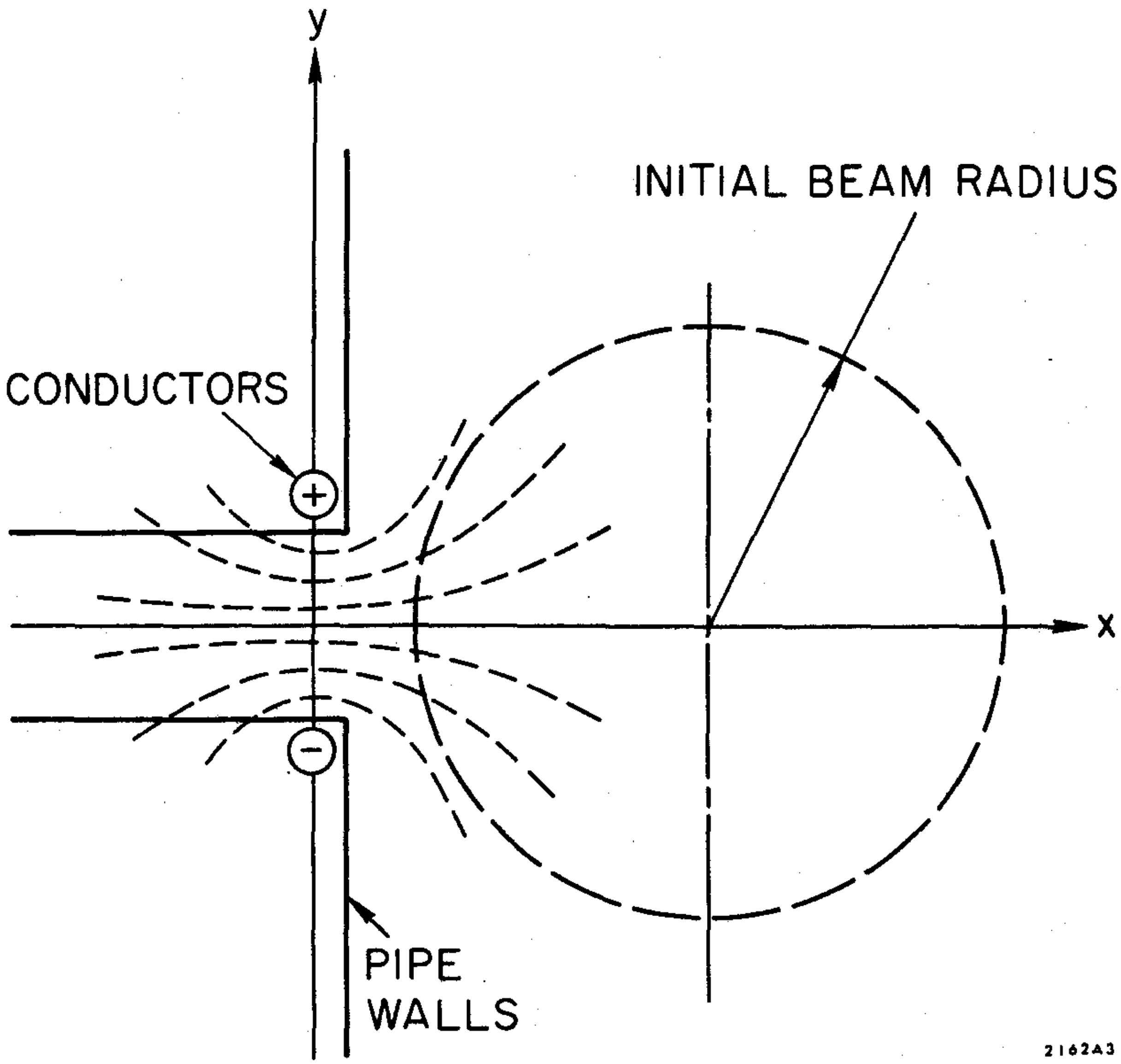

FIG. 26--Bifilar loop for magnetic perturbation suitable for a long-spill extraction device.

energy determination. Future options for more elaborate systems such as beam spilling by scatterinf from a small target or splitting of the beam to different experiments are possible within the framework of the basic system.

D. Low-Energy, High-Duty-Cycle Knockout Extraction System

The conventional slow-spill systems described above produce a flat spill spread in time over the standard 1.6 μsec beam pulse length. Thus, if a 20 mA beam is injected initially into RLA, approximately $(3\times 10^{11})/120 = 2.5\times 10^9$ electrons will spill out in each RLA revolution. This assumes that the beam is stored in RLA for only one interpulse period of 2.8 msec and that the beam is spilled uniformly and at a maximum rate during that time.

However, the initial 20 mA beam is actually composed of many individual "buckets" occurring at a repetition rate of 2856 MHz (0.35 nsec spacing) with a width of approximately 5 psec (5^o in phase). In one 1.6 μsec pulse, there are approximately 4600 buckets. An alternate way of spilling out the beam would be to kick out one bucket every 39 nsec during each 1.6 μsec recirculated beam pulse until all 4600 buckets had been kicked out (after 120 turns). This would allow experiments which normally run with beam knockout at the present time to run with increased average current. The signal-to-noise ratio would be reduced because many more buckets would be filled in this mode than are filled in the existing beam knockout mode.

This mode would also be useful for counter experiments, such as multi-particle coincidence experiments, that cannot presently be done at SLAC because of duty-cycle limitations. In the knockout mode, each bucket will contain $(3\times 10^{11})/4600$ or approximately 6.5×10^7 electrons. Because of the long time between buckets, the experimental electronics will be completely recovered from the effects of one bucket by the time the next bucket arrives. By comparison, in the conventional spill mode, over a time of five nanoseconds, the same counter system would see the effects of (2.5×10^9) $(5/1600) = 7.8\times 10^6$ electrons, or about one-eighth the number of electrons per bucket in the knockout mode. Although 5 nanoseconds represents a typical resolving time for trigger counters, this calculation does not include other experimental considerations such as electronics dead time and accidental effects, nor the length of the gate pulse required for proportional wire chamber hodoscope electronics (presently above 30 nsec -- a tradeoff between chamber efficiency and multiple-track confusion). In addition, the knockout mode would allow a more widespread use of the time-of-flight measurement technique for particle separation and identification. A detailed comparison between the knockout mode and the conventional mode as to which offers the best duty cycle depends critically on the specific details of the experiment under consideration.

The means to effect the knockout mode have not yet been completely developed, although a preliminary scheme using independent multiple frequencies as Fourier components of an appropriate waveform does exist on paper. Whether this scheme will stand up under more detailed scrutiny remains to be seen. However, if a practical system can be developed to implement the knockout mode, the required extraction hardware will be located in a convenient position in the east-bound straight section of the recirculator, so as to utilize as much as possible of the conventional slow-spill transport system to the beam switchyard.

E. Beam Switchyard Modifications

Some modifications to the beam switchyard (BSY) will be required to accommodate the higher energy beams (up to 45 GeV) from RLA. An attempt will be made to minimize disruption of the present beam lines and to utilize existing equipment wherever possible.

Although the bending magnets which are now in the A and B beam lines could produce the magnetic fields required for 45 GeV operation, iron-saturation effects would require the addition of large new power supplies. It is therefore more economical to move four of the present A-line bending magnets with their power supplies to the B line, and to provide the A line with nine new magnets (including a reference magnet) and a new power supply for 45 GeV operation. Four new A-beam dump bending magnets also will have to be built, along with an associated power supply. These four magnets bend the electron beam into a beam dump after high-energy photon beams have been produced for use in End Station A. The existing quadrupole magnets used in the A and B lines are adequate for the higher energy range, but some new power supplies will have to be obtained.

The electron beam to the C-line will be stopped in a target area located in the BSY as far upstream in the C-line tunnel as possible. Secondary beams, both charged and neutral, will be developed and transported through the C-line to experimental set-ups in the research yard. Included in the BSY modifications for RLA will be the equipment to transport and dump the beam in the target area of the C-line.

RLA's high-duty-cycle beams will require some BSY additions in the area of Instrumentation and Control. The long-spill system will require that many monitors be upgraded to make them sensitive to signals which will be essentially dc rather than pulsed, and which will have peak intensities a factor of ~100 lower than the minimum peak intensities that can presently be monitored.

IX. CONVENTIONAL FACILITIES

A. Site and Structures

The east and west loops of RLA are shown superimposed on the existing SLAC facility in Figs. 27 and 28 respectively. Reference to these figures will make the following narrative easier to follow.

Beam-transport components outside the existing accelerator structures will be housed in underground concrete structures of three different types: cast-in-place rectangular structures of cut-and-cover construction; pre-cast concrete pipe of cut-and-cover construction; and bored and lined tunnels.

The rectangular structures will be used in areas where the beam is curved or bent in order to allow space for handling bending magnets. The interior dimensions will be 2.1 m high by approximately 2.4 m wide, and the structures will be designed for the suspension of magnets from the ceiling. Earth shielding will cover them to a height of at least 2.7 m above the ceiling and to a width of at least 8 m horizontally at beam level.

The circular-pipe type of housing will be 2.4 m inside diameter and will be installed where beam runs are straight and beam components consist only of drift tubes, relatively small magnets and monitoring equipment. A flat concrete floor about 1.5 m wide will be cast within the structure. The housing will be covered with an earth shielding fill of dimensions similar to those for the rectangular type structure.

Bored tunnels will be necessary near the accelerator housing to avoid disturbing the Klystron Gallery and the utilities above. A large part of the east loop, where the elevations will be too deep below natural grade for economical cut-and-cover construction, will also be bored and lined.

Approximate lengths of the three structure types are: rectangular cut-and-cover — 591 m; pipe sections — 302 m; bored tunnels — 671 m.

Beams will leave and enter the existing accelerator housing at small angles: three penetrations at 5° and one at 12°. Wherever possible, beam penetrations will be through drilled holes of only a few centimeters in diameter, with nearby ports for man and material access between the SLAC accelerator and RLA housings.

Each loop will have one horizontal access at grade to facilitate the handling of components. In addition there will be a few vertical manhole entries for men,

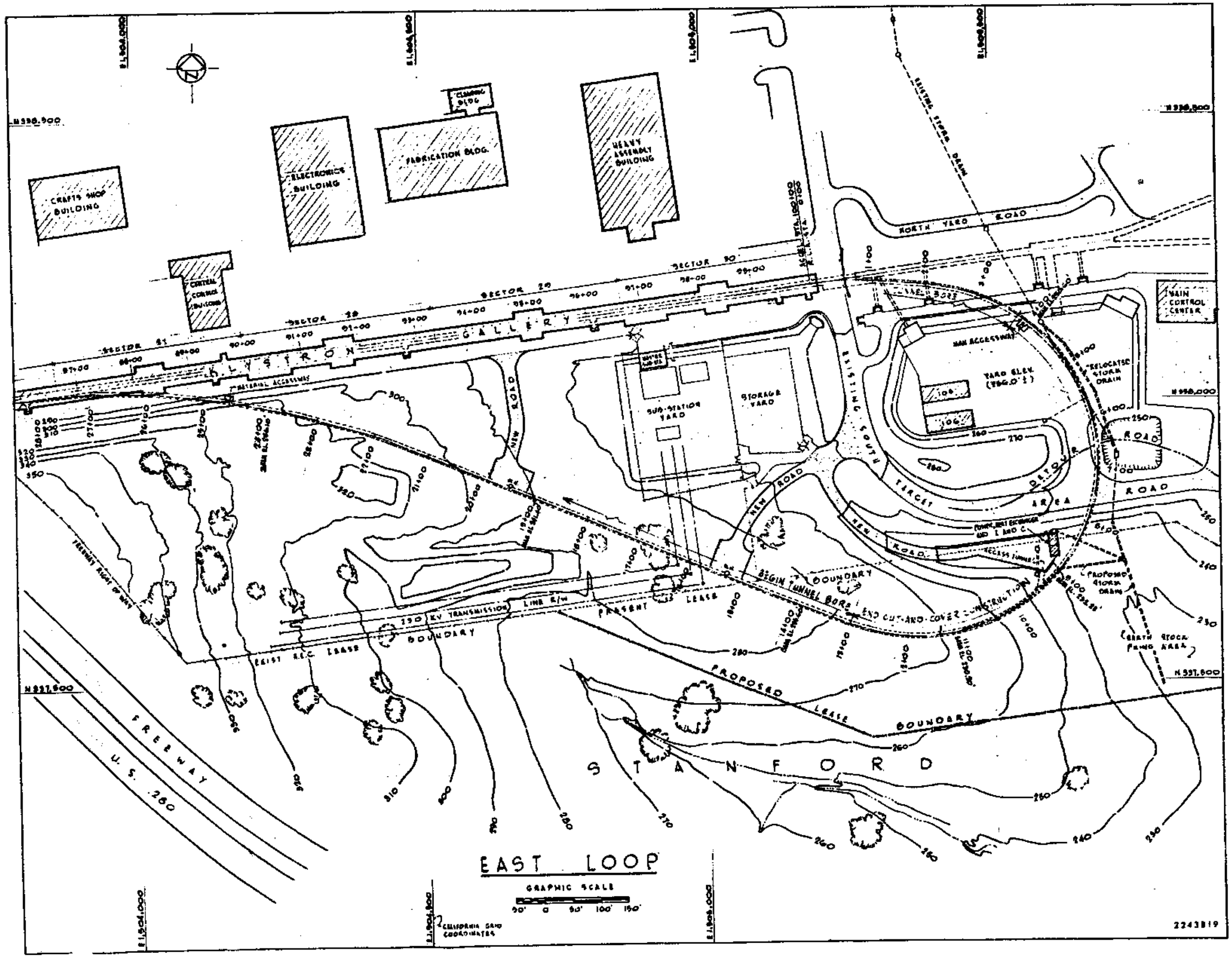

FIG. 27--The east loop of RLA shown superimposed on the present SLAC facility.

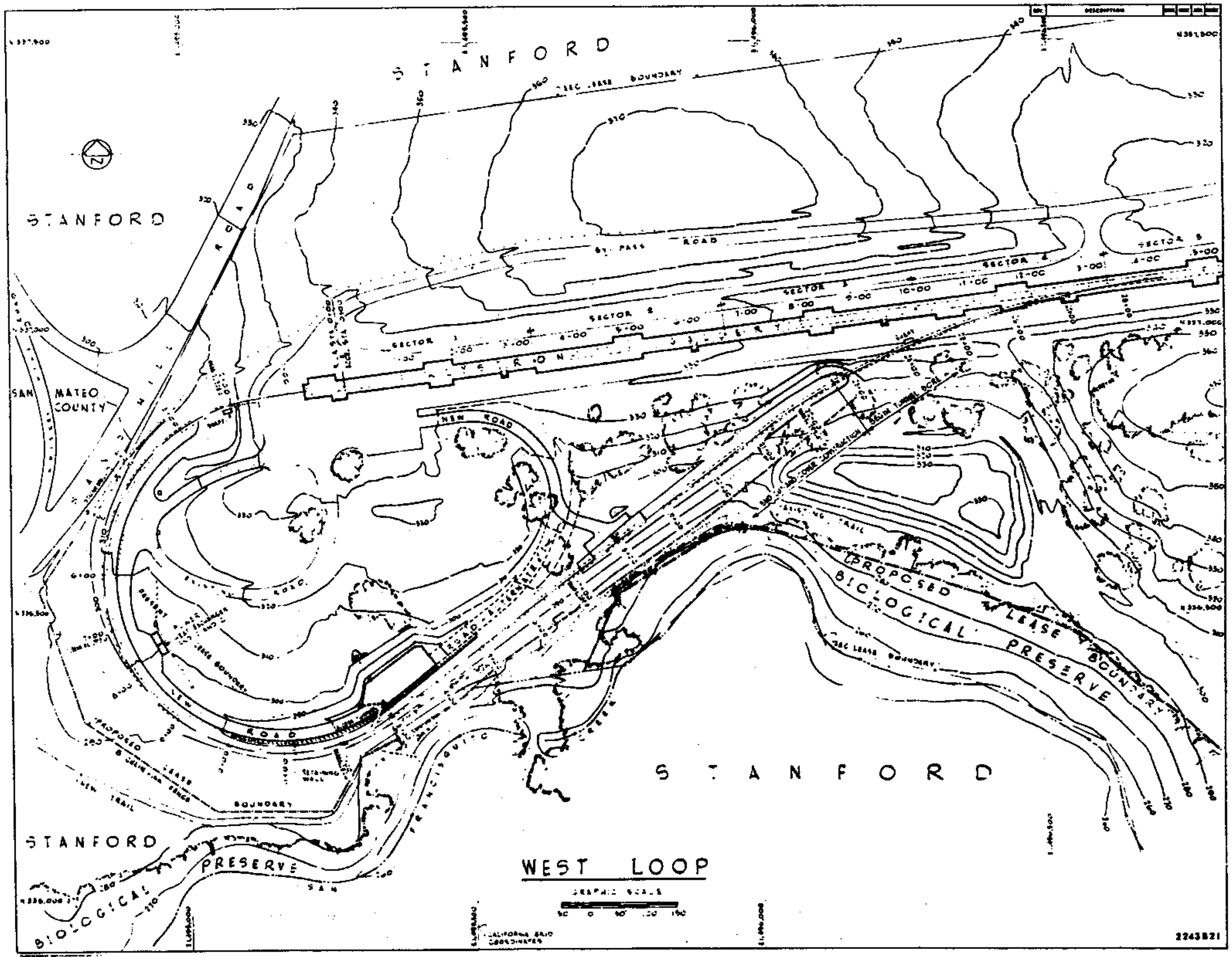

FIG. 28--The west loop of RLA shown superimposed on the present SLAC facility.

materials, services, instrumentation and ventilation; although the number of these shafts will be limited because of interlocking and radiation-safety considerations.

Twenty-foot-wide roads will be constructed between principal access points to RLA and SLAC's existing road system.

Surface facilities will be located within the loops where they can be screened from public view as much as possible. There will be two power supply stations for each loop, housed in shelters about 4.9 m wide by 9.8 m long. Heat exchangers and low-conductivity cooling water pumps will be housed in similar shelters, one per loop. Space will be provided in all shelters for instrumentation and control equipment.

Landscaping with plant materials indigenous to the region will be done to prevent erosion and to minimize the environmental impact of the construction features.

B. Shielding and Radiation

The shielding problems are concerned mainly with limiting the flux of neutrons and muons at the shield surface and at the project boundary. The shielding configuration (combined with operational interlocks and procedures) will limit the radiation at the project boundary to 5 mrem per year. An upper limit of 1.5 rem per year will be maintained for radiation workers (this is 1/3 of the allowable level set by AEC).

At the present time, it is planned to use at least 2.7 m of shielding over the entire recirculation loop. Radiation measurements will be made and any "hot spots" which are found will be remedied by realignment of the beam-transport components, by changes in operating procedures, or by addition of localized shielding. The protection system must be designed with the capability of shutting off the beam within 1 to 2 pulse intervals (2.8 - 5.6 msec) in case the beam-monitoring devices detect an out-of-tolerance radiation condition or in case the beam fails to complete its programmed recirculation schedule.

Calculations indicate that for a continuous 0.003% loss of a 17.5 GeV, 30 mA, 300 kW beam ($\sim$10 W) uniformly spread around the loop, the neutron dose will be well within the design limit while the muon contribution should be entirely negligible. The calculations have also been extended to a 25 GeV, 10 mA, 150 kW beam. The neutron doses at this higher energy will be lower.

Additional localized shielding can be added, if needed, to eliminate any significant dose contribution from muons.

C. Electrical Utilities

The electrical power requirement for the recirculation system operating at a 20 GeV level may be summarized as follows:

East loop	3.0 MW
West loop	2.7 MW
RF system	3.2 MW
TOTAL	8.9 MW

An additional 3 MW will be required to upgrade the BSY to 45 GeV beam capability. The total added power requirement is then approximately 12 MW.

The main SLAC substation has an ultimate capacity of 83 MVA. The present accelerator and research area load is limited to 60 MW or 69 MVA; therefore the present main substation will probably be adequate to supply the increased load when the proposed RLA is operating at 20 GeV.

Taps will be provided at accelerator Sector 16 to divert 12-kV power to two new substations located at the west loop of RLA. These substations will be of the outdoor type. A 3 MVA substation will transform the power from 12 kV to 4160 V for the main-bend-magnet power supplies and cooling water pumps. The other, a 1 MVA substation, will transform power from 12 kV to 480 volts for the smaller magnet power supplies. At the east end, power will be tapped from the master substation feeders and fed to two outdoor substations, similar to those at the west loop.

Power to the radiofrequency system (3.2 MW) will be supplied from the existing 12 kV line at Sector 21. All 16 RLA modulators will be fed from one 5 MVA, 12.47 kV/4160 V outdoor liquid-filled non-inflammable insulated substation with an output voltage range of 2760 to 4600 volts.

A new 3 MVA, 12.47 kV/460 V indoor dry-type unit substation will be added to the BSY substation to provide power for the A and B beam bending magnets for 45 GeV operation. Power for the small bending magnet power supplies for RLA will be taken from the existing BSY 480 V substation.

D. Cooling Water

RLA components which require water cooling will be supplied with low-conductivity water (LCW) which will circulate in closed systems. The LCW will be cooled in heat exchangers by cooling-tower water (CTW). The use of LCW to cool magnets, rf components and power supplies will minimize cooling-circuit corrosion problems. This is especially important since some magnets will have aluminum coils.

The expected heat-load distribution will be as follows:

East loop	2.0 MW
East reverse bend	0.5 MW
West loop	1.8 MW
West reverse bend	0.5 MW
RF system	2.5 MW
Beam switchyard	2.9 MW
TOTAL Heat load	10.2 MW

Two LCW systems are planned to serve the east and west main and reverse bend magnets, vacuum chamber, and power-supply cooling requirements. They will additionally service miscellaneous components in the reinjection and inflection systems. LCW will be supplied at 240 psi ($\sim$17 kg/cm^2) and 35° C, allowing for a magnet coil pressure drop of up to 150 psi (10.5 kg/cm^2). It is expected to achieve an average magnet coil temperature of 45° C. The 45° C temperature was chosen so that conditions in the RLA housings will closely match those in the existing accelerator housing.

The addition of $\sim$200 m of accelerating structure for RLA will require four LCW systems to be added, one in each of Sectors 21 and 22 to cool the klystrons and modulators, and another in each sector to cool the accelerator sections. The klystron LCW systems will require a minimum of work since existing headers have adequate capacity for the additional water flow. Complete systems including distribution piping will be required for cooling the accelerator. Existing waveguide-cooling systems have sufficient capacity to cool the waveguide which is to be added. The cooling systems to be added will be duplicates of the existing systems. The small amount of cooling water required by RLA quadrupoles in the accelerator housing will be supplied from the accelerator cooling systems.

Although the two cooling towers (No. 1201 and No. 1202) serving the accelerator LCW systems are presently very nearly fully loaded; present SLAC plans already call for upgrading and expanding these towers as a part of the program to replace the existing klystrons with higher power tubes. This work is expected to be completed prior to RLA construction, and will thus allow the cooling towers to handle the added RLA load.

The BSY Magnet Cooling LCW system and its cooling tower have sufficient capacity to accommodate the additional 3 MW heat load from RLA. Only minimal additional plumbing will be required.

X. SCHEDULE AND COST ESTIMATES

The estimated time schedule for construction of the Recirculating Linear Accelerator is 36 months from the date of full authorization to the beginning of systems testing, or 39 months to full facility operation. The detailed time schedule included in this section takes as its starting point an assumed date for full authorization in FY 1975.

The total estimated cost of RLA is \$21.8 million, of which ED&I is \$3.1 million, construction is \$15.85 million, and contingency (at 15%) is \$2.85 million. A detailed breakdown of this estimate is given in the cost schedules which follow. The cost estimates for the various RLA components and systems are in general readily identifiable within a single cost schedule. A specific exception, however, is the slow-spill beam extraction system, for which the estimated costs are distributed between the Magnet and Vacuum System cost schedules.

COST ESTIMATE - SUMMARY

($ Thousands)

		Reference Schedule
ED&I	$3,100	A
Construction:		
Site Work & Structures	2,350	B-1
Water & AC Electrical	1,350	B-2
Magnets	3,750	B-3
Magnet Power Supplies	900	B-4
RF System	1,600	B-5
Vacuum System	1,700	B 6
Instrumentation & Control	1,500	B-7
Injection	400	B-8
Beam Switchyard	1,900	B-9
Alignment	400	B-10
Subtotal Construction	15,850	
Contingency at 15%	2,850	
TOTAL	$21,800	

SCHEDULE A

Engineering Design and Inspection

	($ Thousands) Item Cost	Total Cost
Conventional Plant (Sitework, Structures, Water and Electrical) (About 16% of Construction Cost Estimate of $3,700,000)	$ 600	
Machine Hardware (About 21% of Construction Cost Estimate of $12,150,000)	2,500	
TOTAL		$3,100

SCHEDULE B-1

Site Work and Structures

	Item Cost	Total Cost
Sitework		
Relocate Utilities and Fence	$ 60	
Roads and Paving (43,900 sq. ft. at $ .68/sq. ft.)	30	
Earthwork:		
Clean and Strip Topsoil (lump sum)	20	
Excavate and Haul 110,000 cu. yds. at $ .73/cu. yd.	80	
Embankment 75,000 cu. yds at $ .40/cu. yd.	30	
Erosion Control & Drainage	50	
Landscaping	30	
		$ 300
Underground Structures		
Beam Run Structure (5,100 linear ft. at $320/ft)	$1,630	
Shafts, Penetrations and Horizontal Access (lump sum)	255	
Retaining Walls, Painting, and Special Shielding	135	
		$2,020
Surface Structures		
Power Supply and Ventilation Equipment Structures		30
TOTAL		$2,350

SCHEDULE B-2

Water and Electrical

		($ Thousands) Item Cost	Total Cost
Cooling Water Distribution System		$ 650	
AC Electrical Services			
12.47 kV Distribution System	$190		
5 kV Distribution System	120		
480 V Distribution System	100		
Unit substations	290		
		700	
TOTAL			$1,350

SCHEDULE B-3

Magnets

	Item Cost	Total Cost
Main Bending Magnets	$1,900	
Reverse Bending Magnets	310	
Insertion & Reinjection Magnets	170	
Quadrupole Magnets	320	
Long Spill System Magnets	140	
Supports	180	
Bussing and Wiring	280	
Miscellaneous and Installation	430	
TOTAL		$3,750

SCHEDULE B-4

Magnet Power Supplies

Power Supplies	$ 700	
Transistorized Bypass Shunts	40	
Monitoring and Safety Systems	50	
Installation	110	
TOTAL		$ 900

SCHEDULE B-5

RF System

	($ Thousands) Item Cost	Total Cost
Klystrons and Modulators	890	
Phase and Drive	110	
Disk Loaded and Rectangular Waveguide System	600	
TOTAL		$1, 600

SCHEDULE B-6

Vacuum System

Bending Magnet Chambers	$ 710	
Straight Sections	480	
RF Accelerator Sections	200	
Other Vacuum Systems	310	
TOTAL		$ 1, 700

SCHEDULE B-7

Instrumentation and Control

	($ Thousands) Item Cost	Total Cost
Beam Monitors	$ 370	
Machine Protection	50	
Computer and Data Acquisition	290	
Vacuum, Trigger, Power Supply and RF System Instrumentation and Control	170	
Personnel Protection and Communications	50	
Beam Switchyard Instrumentation and Control	120	
Installation	450	
		$1,500

SCHEDULE B-8

Injector

	Item Cost	Total Cost
Main Injector	$ 50	
Second Injector	300	
Positron Source Modifications	50	
TOTAL		$ 400

SCHEDULE B-9

Beam Switchyard

	($ Thousands) Item Cost	Total Cost
Pulse, Quadrupole, Bending, Septum and Dump Magnets	$ 960	
Magnet Power Supplies	340	
Mechanical Components	600	
		$1,900

SCHEDULE-10

Alignment

	Total Cost
Alignment	$ 400

TIME SCHEDULE

RECIRCULATING LINEAR ACCELERATOR

(Assuming Full Authorization-FY 75)

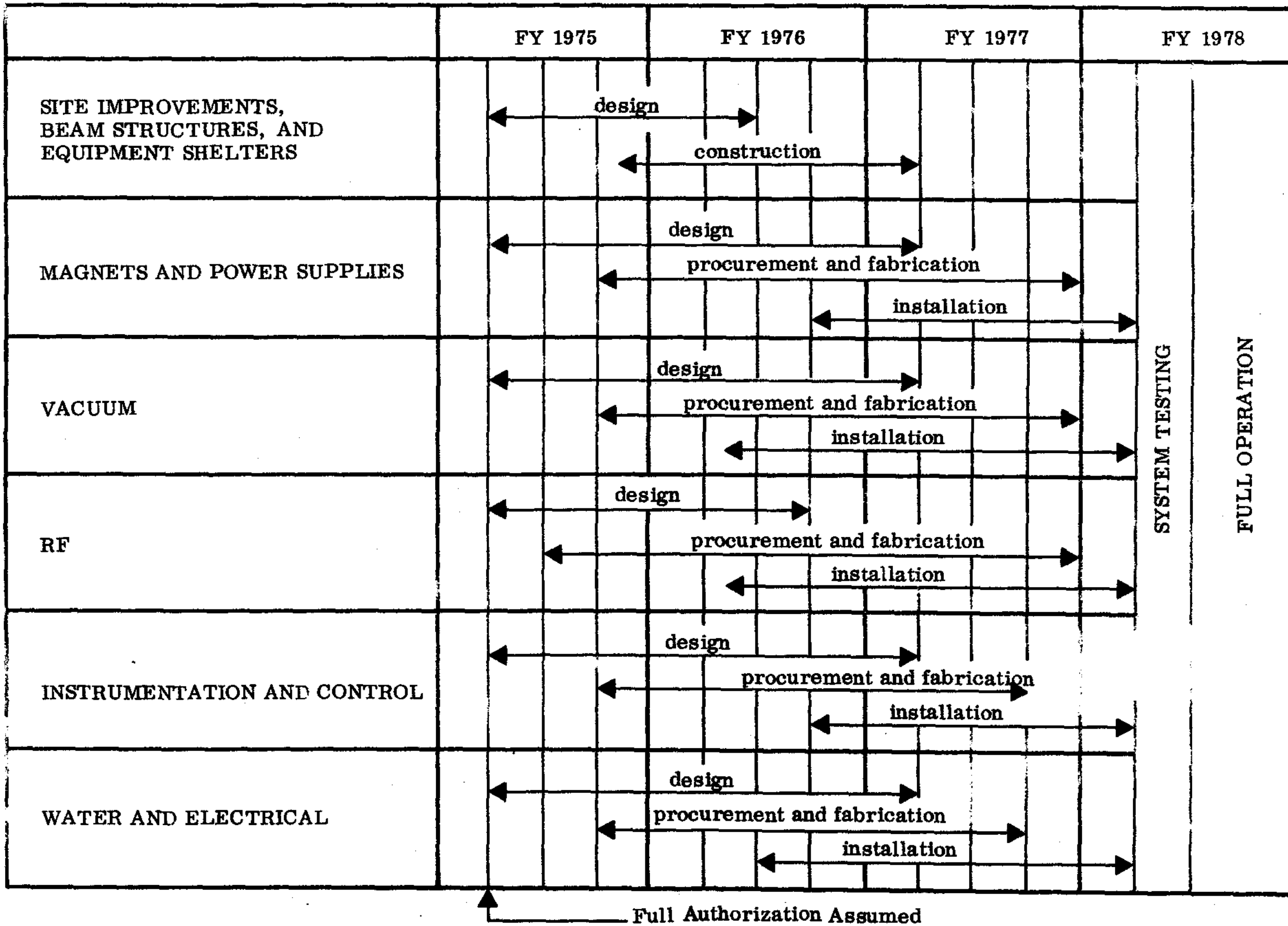

APPENDIX A

INSTABILITIES AND BEAM INTENSITY LIMITATIONS

A number of known incoherent and coherent instabilities could lead to beam loss or deterioration of beam quality, and will have to be taken into account in RLA operation. A brief discussion of some of these instabilities follows.

Synchrotron quantum fluctuations. The incoherent growth in both horizontal and longitudinal phase space, driven by quantum fluctuations, was described in Section III.

Structure resonances. The strong linear integer and half-integer resonances must be avoided by proper choice of tune; the values of ν_x and ν_y can be set independently by rather small adjustments of the quadrupoles. The third integer resonances may also be rather strong because of sextupole corrections that are required for control of chromaticity. It seems unlikely that nonlinear resonances higher than third or fourth integral will be strong enough to drive significant beam growth during the rather short (2.8 msec) storage time.

Transverse cumulative (SLAC-type) beam breakup. This effect arises from a coupling impedance between the beam and an rf deflecting mode in the accelerating structure. The two passes through the SLAC accelerator and the 120 passes through the recirculator linac all contribute to the deflection. Preliminary estimates indicate that the breakup threshold will be no lower than 20 to 30 mA and can be raised if necessary by increasing the focusing in the recirculator linac. Selective detuning of the troublesome mode could also be employed; this approach has proven effective in raising the breakup threshold in SLAC.

Longitudinal cumulative beam breakup. M. Sands has noted the possibility of a longitudinal analogue of the transverse breakup mentioned above. The coupling impedance for this mechanism is provided by the recirculator linac. Analysis shows that there must be an error, of appropriate sign, between the beam-bunching frequency and the linac synchronous frequency in order to produce an instability; hence the effect if observed could probably be tuned out by adjusting the linac temperature. However, preliminary estimates seem to indicate current thresholds of at least several hundred milliamperes even under the worst conditions.

"Two-beam breakup". In 360 pps operation, a low-energy beam and a high-energy beam would be accelerated through the main accelerator simultaneously. Transverse modulation of the beam would be retained during the storage period, so that the reinjected high-energy beam could drive the low-energy beam, and the modulation would be further amplified by the BBU interaction. The effect would thus be cumulative over many machine pulses. This mechanism has not been investigated in detail yet. There is a possibility that 360 pps operation might be limited in maximum current if damping mechanisms (synchrotron and Landau) are not sufficiently effective.

Resistive wall interactions. This mechanism can cause both transverse and longitudinal instabilities. Generally the coupling impedances are much weaker than for interactions which involve high-Q structures such as linacs and cavities. Numerical estimates for machines such as SLAC tend to indicate that resistive wall thresholds are at least one or two orders of magnitude higher than for the above types of effects.

Other beam-structure couplings and head-tail instability. Beam-pipe discontinuities, beam monitors and so on could lead to instabilities either of the cumulative beam breakup or the head-tail type. The microwave position monitors, especially, will have to be analyzed carefully for possible coupling impedances. Sextupole chromaticity corrections will be available to damp the head-tail effect. However, calculations based on coupling impedances observed at Adone and scaling from results at SPEAR indicate that head-tail effect should not be a problem in RLA even without chromaticity correction.

RF noise and phase jitter. RF noise in the recirculator linac can lead to stochastic growth of longitudinal oscillations. Tolerances on pulse-to-pulse jitter have been estimated as a few degrees of rms phase jitter and a few percent of rms amplitude jitter. Very short-period noise, leading to bunch-to-bunch phase error within the beam pulse, probably will not be important during the short 2.8 msec storage time.

Losses in the residual gas. Interaction with the residual gas can cause losses from either longitudinal or transverse effects. The dominant longitudinal effect is bremsstrahlung on the gas nuclei, leading to energy losses outside the rf bucket. The dominant transverse effect is single-scattering events leading to transverse momenta outside the RLA acceptance. At a pressure of 10^{-7} Torr, the bremsstrahlung loss is estimated as 2×10^{-6} and the scattering loss as 5×10^{-7} in 120 turns.

Space-charge effects. Mechanisms such as ion neutralization could produce non-linear tune shifts leading to instabilities. However, it has been estimated that at RLA beam currents (~ 30 mA) such effects should be negligible even with complete neutralization. Similarly, space-charge effects on a completely unneutralized beam are expected to be negligible.

APPENDIX B

This appendix consists of computer print-out sheets from a SYNCH* run for the entire recirculator. It starts at the most western point of the west main bend, i.e., 90° before the beam lines up with the accelerator. Groups of elements which are to be repeated include considerable detail the first time they appear in the listing and are, thereafter, lumped into cells or groups of cells. Thus the main bend cell appears first as half-magnets and thereafter is lumped except where another half-magnet is needed as part of a matching structure. The lumping process causes the integer part of the betatron tune shift to drop whole numbers so that only the final fractional part is correct.

*A. A. Garren and J. W. Eusebio, SYNCH, UCID 10153

BETATRON FUNCTIONS THROUGH RLAA.

	CYCLE	S	NAME	PSIX/2PI	BETAX	ALPHAX	XEQ	DXEQ	WX	PSIY/2PI	BETAY	ALPHAY	WY
WEST MAIN BEND-90DEG	1	0.0	GMDN	0.0	1.28151	-0.00104	0.11506	-0.00000	1.13204	0.0	23.42262	-0.00340	4.83969
	2	2.59517	LE03	0.16554	8.54130	-3.32095	0.19462	0.06433	2.92255	0.02194	12.49985	3.36876	3.53551
	3	2.89517	GMFP	0.17055	10.66061	-3.74343	0.21392	0.06433	3.26506	0.02609	10.56751	3.07239	3.25077
	4	4.14517	GMFN	0.18480	16.06115	0.00031	0.25550	-0.00000	4.00764	0.05057	7.16248	-0.00454	2.67628
	5	5.39517	LE03	0.19906	10.65945	3.74363	0.21391	-0.06434	3.26488	0.07501	10.59660	-3.08952	3.25524
	6	5.69517	GMDP	0.20406	8.54005	3.32105	0.19461	-0.06434	2.92234	0.07916	12.53988	-3.38807	3.54117
	7	8.29034	MB16	0.36968	1.28094	0.00062	0.11502	-0.00001	1.13178	0.10100	23.54914	-0.00391	4.85275
	8	140.93575	GMDN	1.28667	1.28226	0.00118	0.11503	-0.00001	1.13237	0.71587	23.59197	0.00186	4.85716
	9	143.53092	L175	1.45243	8.52238	-3.31416	0.19455	0.06431	2.91931	0.73767	12.56885	3.39440	3.54526
ETA MATCHING QUAD	10	145.28092	Q255	1.47178	24.42824	-5.77491	0.30710	0.06431	4.94249	0.77875	3.73953	1.65093	1.93379
	11	146.78092	L352	1.48016	27.62253	4.04859	0.31478	-0.05454	5.25571	0.88425	1.90048	-0.20911	1.37858
	12	150.30372	XX	1.52120	6.91116	1.83064	0.12264	-0.05454	2.62891	1.03198	10.18932	-2.14380	3.19207
	13	150.30372	BMM	1.52120	6.91116	1.83064	0.12264	-0.05454	2.62891	1.03198	10.18932	-2.14380	3.19207
	14	154.80372	LE2	1.81671	3.18026	-1.00114	0.00001	0.00001	1.78333	1.06751	40.54563	-4.59201	6.36755
BETA MATCH INTO	15	156.80372	Q270	1.87533	9.70323	-2.26034	0.00004	0.00001	3.11500	1.07391	61.09261	-5.68148	7.81618
LONG EASTBOUND	16	157.80372	LE10	1.88807	16.96347	-5.37314	0.00006	0.00002	4.11867	1.07641	62.79337	4.04998	7.92423
DRIFT	17	167.80372	Q271	1.91044	300.51403	-22.98192	0.00028	0.00002	17.33534	1.14406	9.36603	1.27275	3.06040
	18	168.80372	L264	1.91095	319.01601	5.04269	0.00029	-0.00000	17.86102	1.16297	7.82753	0.31198	2.79777
	19	195.22980	L276	1.93344	110.35248	2.85343	0.00018	-0.00000	10.50488	1.41548	89.23788	-3.39266	9.44658
	20	222.80759	Q101	2.04748	15.97571	0.56877	0.00007	-0.00000	3.99696	1.43931	382.98089	-7.25877	19.56990
	21	223.80759	LE71	2.05770	15.33481	0.07787	0.00007	-0.00000	3.91597	1.43972	387.16974	3.10754	19.67663
	22	294.80759	Q103	2.28586	334.99984	-4.58019	-0.00008	-0.00000	18.30300	1.50386	84.65173	1.15327	9.20064
	23	295.80759	LS	2.28633	337.58635	2.01060	-0.00009	-0.00000	18.37352	1.50576	84.01183	-0.50920	9.16580
	24	396.40758	XX	2.38808	84.22132	0.50794	-0.00013	-0.00000	9.17722	1.60755	338.16049	-2.01713	18.38914
SECTOR-SPACED	25	396.40758	QESN	2.38808	84.22132	0.50794	-0.00013	-0.00000	9.17722	1.60755	338.16049	-2.01713	18.38914
QUAD-DEF.	25	396.90758	QESN	2.38902	83.96695	0.00130	-0.00013	-0.00000	9.16335	1.60778	339.17219	-0.00425	18.41663
	27	397.40758	LS	2.38997	84.21872	-0.50533	-0.00014	-0.00000	9.17708	1.60802	338.16898	2.00868	18.38937
SECTOR-SPACED	28	498.00757	QESP	2.49186	336.74414	-2.00486	-0.00035	-0.00000	18.35059	1.70933	84.69893	0.51091	9.20320
QUAD-FOC.	29	498.50757	QESP	2.49210	337.74778	-0.00043	-0.00035	-0.00000	18.37792	1.71027	84.44300	0.00146	9.18929
	30	499.00757	LS	2.49234	336.74500	2.00401	-0.00035	0.00000	18.35061	1.71121	84.69600	-0.50797	9.20304
	31	599.60756	QESN	2.59418	84.28825	0.50550	-0.00014	0.00000	9.18086	1.81269	337.22375	-2.00224	18.36365
	32	600.10756	QAP7	2.59513	84.03651	-0.00153	-0.00014	0.00000	9.16714	1.81292	338.22334	0.00505	18.39085
	33	2022.50744	QESN	3.03624	83.94934	-0.00114	0.00017	-0.00000	9.16239	2.25417	339.38175	0.00378	18.42232
	34	2023.00744	LS	3.03719	84.20350	-0.50768	0.00017	0.00000	9.17625	2.25440	338.36990	2.01791	18.39483
	35	2123.60743	1901	3.13895	337.51550	-2.01033	0.00022	0.00000	18.37159	2.35612	84.06494	0.50998	9.16867
	36	2124.60743	XX	3.13943	335.21099	4.30042	0.00021	-0.00000	18.30877	2.35801	84.63321	-1.08219	9.19963
	37	2124.60743	L436	3.13943	335.21099	4.30042	0.00021	-0.00000	18.30877	2.35801	84.63321	-1.08219	9.19963
	38	2168.25742	2001	3.18522	70.58508	1.76203	0.00006	-0.00000	8.40149	2.40888	227.98698	-2.20197	15.09924
	39	2169.25742	L436	3.18751	68.69631	0.14115	0.00006	-0.00000	8.28832	2.40958	227.16181	3.02082	15.07189
	40	2212.90741	2003	3.28450	84.66222	-0.50692	-0.00004	-0.00000	9.20121	2.47794	48.37069	1.07520	6.95490
	41	2213.90741	L303	3.28639	83.36617	1.79108	-0.00004	-0.00000	9.13051	2.48127	47.56760	-0.26476	6.89693
BEGIN RF STRUCTURE.	42	2244.25740	2101	3.41499	21.14203	0.25914	-0.00008	-0.00000	4.59805	2.56079	84.36045	-0.94752	9.18479
EAST	43	2245.25740	L244	3.42251	21.41494	-0.53525	-0.00008	-0.00000	4.62763	2.56268	83.30110	1.99442	9.12694
	44	2269.65740	QSFP	3.52054	83.30080	-2.00106	-0.00017	-0.00000	9.12693	2.66035	21.54960	0.53638	4.64215
	45	2270.15740	QSFP	3.52149	84.30593	-0.00115	-0.00017	0.00000	9.18183	2.66408	21.28337	-0.00179	4.61339
	46	2270.65740	L244	3.52243	83.30309	1.99881	-0.00017	0.00000	9.12705	2.66780	21.55321	-0.54006	4.64254
	47	2295.05739	QSFN	3.62034	21.46171	0.53567	-0.00006	0.00000	4.63268	2.76527	83.58717	-2.00232	9.14260
	48	2295.55739	XX	3.62407	21.19518	-0.00050	-0.00006	0.00000	4.60382	2.76622	84.59009	0.00450	9.19729
	49	2295.55739	QSFN	3.62407	21.19518	-0.00050	-0.00006	0.00000	4.60382	2.76622	84.59009	0.00450	9.19729
	50	2296.05739	L244	3.62781	21.46272	-0.53670	-0.00006	0.00000	4.63279	2.76716	83.57823	2.01111	9.14211
	51	2320.45739	QSFP	3.72566	83.38309	-2.00102	-0.00002	0.00000	9.13143	2.86512	21.37040	0.53839	4.62281
	52	2320.95739	FS2	3.72661	84.38718	0.00087	-0.00002	0.00000	9.18625	2.86887	21.10014	0.00429	4.59349
	53	2371.75737	QSFP	3.93198	84.22739	-0.00033	0.00016	0.00000	9.17755	3.07493	21.18655	-0.00547	4.60289
	54	2372.25737	L244	3.93293	83.22467	1.99774	0.00016	-0.00000	9.12276	3.07867	21.45899	-0.54159	4.63239
	55	2396.65737	2203	4.03094	21.43853	0.53448	0.00009	-0.00000	4.63018	3.17626	83.77037	-2.01216	9.15262

	56	2397.65737	L303	4.C3846	21.21648	-0.30967	0.00008	0.00000	4.60614	3.17814	84.65573	1.13788	9.20085
END RF STRUCTURE. EAST	57	2428.00736	2205	4.16277	87.59184	-1.87733	0.00009	0.00000	9.35905	3.26480	40.55554	0.31518	6.36832
	58	2429.00736	LE50	4.16456	88.74073	0.73987	0.00009	-0.00000	9.42023	3.26871	41.15981	-0.92543	6.41559
	59	2479.00736	2301	4.28683	58.34706	-0.13200	-0.00004	-0.00000	7.63852	3.35139	246.46048	-3.18058	15.69906
	60	2480.0C736	XX	4.28953	59.92071	-1.45313	-0.00004	-0.00000	7.74085	3.35203	247.41134	2.23668	15.72931
	61	2480.0C736	LE50	4.28953	59.92071	-1.45313	-0.00004	-0.00000	7.74085	3.35203	247.41134	2.23668	15.72931
	62	2530.00736	2303	4.34693	335.05521	-4.04956	-0.00020	-0.00000	18.30451	3.40827	84.39887	1.02357	9.18689
	63	2531.00736	LS	4.34740	337.10931	2.00780	-0.00021	0.00000	18.36054	3.41016	83.88103	-0.50262	9.15866
	64	2631.60735	QESN	4.44926	84.18320	0.50637	-0.00017	0.00000	9.17514	3.51240	336.13809	-2.00491	18.33407
	65	2632.10735	QESN	4.45020	83.93029	-0.00005	-0.00017	-0.00000	9.16135	3.51264	337.14359	-0.00409	18.36147
	66	2632.60735	LS	4.45115	84.18330	-0.50647	-0.00017	-0.00000	9.17515	3.51288	336.14625	1.99678	18.33429
	67	2733.20734	QESP	4.55300	337.13962	-2.00801	-0.00032	-0.00000	18.36136	3.61465	84.54160	0.50426	9.19465
	68	2733.70734	QESP	4.55324	338.14523	-0.00122	-0.00032	0.00000	18.38873	3.61559	84.29185	-0.00427	9.18106
	69	2734.20734	LS	4.55347	337.14205	2.00559	-0.00032	0.00000	18.36143	3.61653	84.55015	-0.51284	9.19512
	70	2834.80733	QESN	4.65518	84.38010	0.50696	-0.00009	0.00000	9.18586	3.71782	338.91147	-2.01560	18.40955
	71	2835.30733	QESN	4.65613	84.12718	-0.00062	-0.00009	0.00000	9.17209	3.71805	339.91939	0.00175	18.43690
	72	2835.80733	XX	4.65707	84.38134	-0.50820	-0.00009	0.00000	9.18593	3.71829	338.90797	2.01909	18.40945
	73	2835.80733	LS	4.65707	84.38134	-0.50820	-0.00009	0.00000	9.18593	3.71829	338.90797	2.01909	18.40945
	74	2936.40732	QESP	4.75871	337.54388	-2.00832	0.00003	0.00000	18.37237	3.81977	84.26690	0.51214	9.17970
	75	2936.90732	QESP	4.75895	338.54860	0.00088	0.00003	0.00000	18.39969	3.82071	84.00848	0.00523	9.16561
	76	2937.40732	LS	4.75918	337.54212	2.01007	0.00003	0.00000	18.37232	3.82166	84.25643	-0.50162	9.17913
	77	3038.00731	QAIN	4.E6092	84.23937	0.50785	0.00011	0.00000	9.17820	3.92374	335.52079	-1.99603	18.31723
	78	3039.00731	LS	4.E6281	84.23716	-0.50564	0.00012	0.00000	9.17808	3.92422	335.51858	1.99824	18.31717
SECTOR 29	79	3139.60730	2901	4.56468	336.82856	-2.00521	0.00034	0.00000	18.35289	4.02643	84.07748	0.50118	9.16938
	80	3140.6C730	LE60	4.56515	335.94541	2.88408	0.00034	-0.00000	18.32881	4.02832	84.30771	-0.73253	9.18192
	81	3200.60730	2903	5.02132	89.70686	1.21990	0.00018	-0.00000	9.47137	4.09796	237.82475	-1.82609	15.42157
	82	3201.60730	L185	5.02310	90.14562	-1.66333	0.00018	0.00000	9.49450	4.09863	233.88400	5.72470	15.29327
	83	3220.19938	3001	5.C4735	166.43823	-2.44018	0.00023	0.00000	12.90109	4.12169	70.92904	3.04006	8.42194
	84	3221.19938	XX	5.04831	159.30238	9.40204	0.00022	-0.00001	12.62150	4.12397	69.98676	-2.07502	8.36581
	85	3221.19938	LE6	5.C4831	159.30238	9.40204	0.00022	-0.00001	12.62150	4.12397	69.98676	-2.07502	8.36581
MATCH TO 12 DEG BEND	86	3227.19938	3003	5.C5758	66.68058	6.03492	0.00014	-0.00001	8.16582	4.13554	97.61615	-2.52988	9.88009
	87	3228.19938	LE2	5.C6015	59.16203	1.64900	0.00013	-0.00000	7.69169	4.13716	96.20121	3.91342	9.80822
	88	3230.19938	L417	5.06584	52.81748	1.52327	0.00012	-0.00000	7.26756	4.14076	81.22589	3.57424	9.01254
BEGIN L2 DEG BEND	89	3234.37478	BEN	5.C8011	41.19291	1.26079	0.00010	-0.00000	6.41817	4.15077	54.33478	2.86613	7.37121
	90	3239.01895	LE5	5.10089	30.84227	0.96897	0.12164	0.05237	5.55358	4.16875	31.25856	2.09591	5.59094
	91	3244.01895	BEN	5.13114	22.72423	0.65464	0.38347	0.05237	4.76699	4.20633	14.61258	1.23329	3.82264
	92	3248.66313	LE8	5.16799	18.00112	0.36282	0.74812	0.10474	4.24277	4.28313	6.85404	0.43501	2.61802
	93	3256.66313	Q307	5.24554	16.21937	-0.14010	1.58603	0.10474	4.02733	4.46961	10.99839	-0.95306	3.31638
	94	3257.66313	LE1	5.25604	13.16554	2.96373	1.51353	-0.24704	3.62843	4.48206	16.02463	-4.44096	4.00308
	95	3258.66313	Q308	5.27159	7.98120	2.22060	1.26649	-0.24704	2.82510	4.48983	26.19970	-5.73411	5.11856
	96	3259.66313	XX	5.29679	5.36699	0.55780	1.13428	-0.02156	2.31668	4.49509	32.78736	-0.42910	5.72602
	97	3259.66313	L141	5.29679	5.36699	0.55780	1.13428	-0.02156	2.31668	4.49509	32.78736	-0.42910	5.72602
	98	3273.77543	XX	5.57475	38.27686	-2.88980	0.82996	-0.02156	6.18683	4.55056	52.09127	-0.93878	7.21743
	99	3273.77543	XX	5.57475	38.27686	-2.88980	0.82996	-0.02156	6.18683	4.55056	52.09127	-0.93878	7.21743
	100	3273.77543	XX	5.57475	38.27686	-2.88980	0.82996	-0.02156	6.18683	4.55056	52.09127	-0.93878	7.21743
	101	3273.77543	XX	5.57475	38.27686	-2.88980	0.82996	-0.02156	6.18683	4.55056	52.09127	-0.93878	7.21743
	102	3273.77543	BEN	5.57475	38.27686	-2.88980	0.82996	-0.02156	6.18683	4.55056	52.09127	-0.93878	7.21743
	103	3278.41961	LE05	5.58901	70.37043	-4.02385	0.85142	0.03081	8.38871	4.56364	61.43520	-1.07043	7.83806
	104	3278.91961	Q320	5.59011	74.45536	-4.14600	0.86682	0.03081	8.62875	4.56492	62.51437	-1.08790	7.90660
	105	3279.91961	LE1	5.59230	65.21146	12.63771	0.79438	-0.17277	8.07536	4.56724	81.34922	-19.23125	9.01998
	106	3280.91961	Q321	5.59533	42.40050	10.17324	0.62161	-0.17277	6.51157	4.56883	124.37035	-23.78988	11.15215
	107	3281.91961	L530	5.59983	31.63258	1.37434	0.51218	-0.05008	5.62428	4.56997	144.03986	5.58704	12.00166
	108	3287.21961	XX	5.63395	19.62983	0.89033	0.24675	-0.05008	4.43056	4.57734	91.09967	4.40168	9.54461
END 12 DEG BEND	109	3287.21961	BEMH	5.63395	19.62983	0.89033	0.24675	-0.05008	4.43056	4.57734	91.09967	4.40168	9.54461
	110	3291.86379	L887	5.68019	13.37444	0.46697	0.13616	0.00232	3.65711	4.58782	54.65208	3.39251	7.39270
	111	3300.74209	BEM2	5.80211	12.26141	-0.34161	0.15678	0.00232	3.50163	4.64309	12.45442	1.36039	3.52908
	112	3303.06418	L414	5.83013	14.33882	-0.55308	0.18497	0.02196	3.78666	4.68206	7.36714	0.83001	2.71425
ETA MATCH QUAD	113	3307.20728	Q334	5.86899	20.48504	-0.93041	0.27594	0.02196	4.52604	4.81129	4.42464	-0.11980	2.10348
	114	3308.7C728	LE75	5.88186	14.29971	4.37365	0.24283	-0.06433	3.78150	4.85527	7.99356	-2.62771	2.82729
BEGIN EAST MAIN	115	3309.45728	GMOP	5.89268	8.53103	3.31792	0.19458	-0.06433	2.92079	4.86723	12.49139	-3.36939	3.53432

	116	3312.05245	SE19	6.C5842	1.28118	-0.00049	0.11502	-0.00000	1.13189	4.88917	23.42593	0.00042	4.84003
MATCH EAST LOOP	117	3627.08530	TP2	6.11140	1.28178	-0.00088	0.11502	0.00000	1.13216	5.72544	23.53421	0.00236	4.85121
TO OBLIQUE DRIFT	118	3640.95326	LE6	6.64144	3.18158	-1.00361	0.00003	0.00001	1.78370	6.07694	40.59443	-4.59534	6.37138
	119	3646.95326	Q400	6.73339	37.93700	-4.78896	0.00007	0.00001	6.15930	6.09091	115.35245	-7.86433	10.74023
	120	3647.95326	XX	6.73693	56.83672	-15.25760	0.00009	0.00002	7.53901	6.09228	109.74964	13.11871	10.47615
	121	3647.95326	LE2	6.73693	56.83672	-15.25760	0.00009	0.00002	7.53901	6.09228	109.74964	13.11871	10.47615
	122	3649.95326	Q401	6.74057	134.32085	-23.48447	0.00013	0.00002	11.58969	6.09609	63.58374	9.96425	7.97394
	123	3650.95326	L710	6.74163	157.83520	1.35141	0.00014	-0.00000	12.56325	6.09887	54.66280	-0.53130	7.39343
	124	3721.96625	Q410	6.87757	56.20042	0.07980	-0.00002	-0.00000	7.49669	6.20317	248.41736	-2.19713	15.76126
	125	3722.96625	L710	6.88039	57.00516	-0.88904	-0.00002	-0.00000	7.55018	6.20381	248.64168	1.97407	15.76838
	126	3793.97923	Q420	6.96535	341.65414	-3.11937	-0.00020	-0.00000	18.48389	6.29607	67.59014	0.57548	8.22132
	127	3794.97923	LE73	6.96582	341.15577	3.61447	-0.00021	0.00000	18.47040	6.29843	67.78416	-0.77077	8.23311
	128	3867.97923	Q430	7.C8627	33.13512	0.60499	-0.00010	0.00000	5.75631	6.38308	305.63954	-2.48752	17.48255
	129	3868.97923	L178	7.C9109	33.33747	-0.81015	-0.00010	-0.00000	5.77386	6.38361	297.90092	10.11802	17.25981
	130	3886.80940	Q434	7.14793	78.02290	-1.69602	-0.00014	-0.00000	8.83306	6.40758	47.40834	3.93079	6.88537
	131	3887.80940	LE8	7.15002	70.87046	8.51613	-0.00014	0.00002	8.41846	6.41106	46.02017	-2.47929	6.78382
	132	3895.80940	XX	7.34748	1.00910	0.21654	-0.00000	0.00002	1.00454	6.43030	95.62799	-3.72169	9.77896
	133	3895.80940	Q438	7.34748	1.00910	0.21654	-0.00000	0.00002	1.00454	6.43030	95.62799	-3.72169	9.77896
	134	3896.80940	L275	7.48515	1.81553	-1.07065	0.00002	0.00002	1.34742	6.43200	86.19870	12.58003	9.28433
BEGIN EAST REV BND	135	3899.55940	L413	7.56853	16.64432	-4.32164	0.00007	0.00002	4.07974	6.44048	30.98071	7.49924	5.56603
HORIZ FOCUS BEND	136	3899.97240	B1H	7.57210	20.41563	-4.80988	0.00008	0.00002	4.51837	6.44283	25.10147	6.73620	5.01014
	137	3907.47240	L425	7.60479	26.73529	4.81310	0.13261	0.02773	5.17062	6.81790	9.64864	-3.20541	3.10623
VERT FOCUS BEND	138	3907.89740	B1V	7.60753	22.80742	4.42894	0.14439	0.02773	4.77571	6.82404	12.58430	-3.70203	3.54744
	139	3915.39740	L291	7.75145	8.58335	-1.17621	0.86826	0.20363	2.92974	6.86611	26.44986	3.71085	5.14294
	140	3918.30990	Q446	7.78932	17.79025	-1.98496	1.46133	0.20363	4.21785	6.89541	9.57114	2.08442	3.09373
	141	3919.30990	LE2	7.79754	20.57610	-0.73290	1.60958	0.09107	4.53609	6.91592	6.48341	1.07793	2.54625
	142	3921.30990	Q447	7.81194	23.80650	-0.88231	1.79173	0.09107	4.87919	6.98482	3.50551	0.41102	1.87230
	143	3922.30990	L112	7.81873	21.94190	2.64900	1.74260	-0.18805	4.68422	7.03199	3.52196	-0.42832	1.87669
	144	3933.55990	XX	8.16578	8.58318	-1.46155	-0.37297	-0.18805	2.92971	7.18045	55.68677	-4.20856	7.46236
	145	3933.55990	Q450	8.16578	8.58318	-1.46155	-0.37297	-0.18805	2.92971	7.18045	55.68677	-4.20856	7.46236
	146	3934.55990	L425	8.18049	14.93295	-5.43955	-0.61997	-0.31681	3.86432	7.18335	49.49972	9.83907	7.03560
	147	3934.98490	B1H	8.18441	19.92656	-6.31012	-0.75461	-0.31681	4.46392	7.18485	41.49341	8.99930	6.44154
	148	3942.48490	L425	8.20946	46.37193	6.32359	-1.37538	0.18686	6.80969	7.36343	3.59212	-0.33929	1.89529
	149	3942.90990	Q453	8.21101	41.15653	5.94794	-1.29596	0.18686	6.41534	7.38146	3.93659	-0.47123	1.98408
	150	3943.40990	Q453	8.21304	38.25326	0.00088	-1.24953	-0.00000	6.18492	7.40089	4.17700	0.00230	2.04377
	151	3943.90990	L425	8.21507	41.15470	-5.94592	-1.29597	-0.18687	6.41519	7.42033	3.93220	0.47517	1.98298
	152	3944.33490	B1H	8.21662	46.36828	-6.32135	-1.37538	-0.18687	6.80943	7.43839	3.58462	0.34268	1.89331
	153	3951.83490	L425	8.24168	19.91427	6.30787	-0.75464	0.31681	4.46254	7.61763	41.41511	-8.98652	6.43546
	154	3952.25990	Q456	8.24561	14.92255	5.43737	-0.62000	0.31681	3.86297	7.61913	49.41023	-9.82551	7.02924
	155	3953.25990	LE9	8.26020	8.78306	1.27448	-0.37838	0.17785	2.96362	7.62205	54.53691	5.19529	7.38491
REVERSE BEND CELL	156	3962.25990	XX	8.55638	10.04451	-1.41464	1.22228	0.17785	3.16931	7.75861	2.59490	0.57605	1.61087
	157	3962.25990	Q459	8.55638	10.04451	-1.41464	1.22228	0.17785	3.16931	7.75861	2.59490	0.57605	1.61087
	158	3962.75990	Q459	8.56394	10.76958	-0.00100	1.26702	0.00004	3.28170	7.79173	2.31123	0.00466	1.52027
	159	3963.25990	LE9	8.57151	10.04642	1.41292	1.22232	-0.17777	3.16961	7.82491	2.58514	-0.56537	1.60784
	160	3972.25990	Q456	8.86740	8.77208	-1.27132	-0.37762	-0.17777	2.96177	7.96255	54.11036	-5.15965	7.35597
	161	3973.25990	L425	8.88202	14.89993	-5.42782	-0.61905	-0.31649	3.86004	7.96549	49.03310	9.74523	7.00236
	162	3973.68490	B1H	8.88595	19.88284	-6.29668	-0.75356	-0.31649	4.45902	7.96700	41.10318	8.91341	6.41118
	163	3981.18490	L425	8.91105	46.28095	6.31013	-1.37388	0.18664	6.80301	8.14601	3.61699	-0.34824	1.90184
	164	3981.60990	Q453	8.91260	41.07665	5.93530	-1.29456	0.18664	6.40911	8.16390	3.96899	-0.47999	1.99223
	165	3982.10990	REV2	8.91464	38.18010	-0.00027	-1.24819	-0.00002	6.17901	8.18316	4.21530	-0.00044	2.05312
	166	4059.50990	REV4	9.31755	38.19878	0.00097	-1.24941	0.00001	6.18052	8.74698	4.21038	0.00319	2.05192
END EAST REV BEND	167	4103.36040	L275	9.56235	16.62029	4.31357	-0.00017	0.00004	4.07680	9.70774	31.27998	-7.57063	5.59285
	168	4106.11040	2602	10.C4576	1.81711	1.06941	-0.00007	0.00004	1.34800	9.71614	87.01705	-12.69739	9.32829
BEGIN WESTBOUND	169	4107.11040	LE8	10.18314	1.01152	-0.21608	-0.00003	0.00003	1.00574	9.71782	96.49098	3.79852	9.82298
DRIFT	170	4115.11040	2604	10.38062	70.69404	-8.49423	0.00021	0.00003	8.40797	9.73699	45.94821	2.51933	6.77851
	171	4116.11040	L173	10.38271	78.35723	1.16886	0.00023	0.00000	8.85196	9.74049	46.91573	-3.52877	6.84951
	172	4133.44159	2502	10.42885	46.91231	0.64549	0.00025	0.00000	6.84926	9.76580	255.35659	-8.49815	15.97988
	173	4134.44159	L498	10.43224	47.62867	-1.37193	0.00025	0.00001	6.90135	9.76641	261.50527	2.43645	16.17112
	174	4184.24158	2504	10.49680	334.34868	-4.38550	0.00085	0.00001	18.28520	9.82074	84.61642	1.11553	9.19872
	175	4185.24158	LS	10.49728	336.74487	2.00453	0.00085	-0.00000	18.35061	9.82264	84.00455	-0.49979	9.16540

	176	4285.84157	QESN	10.59915	84.24599	0.50540	0.00042	-0.00000	9.17856	9.92497	335.12828	-1.99647	18.30651
WESTBOUND	177	4286.34157	ACC	10.60010	83.99424	-0.00139	0.00042	-0.00000	9.16484	9.92520	336.12834	-0.00167	18.33380
RF-SYSTEM	178	4895.94149	QESN	11.01409	83.93298	-0.00064	-0.00044	-0.00000	9.16149	10.18274	340.20418	0.00229	18.44462
	179	4896.44149	LS	11.01504	84.18658	-0.50708	-0.00044	-0.00000	9.17532	10.18297	339.19138	2.02131	18.41715
	180	4997.04148	XX	11.11685	337.33348	-2.00930	-0.00080	-0.00000	18.36664	10.28442	84.24414	0.51296	9.17846
	181	4997.04148	QESP	11.11685	337.33348	-2.00930	-0.00080	-0.00000	18.36664	10.28442	84.24414	0.51296	9.17846
	182	4997.54148	QESP	11.11709	338.33980	-0.00135	-0.00080	0.00000	18.39402	10.28537	83.98483	0.00618	9.16432
	183	4998.04148	LS	11.11732	337.33617	2.00661	-0.00080	0.00001	18.36671	10.28631	84.23176	-0.50053	9.17779
	184	5098.64147	QESN	11.21898	84.40447	0.50762	-0.00020	0.00001	9.18719	10.38847	335.18763	-1.99406	18.30813
	185	5099.14147	QESN	11.21992	84.15097	-0.00010	-0.00020	0.00000	9.17338	10.38871	336.18510	0.00109	18.33535
	186	5099.64147	LS	11.22087	84.40468	-0.50782	-0.00020	0.00000	9.18720	10.38895	335.18545	1.99623	18.30807
	187	5200.24146	EL11	11.32252	337.40264	-2.00707	0.00016	0.00000	18.36852	10.49123	84.05534	0.50009	9.16817
	188	6013.04139	QESP	12.14622	337.49152	-2.01005	-0.00072	-0.00000	18.37094	11.31386	84.05912	0.51123	9.16838
	189	6013.54139	QESP	12.14646	338.49812	-0.00116	-0.00072	0.00000	18.39832	11.31480	83.80099	0.00554	9.15429
	190	6014.04139	LS	12.14669	337.49383	2.00775	-0.00071	0.00001	18.37101	11.31575	84.04802	-0.50009	9.16777
	191	6114.64138	QESN	12.24833	84.40030	0.50810	-0.00013	0.00001	9.18696	11.41804	335.19139	-1.99637	18.30823
	192	6115.14138	QESN	12.24927	84.14630	0.00040	-0.00013	0.00001	9.17313	11.41828	336.19115	-0.00119	18.33552
	193	6115.64138	LS	12.25022	84.39950	-0.50729	-0.00012	0.00000	9.18692	11.41852	335.19376	1.99400	18.30830
	194	6216.24137	SQ2	12.35190	337.23462	-2.00598	0.00031	0.00000	18.36395	11.52067	84.23993	0.50057	9.17823
	195	6217.24137	LE60	12.35237	333.81568	5.39973	0.00031	-0.00000	18.27062	11.52256	85.11154	-1.37857	9.22559
	196	6277.24137	SQ4	12.57652	11.07396	-0.02070	0.00016	-0.00000	3.32776	11.57720	373.22153	-3.42326	19.31894
	197	6278.24137	L189	12.59063	11.69092	-0.60506	0.00016	0.00000	3.41920	11.57763	364.09819	12.41555	19.08136
	198	6297.23417	SQ6	12.69987	76.82576	-2.82439	0.00024	0.00000	8.76503	11.60102	46.19527	4.32253	6.79671
	199	6298.23417	LE8	12.70197	70.83034	8.51006	0.00022	-0.00003	8.41608	11.60462	44.54334	-2.58698	6.67408
	200	6306.23417	SQ8	12.89928	1.01033	0.21744	-0.00003	-0.00003	1.00515	11.62404	96.98751	-3.96854	9.84822
	201	6307.23417	L275	13.03685	1.81654	-1.07187	-0.00007	-0.00004	1.34779	11.62572	87.59002	12.79023	9.35895
WEST REVERSE BEND	202	6309.98417	REVB	13.12017	16.65801	-4.32503	-0.00018	-0.00004	4.08142	11.63406	31.65442	7.62272	5.60842
	203	6513.78516	L275	13.51406	16.62614	4.31433	0.00007	-0.00002	4.07752	11.90297	30.88170	-7.48610	5.55713
WEST OBLIQUE DRIFT	204	6516.53516	Q160	13.59741	1.81863	1.07023	0.00002	-0.00002	1.34856	11.91146	86.02395	-12.56563	9.27491
	205	6517.53516	LE8	13.73511	1.00478	-0.21007	0.00000	-0.00002	1.00239	11.91317	96.08756	3.08795	9.80243
	206	6525.53516	Q165	13.93357	70.87245	-8.52338	-0.00013	-0.00002	8.41858	11.93093	53.69757	2.21080	7.32786
	207	6526.53516	L176	13.93566	77.94491	1.78253	-0.00013	0.00000	8.82864	11.93388	56.80546	-5.46173	7.53694
	208	6544.23415	Q170	13.99366	31.63556	0.83396	-0.00009	0.00000	5.62455	11.95215	420.15444	-15.06764	20.49767
	209	6545.23415	LE67	13.99875	31.35948	-0.55392	-0.00009	-0.00000	5.59995	11.95252	432.08058	3.31367	20.78655
	210	6612.23415	Q180	14.12203	292.65197	-3.34597	-0.00020	-0.00000	17.10707	12.00166	112.51655	1.45594	10.60738
	211	6613.23415	LE67	14.12257	292.86303	3.13647	-0.00020	0.00000	17.11324	12.00308	112.09602	-1.03232	10.58754
	212	6680.23415	Q185	14.23092	38.69215	0.65712	-0.00001	0.00000	6.22030	12.05943	333.14873	-2.26698	18.25236
	213	6681.23415	LE67	14.23508	38.03789	0.00070	-0.00001	0.00000	6.16749	12.05991	332.22499	3.18567	18.22704
	214	6748.23415	Q190	14.40298	155.95770	-1.76070	0.00017	0.00000	12.48830	12.14165	55.98287	0.93735	7.48217
	215	6749.23415	LE2	14.40405	133.17982	23.18359	0.00016	-0.00003	11.54036	12.14438	64.38239	-9.82492	8.02386
	216	6751.23415	XX	14.40772	56.61844	15.09710	0.00010	-0.00003	7.52452	12.14816	109.74145	-12.85461	10.47576
	217	6751.23415	Q191	14.40772	56.61844	15.09710	0.00010	-0.00003	7.52452	12.14816	109.74145	-12.85461	10.47576
	218	6752.23415	LE6	14.41126	37.86542	4.78014	0.00009	-0.00001	6.15349	12.14954	115.07567	7.84802	10.72733
	219	6758.23415	RTP2	14.50336	3.17853	1.00101	0.00003	-0.00001	1.78284	12.16355	40.48035	4.58453	6.36242
BEGIN WEST MAIN	220	6772.10212	TP23	15.03342	1.28141	-0.00100	0.11502	0.00000	1.13200	12.51505	23.60101	-0.00029	4.85809
BEND	221	6962.77990	GMDN	15.53916	1.28151	-0.00104	0.11506	-0.00000	1.13204	12.83734	23.42262	-0.00340	4.83969

QX = 15.53916142 XRMS = 0.49319142 QY = 12.83734068 YRMS = 0.0

TRANSITION GAMMA = 141.460345

ELEMENT MATRICES

ELEMENT	RX(I,J)				RY(I,J)	
RLAA	-0.96962575	-0.31216113	0.22662421	0.	0.52455505	-19.98322859
	0.19008004	-C.97013142	-0.02187457	0.	0.03642503	0.51874507
	0.	0.	1.	0.		
	0.02186659	-C.22668366	-0.35046354	1.		

APPENDIX C

RLA ALL-SYSTEM SCHEMATIC DIAGRAM